QATAR UNIVERSITY

Graduate Studies

College of Pharmacy

Synthesis and Pharmacological Evaluation of Different Piperine

Analogs for Therapeutic Potential to Prevent ER Stress

A Thesis in

Pharmacology

By

Ayat Samir Hammad

Submitted in Partial Fulfillment

of the Requirements

for the Degree of

Master of Sciences in Pharmacy

June 2015

The thesis of Ayat Hammad was reviewed and approved by the following:

We, the committee members listed below, accept and approve the Thesis/Dissertation of the student named above. To the best of this committee's knowledge, the Thesis/Dissertation conforms the requirements of Qatar University, and we endorse this Thesis/Dissertation for examination.

Name: Dr. Feras Qasem Alali_____

Signature _____Date_____

Name: Dr. Shankar Munusamy_____

Signature _____Date_____

Name: Dr. Ashraf Khalil_____

Signature _____Date_____

Name: Dr. Ali Hussein Eid _____

Signature _____Date_____

Name: Dr. Michael Pungente_____

Signature _____Date_____

Abstract

Background: Endoplasmic reticulum (ER) is the chief organelle involved in protein folding and maturation. Emerging studies implicate the role of ER stress in the development of chronic kidney disease (CKD). Thus, there is an urgent need for compounds, which have the ability to ameliorate ER stress and prevent CKD. Piperine and its analogs have been reported to exhibit multiple pharmacological activities; however, their efficacy against ER stress in kidney cells has not been studied yet. Hence, the goal of this study was to synthesize different piperine analogs and screen them for pharmacological activity to relieve ER stress using an *in vitro* model of tunicamycin-induced ER stress using rat renal cells (NRK-52E).

Methods: Five piperine analogs were prepared and their chemical structures were elucidated by pertinent spectroscopic techniques. An *in vitro* model of ER stress was developed using tunicamycin, and the compounds of interest were screened for their effect on cell viability (by MTT assay), and the ER chaperone GRP78 and the pro-apoptotic ER stress marker CHOP (via western blotting).

Results: Five piperine analogs were synthesized and their structures were confirmed. Our findings indicate that exposure to tunicamycin (0.5 µg/mL) for 2 hours induces the expression of GRP78 and CHOP, and causes a significant reduction in renal cell viability. Pre-treatment of cells with piperine and its cyclohexylamino analog decreased the tunicamycin-induced upregulation of GRP78 and CHOP.

Conclusion: Our findings demonstrate that piperine and its analogs differentially regulate ER stress, and thus represent potential therapeutic agents to treat ER stress-related renal disorders.

Key Words: Piperine; Amide Piperine Analogs; ER Stress; NRK-52E; Tunicamycin.

Contents

List of Figures

List of Tables

List of Abbreviations

4-PBA	4-Phenylbutyrate
APAF-1	Apoptotic protease activating factor 1
ASK1	Apoptotic signaling kinase-1
ATF4	Activating transcription factor 4
ATF6	Activating transcription factor 6
BH	Bcl-homology domain
BiP	Binding immunoglobulin protein
BIX	BiP/GRP78 inducer X (1-(3,4-dihydroxyphenyl)-2-thiocyanate-ethanone)
CHOP	CCAAT-enhancer-binding protein homologous protein
CKD	Chronic kidney disease
CREB	cAMP-responsive element–binding protein
DM	Diabetes mellitus
DMEM	Dulbecco's modified Eagle medium
DMSO	Dimethyl sulfoxide
DN	Diabetic nephropathy
DTT	Dithiothreitol
eIF2α	Eukaryotic initiation factor 2α
ER	Endoplasmic reticulum
ERAD	ER-associated degradation
ESRD	End stage renal disease
FBS	Fetal bovine serum
FTIR	Fourier transform infrared spectroscopy
GADD34	Growth arrest and DNA damage-inducible protein 34
GADD153	Growth arrest and DNA damage-inducible protein 153
GRP78	Glucose-regulated protein 78
GSK-3	Glycogen synthase kinase-3
HFD	High fat diet
IRE1	Inositol- requiring enzyme 1
JNK	Jun-N-terminal kinase
MAPK	P38 mitogen activated protein kinase
MS	Mass spectrometry
MTT	Thiazolyl blue tetrazolium bromide
NE	Nuclear envelope

NMR	Nuclear magnetic resonance
NRK-52E	Normal rat kidney cells
ORP150	Oxygen-regulated protein 150
PBS	Phosphate-buffered saline
Pen-strep	Penicillin-streptomycin
PERK	PKR-like endoplasmic reticulum kinase
PGD	Primary glomerular diseases
PP1α	Protein phosphatase 1 alpha
PTMs	Post-translational modifications
RER	Rough endoplasmic reticulum
S1P	Site-1 protease
S2P	Site-2 protease
SER	Smooth endoplasmic reticulum
SERCA	Sarco/endoplasmic reticulum Ca^{2+}-ATPase
TM	Tunicamycin
TUDCA	Tauroursodeoxycholic Acid
UATR	Universal attenuated total reflectance
UDCA	Ursodeoxycholic acid
UPR	Unfolded protein response
XBP1	X-box binding protein-1

Acknowledgments

I would like to sincerely thank my supervisors, Prof. Shankar Munusamy and Prof. Ashraf Khalil for their guidance and support during my master degree. You were the ideal thesis supervisors. You trained me to the highest standards and your patience and passion for teaching will always be remembered. I am extremely grateful for your sincere efforts and time spent towards shaping me as a research professional. I appreciate all the support, suggestions and guidance you have provided to me. On this special day, I promise to remember them at all times in my life; I will work diligently to establish my research career that I have embarked under your supervision.

I would like also to thank Prof. Lee Ann MacMillan-Crow for her support and guidance for me during my summer internship at the University of Arkansas for Medical Sciences (UAMS), Little Rock, USA.

Finally I would like to thank my Supervisory Committee members: Prof. Ali Hussein Eid, Prof. Michael Pungente and the committee chair Prof. Feras Qasem Alali, for all their efforts and time. I appreciate all the suggestions and constructive feedback that were provided by you to improve my knowledge and skills. Your constant encouragement and support have provided me with the strength to complete this learning experience.

Dedication

First and foremost, I dedicate my thesis to my parents and my family. Thanks to my beloved parents, Samir Hammad and Fadwa Omar, for their love, support and encouragement. Today is the day to share this success with you and I deeply know by my heart that I would have never been able to accomplish my dreams without your continuous and boundless belief in my abilities. I pray to the God to protect you and to give you all the happiness that you have provided me through your guidance and support in every stage of my life. I also would like to thank my brothers, Mahmoud and Mohammad, and my sisters, Diana, Aphrodite, Elyaa, and Alaa for being with me at all times. I am truly blessed to have you in my life. I feel safe in your arms and I know you will always be around me. To my parents, my brothers, my sisters, and the new addition to my family, you are the source of love, strength and happiness for me. No word can ever describe my gratefulness and love for you.

Last but not least, I would like to thank Allah for giving me this experience in life and for providing me with the strength. The best gifts in my life are those who loved me and supported me at all times. There is nothing more I could ask from you. Thank you God for all that you gave me right from the day that I was born to this minute in my life.

1. Introduction

1.1   Endoplasmic Reticulum

1.1.1 Physiological Role

Endoplasmic reticulum (ER) is one of the most versatile and adaptable organelles in eukaryotic cells (1, 2). ER plays a principal role in controlling the synthesis, folding and maturation of luminal, secreted and transmembrane proteins besides controlling the cytosolic calcium levels (1-3). In addition, it serves as a major site for the synthesis of phospholipids and steroids (4). Progresses in cell biology indicate that all signaling proteins are assembled in the ER (5).

The ER is the largest organelle in most cell types, and is composed of three compartments, 1) the rough ER (RER), 2) smooth ER (SER) and 3) the nuclear envelope (NE) (2, 4). The fundamental difference between the RER and the SER is the presence of ribosomes in the RER (6). Moreover, the ultrastructure of the RER has been visualized to be tubular in appearance, while the SER appear to be more convoluted and dilated (4). The abundance of SER and RER differs between cells; however, it is well demonstrated that cells that secrete large quantities of proteins are chiefly composed of RER (4). Recent progress in cell biology has also highlighted the specific role of RER in the synthesis of membrane and secretory proteins due to the presence of ribosome and mRNA on RER (6). On the other hand, the SER is composed of several subdomains

including the cortical ER, ER quality control compartment, mitochondria-associated membrane and ER exit sites (6).

During protein synthesis, which occurs within the RER, the stoichiometry of the amino acid residues in a nascent protein is most often altered by post-translational modifications (PTMs) while folding of the emerging peptide into a proper configuration (3). It was found that the protein glycosylation, (a common PTM), as well as, the translocation of proteins are regulated by the ER (6). Thus, only those proteins folded in proper configuration, which undergo specific post-translational modifications, will be processed through the ER secretory pathway and translocated to Golgi bodies (3). If cells cannot mitigate the unfolded or misfolded proteins and reestablish homeostasis, it results in ER stress (5).

The balance between protein folding and degradation is thought to be the principal mechanism that governs the dynamics of ER (1); this intricate balance is tightly controlled by the unfolded protein response (UPR), and the ER-associated degradation (ERAD) pathways that exist within the ER (3). Numerous studies have documented the vulnerability of the ER to undergo stress, or to develop "ER stress", when the misfolded proteins accumulate in the ER either due to saturation of the UPR and/or ERAD response pathways (3, 7-9). This fact has been well established, particularly in chronic diseases such as diabetes, where the UPR pathway is continuously activated in most tissues (3). Cells with high rate of protein synthesis such as those within the kidney and liver demonstrate high dependence to the UPR.

The ER plays a central role in the synthesis of proteins, steroids, cholesterol and other lipids, and acts as an intracellular reservoir for Ca^{2+}, which is essential for the synthesis of proteins. Thus, a functional ER is essential to maintain the highly regulated and coordinated homeostatic balance within the cells (10, 11). However, physiological conditions are not always maintained and numerous stimuli such as hypoxia, hypoglycemia, hyperglycemia and certain chemicals can lead to improper folding or glycosylation of newly synthesized protein and activate UPR as a defense mechanism (10, 12). The UPR attempts to re-establish homeostasis through inducing several chaperones, which allows the cells to adapt and restore the balance between protein folding and degradation (10).

1.1.2 ER Stress and the Unfolded Protein Response (UPR)

The UPR is a collection of phylogenetically conserved signaling pathways that is composed of three principal pathways: PERK (PKR-like endoplasmic reticulum kinase), IRE1 (inositol- requiring enzyme 1) and ATF6 (activating transcription factor 6) (5, 10). Under normal conditions, a chaperone called GRP78 (glucose-regulated protein 78), also known as BiP (binding immunoglobulin protein), is connected to the three transducers of UPR in the intraluminal domains (amino-terminal in the IRE1 and PERK, whereas carboxy-terminal in the ATF6) and retains them inactive (as shown in **Figure 1.1**) (10, 11, 13). Dissociation of GRP78 from PERK, IRE1 or ATF6, results in the activation of UPR signaling (10). However, several studies have suggested that other mechanisms may be involved in the activation of the previous sensors and GRP78 may not always lead to constitutive activation (11). In addition, GRP78 is regarded as the master

chaperone that binds to Ca^{2+}, and has been shown to reduce cell death induced by Ca^{2+} efflux of the ER (10).
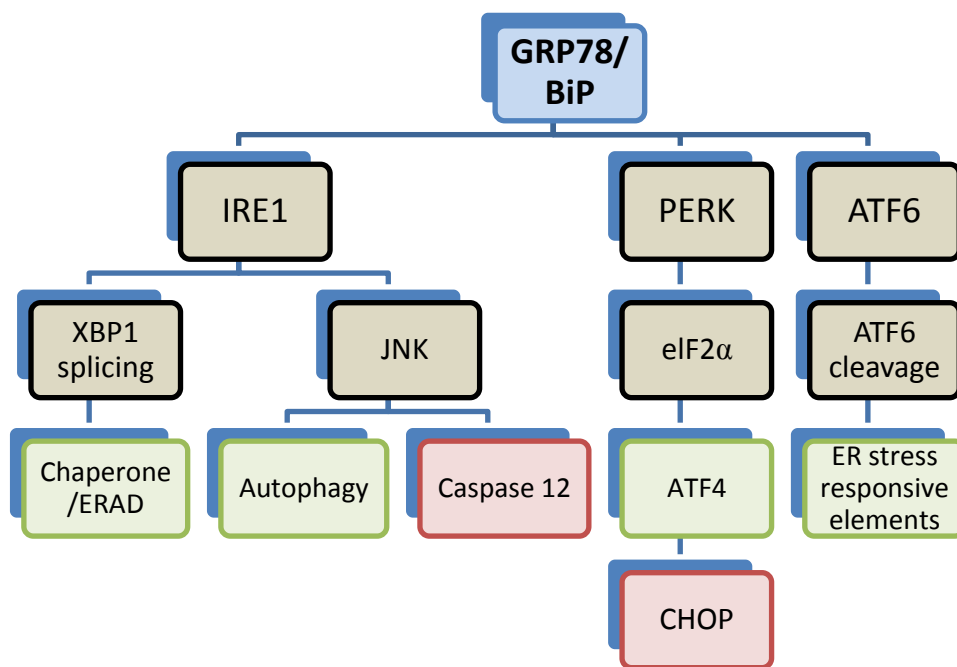
Figure 1.1 The signaling pathway and the downstream targets of the unfolded protein response (UPR). **GRP78/BiP**, glucose-regulated protein-78/ binding immunoglobulin protein; **PERK**, PKR- like ER kinase; **IRE-1**, inositol requiring enzyme 1; **ATF6**, activating transcription factor 6; **XBP-1**, X-box binding protein 1; **JNK**, Jun amino-terminal kinase; **eIF2α**, eukaryotic translation initiation factor 2 subunit a; **ATF4**, activating transcription factor 4; **CHOP**, C/EBP homologous protein, growth arrest and DNA damage inducible gene 153; and **ERAD,** ER-associated degradation.

Tremendous progress has been made towards understanding the mechanisms of ER stress, and several studies have provided evidence that the UPR sensors work to either reduce protein synthesis to prevent the formation of more misfolded proteins, increase

production of chaperones to modify and refold the unfolded proteins, or facilitate protein degradation by the ubiquitin-proteasome pathway (14). If ER stress persists, the cells fail to survive and undergo cell death through apoptosis (11).

1.1.2.1 The PERK-arm of the UPR

PERK signaling is of great importance to ER stressors, and it was first defined by Shi et al and Harding et al (10). The activation of PERK leads to the phosphorylation of the α-subunit of the eukaryotic initiation factor 2 (eIF2α) on its serine residue 51 and consequently causes translational arrest (10, 15, 16). Moreover, the phosphorylation of eIF2α leads to increase in the activity of a transcription factor called ATF4 (activating transcription factor 4), which plays an important role in the activation of growth arrest and DNA damage-inducible protein 34 (GADD34). GADD34 acts as an activator of protein phosphatase 1 alpha (PP1α), which dephosphorylate eIF2α and serves as a negative feedback (10, 13, 17). In addition, AFT4 also activates another transcription factor named CHOP (CCAAT-enhancer-binding homologous protein), also known as GADD153 (growth arrest and DNA damage-inducible protein 153), which promotes apoptosis in cells undergoing ER stress (10, 13).

1.1.2.2 The IRE1-arm of the UPR

The IRE1 operates in parallel to the other branches; however, it is unique as it is the only transducer of the UPR in lower eukaryotes, and conserved from yeast to humans (5, 11). IRE1 has two isoforms, IRE1α (termed IRE1 hereafter) and IRE1β (13). It has a bi-functional transmembrane kinase domain and an endoribonuclease (C-terminal RNase)

domain (5, 13). Activation of IRE1 by oligomerization in the ER membrane leads to conformational changes, which stimulate RNase to remove an intron from unspliced XBP1 (XBP1u) mRNA to form spliced XBP1 (XBP1s) (13). XBP1s is one of the most active transcription factors used to improve ER protein-folding capacity and enhance the ability of cells to degrade misfolded proteins (13). By these means, IRE1 serves as an essential adaptive response that acts mainly to improve the protein folding capacity to match the increased protein folding demand (13).

1.1.2.3 The ATF 6–arm of the UPR

ATF6 is a transcription factor with a large luminal domain and has two isoforms of transmembrane receptors, AFT6α and AFT6β (13). It belongs to cAMP-responsive element–binding protein (CREB) family of basic zipper-containing proteins (15). Studies have revealed that the AFT6α isoform is highly related to the UPR (13). Upon activation of AFT6α, it is packaged into transporter vehicles and transported to Golgi apparatus where it is converted by serine protease site-1 protease (S1P) and the metalloprotease site-2 protease (S2P) to the active form (5, 11, 13). Following this event, AFT6α becomes proteolytically removed from its transmembrane anchor, and the N-terminal cytosolic fragment, ATF6(N) is translocated to the nucleus where it binds to the promoters of the ER stress-induced genes (5, 13). Consequently, genes that code for ER chaperones such as GRP78/BiP, Glucose–regulated protein 94 and protein disulfide isomerase are stimulated (5, 13). In addition, ATF6(N) also activates the proteins involved in the ERAD pathway (13).

1.1.3 ER Stress and Apoptosis

If the ER stress is severe and prolonged, and homeostasis is not restored by the adaptive mechanism of the UPR, then the cell initiates a pro-apoptotic response rather than a pro-survival response (18). Both extrinsic and intrinsic pathways of cell death could be triggered due to ER stress through caspases, which is a family of cysteine aspartyl proteases (14, 18-20). The extrinsic (death receptor-mediated) pathway is mainly activated by caspase-8, which activates caspase-3 and caspase-7, and leads to apoptosis (21, 22). However, the apoptosis mechanism as a result of ER stress is thought to be mediated mainly through the intrinsic pathway (22).

The intrinsic (mitochondrial) pathway is activated through Bcl-2 family members (18, 23). The pro-apoptotic family is classified into two types based on their Bcl-homology domain (BH) (18, 24, 25). The first type contain BH domains 1, 2 and 3 such as Bax, Bok and Bak, while the other type contain only BH domain 3 such as Bad, Bim, Bmf, Bik, Bid, Hrk, Noxa and Puma (18, 24, 25). In contrast, the anti-apoptotic members contain four BH domains such as Bcl-2, Bcl-xL, A1 and Mcl-1 (18, 25).

Upon activation of the pro-apoptotic members, cytochrome c is released from the mitochondrial intermembrane space (18, 26, 27). Following its release, cytochrome c assembles with pro-caspase 9 and apoptotic protease activating factor 1 (APAF-1) to form a complex called "apoptosome", which in turn activates caspase-9 and consequently caspase 3, leading to cell death (18, 26, 27).

When ER stress is severe and prolonged, the IRE1α activates apoptotic signaling kinase-1 (ASK1) and stimulates the expression of stress kinases, Jun-N-terminal kinase (JNK) and P38 mitogen activated protein kinase (MAPK), and results in cell death (14, 28, 29). JNK is of great importance as its phosphorylation leads to apoptosis via inactivation of anti-apoptotic Bcl-2 and activation of pro-apoptotic Bim (14). On the other hand, P38 MAPK activates CHOP, which in turn activates Bim and death receptor 5 (DR5), and reduces the expression of Bcl-2 (14). Numerous studies have established a strong link between activation of CHOP and the PERK pathway, while the activation of JNK, caspase-12, and pro-apoptotic Bcl-2 proteins Bax and Bak were shown to associated with IRE1α activation (11, 30, 31).

1.2   Chronic Kidney Disease and ER stress

As described earlier, ER performs several essential cellular functions; many diseases have been shown to affect the signaling pathways within the ER and induce ER stress. Accumulating evidences identified the involvement of ER stress in diverse disease states such as Parkinson's disease, Alzheimer's disease and most importantly, in a wide range of renal pathologies, which results in chronic kidney disease (32-34). Numerous studies have provided evidence for the involvement of ER stress in CKD (32-35).

Chronic kidney disease is defined as the presence of abnormalities in the structure or function of kidney for more than 3 months (32, 36). According to a study that was conducted in Qatar between 2002 and 2006, it was estimated that the prevalence of end stage renal disease is 624 patients per million populations with an incidence of 202

patients per million population per year (37). Currently, CKD is considered as one of the most significant global health issue, which not only endangers the health of our society but also places a huge burden on our health-care cost (32, 38). Early identification or prevention of CKD provides the opportunity to avoid its complications and improve kidney function (38). However, studies have found that once the diagnosis of CKD is established, the rate of decline in kidney function was found to be 2.3 to 4.5 mL/min/year (38). This rapid progression necessitates the use of more aggressive and costly interventions (38). Thus, prophylaxis to hinder the deterioration of kidney function is a better strategy than treatment, especially in high-risk populations such as patients with diabetes and/or hypertension (38, 39).

1.2.1 CKD, Diabetic Nephropathy and ER Stress

Diabetic nephropathy is one of the major complications of diabetes mellitus (DM), and it is the leading cause for CKD and end stage renal disease (ESRD) around the world (40). Among DM patients, 30 to 40% progress to diabetic nephropathy (DN), which is characterized by persistent microalbuminuria (41). About 40% of patients with DN in the US progress to ESRD, a severe and the most advanced stage of CKD (42). In Qatar, DN accounts for 48% of ESRD cases, which makes diabetes the most prevalent cause of ESRD in the nation (37).

Given the direct association between the ER and cellular metabolism, several studies have provided evidence for the involvement of ER stress in metabolic disorders such as DM (11, 43-48). A study conducted by Matsuhisa et al. has demonstrated that

overexpression of oxygen-regulated protein 150 (ORP150), an ER chaperone, in diabetic mice leads to improvements in insulin receptor signaling and glucose tolerance (11, 49). Conversely, a study by Liu et al. revealed marked upregulation of ER stress markers GRP78, CHOP and caspase-12 in diabetic rat kidneys (50). It was also found that ER stress-associated apoptosis was linked to the loss of renal cells (50). Moreover, a recent study on the kidney biopsies obtained from DN patients revealed increased levels of XBP1 and ER chaperones (GRP78 and ORP150) (3) Thus, it is clear that activation of ER stress contributes to the development of DN in diabetic patients (51).

1.2.2 Non-diabetic CKD and ER stress

Apart from DN, abnormalities in ER stress response pathway and other stimuli such as lipotoxicity and inflammation could also result in CKD (34, 52, 53). Mutations to ER chaperone GRP78/BiP have been shown to cause tubulointerstitial lesions in the kidney (52), which suggests the involvement of ER stress in the development of CKD. Interestingly, a study by Chatterjee et al. demonstrated that micromolar concentrations of palmitic acid cause increase in phosphorylation of eIF2α and induction of CHOP expression, and decrease in cell viability in rat renal proximal tubular cells (53).

Findings from a study conducted on kidney biopsies taken from patients with primary glomerulonephritis, one of the primary glomerular diseases (PGD), revealed increased expression of GRP78 and GADD153/CHOP, and decrease in the expression of anti-apoptotic Bcl-2 proteins in PGD (34). Several other studies also confirmed the involvement of ER stress in a wide variety of kidney diseases (54-58), and some of those

studies are mentioned in the table below (Table 1.1). Thus, prevention or treatment of ER stress could serve as a therapeutic strategy to combat kidney disease and the onset of CKD in patients.

Table 1.1: Reports on the involvement of ER stress in kidney disease

Site	Species	Disease	Reference
Glomerulus	Rat	Passive Heymann nephritis	(55)
Glomerulus	Rat	Misfolded protein accumulation in podocytes	(56)
Glomerulus	Mouse	Focal segmental glomerulosclerosis model	(58)
Glomerulus	*In vitro*	Misfolded nephrin accumulation in the ER	(54)

1.3 Therapeutic Targeting for ER Stress

1.3.1 Chemical Chaperones

1.3.1.1 Tauroursodeoxycholic Acid (TUDCA)

TUDCA, an hydrophilic conjugate of ursodeoxycholic acid (UDCA) (57), is known for its effect in improving clinical symptoms and biochemical markers of liver diseases (59). Specifically, TUDCA was shown to decrease intracellular calcium through blocking caspase-12 activation and prevent calcium-mediated apoptosis induced by tunicamycin in liver cells *in vitro* (59). A study by Ozcan et al highlighted that TUDCA is one of the potent chemical chaperones to alleviate ER stress both *in vivo* and *in vitro* (60). In further support to these findings, Mei et al. demonstrated the ability of TUDCA

to downregulate the expression of GRP78, CHOP and Caspase-12 in mouse model of ischemia/reperfusion-induced acute kidney injury (61).

1.3.1.2 4-Phenylbutyrate (4-PBA)

4-PBA is a well-established low molecular weight inhibitor of ER stress with chemical chaperone properties (62, 63). It has several clinical indications; it is used as a urea cycle scavenger, and in the treatment of cystic fibrosis, sickle cell disease, cancer, and neurodegenerative diseases. The US FDA recommended dose for patients with cystic fibrosis is 9.9 - 13.0 g/m^2 /day in children weighing more than 20 kg, adolescents and adults, and there is no safety data on its use at a concentration greater than 20 g/d.
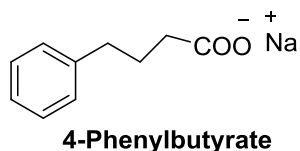
4-Phenylbutyrate

Figure 1.2: Chemical structure of sodium 4-phenylbutyrate

Several studies have confirmed the efficacy of 4-PBA to relieve ER stress both *in vivo* and *in vitro* (62). 4-PBA was shown to suppress ER stress through stabilizing protein conformation in the ER (62). A study by Ozcan et al. has demonstrated the efficacy of 4-PBA to prevent tunicamycin-induced phosphorylation of PERK, eIF2α and JNK in rat hepatoma cells (60). In addition, a recent study in 3T3-L1cells has shown that 4-PBA decreases the expression of GRP78, spliced XBP1 and phospho-eIF2α (62). Similarly, Kang et al. demonstrated that low doses of palmitate induce ER stress in pancreatic beta cells, and the use of 4-PBA (at 0.5 mM concentration) decreases palmitate-induced ER stress *in vitro* (64). Studies by Dickhout et al. further demonstrated the efficacy of 4-

PBA *in vitro* as well as *in vivo* to prevent tunicamycin-induced acute kidney injury through downregulation of CHOP expression (63). In the above study, 4-PBA was used at 1 mM concentration *in vitro* and at the dose of 1 g/kg/day *in vivo* (63).

1.3.2 Inducers of Chaperone Activity

1.3.2.1 Lithium

Lithium, a drug that is well known for its mood-stabilizing properties, has been recently shown to possess activity against ER stress (65). Lithium was demonstrated to increase the expression of GRP78 and decrease the rate of Ca^{2+} efflux from the ER (65). In addition, lithium was also shown to decrease the pro-apoptotic factors in neuroblastoma cells by inhibiting the activity of glycogen synthase kinase-3 (GSK-3), which activates caspases during ER stress (65).

1.3.2.2 Valproate

Valproate is one of the most widely used anticonvulsant drugs (66). Similar to lithium, it was also shown to ameliorate ER stress through the inhibition of GSK-3 activity (66). In addition, evidences also suggest that valproate decreases the activity of caspase-3 mediated apoptosis in ER stress (66).

1.3.2.3 BiP/GRP78 inducer X (1-(3,4-dihydroxyphenyl)-2-thiocyanate-ethanone) (BIX)

BIX is an inducer for the cytoprotective ER sensor protein BiP/GRP78, which binds to Ca^{2+} and inhibits cell death caused by ER stress (67, 68). BIX was shown to decrease tunicamycin-induced cell death in mouse retinal ganglion cells (68).

1.3.3 Benzodiazepinones

Benzodiazepinones were first discovered in the 1950s. A study conducted by Kim et al. (2009) demonstrated the ability of these compounds to inhibit ASK1 via phosphorylation of its serine-967 residue, and thus prevent the activation of JNK and p38 MAPK (69).

1.3.4 Inhibitors of eIF2-alpha phosphatase

Salubrinal is reported to be the most commonly used inhibitor of ER stress (70). It is a selective inhibitor of dephosphorylation of eIF2α (70). While guanabenz, an α2-adrenergic receptor agonist, was found to disturb PPPP1R15A-PP1c complex thereby it also inhibits dephosphorylation of eIF2α and prevents protein synthesis during ER stress (71).

1.3.5 Others

Agents that act as antioxidants (BHA, TM2002, baicalein), inducers of antioxidant pathways (Carnosic acid, Triterpenoids), and stress kinase inhibitors (JNK, p38 MAPK inhibitors) have also been reported to ameliorate ER stress (57).

1.4   Pepper as a spice

Black pepper is considered as the king of spices as it is the most widely used spice in the world. It was reported that black pepper contains 4.9 to 7.7% of piperine ($C_{17}H_{19}O_3N$), its active constituent, and the rest of which is composed of essential oils mainly monoterpenes and sesquiterpenes (1.0 to 1.8%), protein (10.9 to 12.7%), fiber (9.7 to 17.2%), water (9.5 to 12%), starch (25.8 to 44.8%), and ash (3.4 to 6%).

1.4.1 Piperine

Natural products have served as a valuable source of drugs, and are considered as potential leads for drug development (72). Since ancient times, spices were used as natural food additives for their multiple medicinal properties. Apart from its use as a condiment, black pepper (*Piper nigrum*) is commonly used in conventional medicine especially in Chinese and Indian medicine to treat several ailments (72, 73). The medicinal properties of black pepper are mainly attributed to its major phytoconstituent piperine.

Piperine [1-[5-[1,3-benzodioxol-5-yl]-1-oxo-2,4-pentadienyl] piperidine] **(1)** is one of the four diastereomeric geometric isomers isolated from black pepper (74). Chemically, it is an amide alkaloid and a trans-trans isomer of 1-piperoylpiperidine. It is also found in *Piper longum* plants (75), which belongs to the family *Piperaceae* (75).
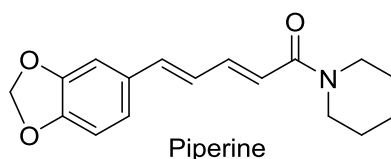
Piperine

Figure 1.3: Chemical structure of Piperine [1-[5-[1,3-benzodioxol-5-yl]-1-oxo-2,4-pentadienyl] piperidine] **(1)**

Historically, piperine has been used as a food additive and to treat several illnesses (76). Ancient Indian medicine has used piperine as a treatment for DM (75). Many recent studies have confirmed its medical properties, and further demonstrated its efficacy as anti-carcinogenic, hepatoprotective, anti-inflammatory, anti-arthritic, antidepressant and antimicrobial (75, 77).

The chemical structure of piperine is composed of three essential components: piperidine moiety linked through carbonylamide linkage to the side chain, methylenedioxyphenyl ring and conjugated double bond chain (Figure 1.3) (78).

Several studies were conducted to evaluate the pharmacological potential of piperine. Ferreira et al. demonstrated that piperine exhibits leishmanicidal effects (at 50-µM concentration), and inhibits promastigote growth by 96% (79). In the same study, its metabolite piperic acid was also screened, and it was found to be 9 times less active than piperine (79). In another study, topical application of piperine and its cyclohexylamino analog for 4 weeks was found to stimulate the development of even skin pigmentation (80). These findings provide evidence that piperine and its derivatives have the potential to treat vitiligo (80).

Tankamnerdthai et al. had reported that administration of piperine (at doses ranging from 5, 10 and 20 mg/kg, once daily for 4 weeks) in rats is associated with anti-depressant and cognitive enhancement properties (81). It is important to note that the effects observed with piperine were similar to that of the well-known antidepressants such as fluoxetine and donepezil hydrochloride (81).

A study by Koul et al. introduced changes to the phenyl nucleus, side chain and basic moiety of piperine to prepare diethylamino- and pyrrolidinyl analogs and compared the ability of piperine and its analogs to inhibit the activity of both constitutive and inducible cytochrome P450 (CYP) (82). Findings from the study confirmed that the CYP inhibition caused by piperine is similar to that of its diethylamino- analog (82). However, the CYP inhibitory potential was completely lost when the piperidine nucleus is replaced by pyrrolidinyl moiety (82).

1.4.2 Piperine as a Putative Agent to relieve ER Stress

Although numerous studies have documented the anti-cancer properties of piperine in various types of cancer (83-86), the precise mechanisms by which piperine exerts its anti-cancer effects are still unclear (83). A study by Yaffe et al. attempted to investigate the mechanisms by which piperine mediates cell cycle arrest and apoptosis in colon cancer (83). This study revealed that piperine-induced apoptosis in colon cancer cells is mediated through increased expression of CHOP and GRP78 (83). This was the first study to show that piperine modulates ER stress response.

Paradoxical to the findings by Yaffe et al. (83), a study using a high fat diet (HFD)-induced model of hepatic steatosis indicated that piperine decreases the mRNA expression of GRP78 in the liver tissues of mice fed an HFD (87). Moreover, the use of piperine was also associated with a significant decrease in the expression of the phosphorylated JNK and eIF2α (87). These findings suggest the putative role of piperine as a chemical chaperone to relieve high-fat diet induced ER stress in the liver. However, the effect of piperine on ER stress in kidney has not yet been studied. Furthermore, based on the previously reported activities of its amide piperine analogs, piperine and its analogs have different activities towards different diseases. However, none of those studies were targeted to elucidate the impact of piperine and its analogs on ER stress markers in kidney cells.

2. Objectives of the Study

Since the establishment of ER stress in organ pathologies, the search for new agents that decrease or prevent ER stress has become an active area for research. Unlike most other natural compounds, piperine exhibits very low cytotoxicity but still possess multiple pharmacological properties (82), which make it a promising pharmacophore to develop lead compounds. Hence, the goal of this study is to elucidate whether structural modifications in the parent molecule piperine would result in a lead compound with higher potency and efficacy to that of piperine. We investigated the effect of structural modifications to piperine on relieving ER stress induced by tunicamycin in renal cells *in vitro*.

Objective 1: To synthesize a variety of piperine analogs.

Objective 2: To characterize the prepared analogs using melting point, LC/MS, GC/MS, FT-IR and NMR.

Objective 3: To establish an *in vitro* model of ER stress-induced cell injury using tunicamycin in normal rat kidney (NRK-52E) cells.

Objective 4: To evaluate the tolerability of NRK-52E cells to the prepared analogs (using MTT assay).

Objective 5: To investigate the pharmacological activity of the prepared compounds to relieve ER stress in the established *in vitro* model.

3. Experimental Methods

3.1 Synthesis of Piperine Analogs

Piperine, silica gel 60 F254 and all solvents used were purchased from Sigma-Aldrich, Germany. All reactions were monitored by thin layer chromatography (TLC) and the spots were visualized using ultraviolet (UV) transilluminator. Thin layer chromatography (TLC) was conducted on pre-coated silica gel aluminum plates (Merck, USA). Melting points of the synthesized compounds were measured as range using Stuart SMP40 automatic melting point apparatus. The infrared (IR) spectra were recorded on Perkin Elmer Spotlight 400 Fourier transform infrared (FTIR) spectrophotometer. The spectra were acquired using a universal attenuated total reflectance sensor (FTIR-UATR) to allow the application of the solid samples.

All of the prepared compounds were analyzed for C, H and N (elemental analysis) using Thermo Scientific Flash 2000 in the Central Laboratory Unit, Qatar University. Mass spectra (MS) were recorded on an Agilent 6460 Triple Quadrupole LC/MS system using electrospray ionization (ESI) by direct injection technique and reported as $[M+1]^+$. Proton (^1H) and carbon (^{13}C) NMR spectra were recorded using Bruker Avance III 400 MHz apparatus, and the chemical shifts were expressed in δ (ppm) with reference to DMSO-d6 peak.

3.1.1 Synthesis of Piperic Acid from Piperine

Piperine (2 g, 7 mmol) was refluxed with 100 mL of 2 M ethanolic potassium hydroxide for 25 hours, and the ethanol was removed by evaporation under reduced pressure.

Completion of reaction was monitored by thin-layer chromatography (TLC). The separated solid (potassium piperate) was filtered and washed with cold ethanol, and then dissolved in warm water and gradually acidified with diluted HCl. The obtained yellow precipitate (piperic acid) was filtered and washed with cold water. The crude product (**2**) was recrystallized from ethanol to yield 1.4 g (6.4 mmol) of yellow crystalline piperic acid (90% yield).

3.1.2 Synthesis of Amide Piperine Analogs

To a solution of piperic acid (10 mmol) in 25 mL dichloromethane (DCM), 2.0 mL (27.6 mmol) of thionyl chloride was added. The mixture was kept under reflux for 1 hour. Excess thionyl chloride was removed under reduced pressure using rotary evaporator. The obtained residue (piperoyl chloride) was dissolved in 20 mL DCM and the amine (10 mmol) or alcohol (10 mmol) in 20 mL DCM was added drop-wise. The mixture was stirred for 1 hour at room temperature. The solvent was evaporated and the residue was crystallized from ethyl acetate. The yield of the final products (**3** to **6**) was in the range of 40-65%.

3.2 Pharmacological Screening

3.2.1 Materials

NRK-52E (rat renal proximal tubular cell line) was purchased from Health Protection Agency, UK. BCA protein assay reagent was obtained from Pierce, UK. Dimethyl sulfoxide, Piperine, Thiazolyl blue tetrazolium bromide (MTT) and Tunicamycin were

purchased from Sigma-Aldrich. Dulbecco's modified Eagle medium (DMEM), Fetal bovine serum (FBS), L-Glutamine, Penicillin-streptomycin (pen-strep) and phosphate-buffered saline (PBS) were purchased from Life technologies. All primary and secondary antibodies were purchased from Abcam, UK except for CHOP (GADD153) primary antibody, which was obtained from Santa Cruz Biotechnology, Germany.

3.2.2 Preparation of Stock Solutions of Tunicamycin, MTT, Piperine and Its Analogs

Tunicamycin (5 mg) was dissolved in 1 mL of DMSO to prepare a 5-mg/mL stock solution. All stock solutions were stored at 4 ^{0}C. Working solutions of tunicamycin were freshly prepared before each experiment. MTT stock solution was prepared by dissolving 0.02 g of MTT reagent in 4 mL of DMSO. 100 μM stock solutions of piperine and its analogs were prepared by dissolving the powder in DMSO.

3.2.3 Cell Culture

NRK-52E cells were maintained in DMEM (1X) with 10% FBS and 1% Penicillin/Streptomycin and 1% L-Glutamine 200 mM (Complete cell culture media). Cells were grown in 100-mm tissue culture dish and kept in a 5% CO_2 humidified incubator at 37 ^{0}C. Once 90% confluency was reached, cells were split in 1:5 to 1:7. For splitting cells, the monolayer was washed with 5 mL of PBS and cells were detached using 1 mL of 0.25% trypsin-EDTA (1X) and plated into a new 100-mm dish containing 10 mL of fresh complete cell culture media.

3.2.4 Cell Treatments

Every trial followed the same three-day routine as shown in Figure 3.1. In brief, 24 hours after seeding the cells, the analogs were added to cells at either 250 nM or 500 nM concentrations for 24 hours. After 24 hours of pre-treatment, the old media was removed and the cells were washed with PBS and another fresh media containing 0.5 μg/mL tunicamycin was added and cells were incubated for 2 hours. After the completion of tunicamycin treatment, the media was removed and cells were washed twice with PBS and new fresh complete media was added for another 22 hours.
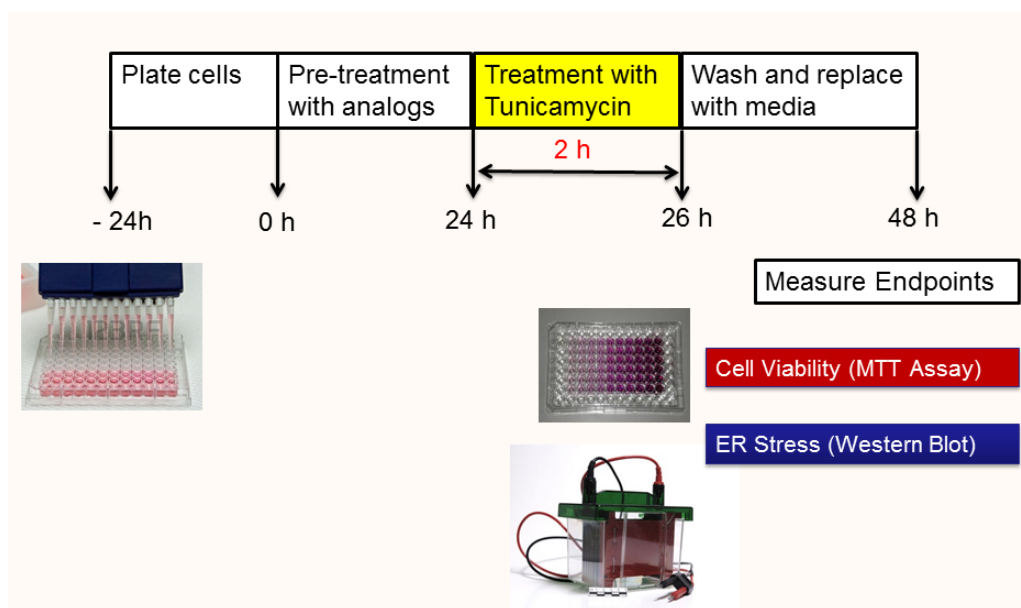

Figure 3.1: Experimental Design for the *In Vitro* Model of Tunicamycin-induced ER Stress using NRK-52E cells.

3.2.5 Cell Viability and Tolerability Studies using MTT Assay

NRK cells were seeded in 48-well plates and incubated at 37 ^{0}C for 24 hours (day-0). After 24 hours of seeding, cells were treated with different concentrations of tunicamycin (0.25, 0.5, 1.0 and 2 μg/mL) for 15 minutes, 2 hours and 24 hours. After the completion of tunicamycin treatment, the cells were washed with PBS and 250 μL of complete media was added to each well and incubated for 24 hours at 37 ^{0}C. After 24 hours, the media was removed and replaced with fresh media containing 25 μL MTT (0.5 mg/mL) for 3-4 hours. Next, the media was removed carefully and 100 μL of DMSO was added to dissolve the formazan crystals. The cell viability in the developed *in vitro* model was assessed by MTT assay, which is based on the enzymatic conversion of yellow tetrazolium salt 3-(4,5-dimethylthiazol-2-yl)-2,5-diphenyltetrazolium bromide by mitochondrial dehydrogenases into purple formazan. The absorbance was read at 570 nm using SpectraMax M2 multimode plate reader (Molecular Devices, USA).

3.2.6 Quantification of Expression of ER Stress Markers

3.2.6.1   *Preparation of Cell Lysates*

NRK-52E cells were seeded in 6-well plates at a seed density of 150,000 cells per well for 24 hours. Then tunicamycin was added to cells at various concentrations at different time points. After the treatment period, cells were washed with PBS and the media was replaced with complete media for the rest of 24 hours. Thereafter, cells were washed with 2 mL PBS twice and about 60 to 70 μL lysis buffer (0.5 M Tris pH 6.8 and 20% SDS) was added. The cells were scraped; the cell lysate was collected and sonicated for

10 to 15 seconds. The cell lysates were centrifuged at 16,000 x g for 15 minutes at 4 ^{0}C. The supernatant was collected and stored at -20 ^{0}C until use.

3.2.6.2   Protein Assay

The frozen cell lysates were thawed and kept on ice. The samples were then centrifuged at 10,000 x g for 5 minutes at 4 ^{0}C. The protein concentrations were determined using Bicinchoninic acid (BCA) protein assay kit (Pierce, USA). The samples were incubated at 37 ^{0}C for 30 minutes, and then, their absorbance was recorded at 562 nm using SpectraMax M2 multimode plate reader (Molecular Devices, USA).

3.2.6.3   Western blotting

Proteins were separated using SDS-PAGE with an acrylamide concentration 15%. Equal concentrations (25 μg) of sample protein was mixed with 4X sample buffer and electrophoresed for 20 minutes at 70 volts followed by 90 minutes at 140 volts (BioRad, USA). Following gel electrophoresis the proteins were transferred to a PVDF membrane at 100 volts for 90 minutes. The membrane was then removed and blocked with 5% milk for 1 hour at room temperature. Next, the membrane was incubated overnight at 4 ^{0}C with the primary antibody for GRP78 or CHOP at the concentrations shown in Table 3.1. The PVDF membrane was then washed 3 times with tris-buffered saline containing 0.1% tween 20 (TBST) at 10 minutes intervals. The membrane was then incubated with an HRP-conjugated goat-anti-rabbit IgG secondary antibody for 1 hour at room temperature. The membrane was washed again with TBST for 3 times at 10 minutes

interval. Bands were visualized using enhanced chemiluminesence (ECL) detection kit (Abcam, UK) and quantified using a FC-2 imaging system (Protein Simple, USA).

Table 3.1: Antibodies used for Western Blotting

Primary Antibody	Dilution	Molecular Weight (kD)	Supplier	Catalog #
GRP78	1:1,000	78	Abcam, UK	ab21685
CHOP	1:500	30	Santa-Cruz Biotech, Germany	sc-793

4. Results

4.1 Synthesis and Characterization

4.1.1 Chemical Synthesis

The prepared compounds 3 to 6 (shown in Table 4.1) were obtained by alkaline hydrolysis of piperine (**1**, the starting material) to the intermediate compound piperic acid (**2**). The obtained piperic acid was activated to its acid chloride (i.e., piperoyl chloride) by thionyl chloride as described by Koul et al. and Qazi et al. (78, 88). The obtained acid chloride served as the key intermediate in the preparation of the proposed compounds as it was reacted with different amines and alcohols as shown in the Table 4.1. The proposed scheme for the preparation of the compounds 2 to 6 is shown in Figure 4.1.
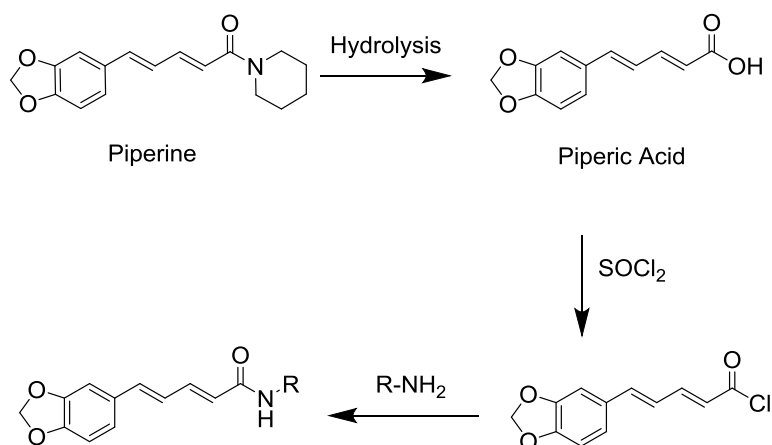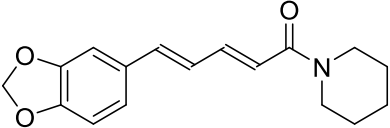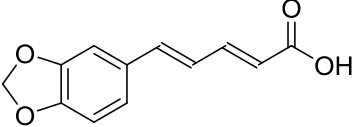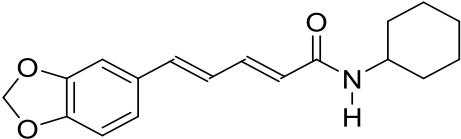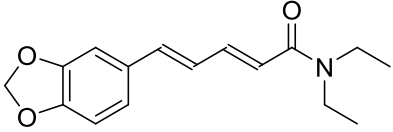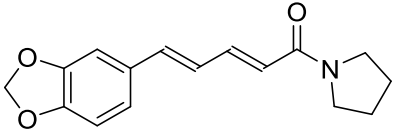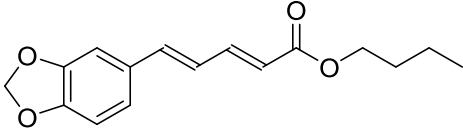

Figure 4.1: Scheme for synthesis of amide piperine analogs

Table 4.1: Physical properties and molecular formulae for of the synthesized compounds analogs and the parent compound piperine.

Name and Chemical Structure	Melting point	Molecular Formulae	MW
Piperine [(2*E*,4*E*)-5-(benzo[*d*][1,3]dioxol-5-yl)-1-(piperidin-1-yl)penta-2,4-dien-1-one] **(1)**	128-131°C (89)	$C_{17}H_{19}NO_3$	285.14
Piperic Acid [(2*E*,4*E*)-5-(benzo[*d*][1,3]dioxol-5-yl)penta-2,4-dienoic acid] **(2)**	220-224°C	$C_{12}H_{10}O_4$	218.06
Cyclohexylamino Analog [(2*E*,4*E*)-5-(benzo[*d*][1,3]dioxol-5-yl)-*N*-cyclohexylpenta-2,4-dienamide] **(3)**	202-205°C	$C_{18}H_{21}NO_3$	299.15

Diethylamino Analog [(2*E*,4*E*)-5-(benzo[*d*][1,3]dioxol-5-yl)-*N*,*N*-diethylpenta-2,4-dienamide] **(4)**	94-98°C	$C_{16}H_{19}NO_3$	273.14
Pyrrolidinyl Analog [(2*E*,4*E*)-5-(benzo[*d*][1,3]dioxol-5-yl)-1-(pyrrolidin-1-yl)penta-2,4-dien-1-one] **(5)**	143-146°C	$C_{16}H_{17}NO_3$	271.12
Butyl ester Analog [butyl (2*E*,4*E*)-5-(benzo[*d*][1,3]dioxol-5-yl)penta-2,4-dienoate] **(6)**	NA	$C_{16}H_{18}O_4$	274.12

4.1.2 Spectroscopic Investigations

4.1.2.1 Diethylamino Analog [(2E,4E)-5-(benzo[d][1,3]dioxol-5-yl)-N,N-diethylpenta-2,4-dienamide] (4)
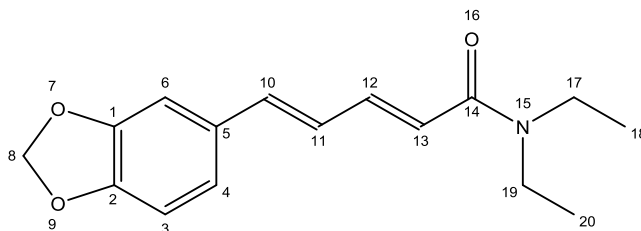
(2*E*,4*E*)-5-(benzo[*d*][1,3]dioxol-5-yl)-*N*,*N*-diethylpenta-2,4-dienamide
Chemical Formula: $C_{16}H_{19}NO_3$
Molecular Weight: 273.33
Elemental Analysis: C, 70.31; H, 7.01; N, 5.12; O, 17.56

All data obtained for the piperine analogs were consistent with those previously reported in the literature (78, 90). For example, **4** was prepared from **2** and N, N-diethylamine as described in section 3.1.2.   The mass spectrum of **4** (Figure 4.2) showed $[M+1]^+$ appearing at m/z 274. This value confirmed the molecular weight of the prepared **4**, which was calculated to be 273. Elemental analysis for $C_{16}H_{19}NO_3$ found C, 70.02, H, 7.04, N, 5.03%; calculated C, 70.31, H, 7.01, N, 5.12%. IR (conducted on the solid sample using UATR) (Figure 4.3): 3164 (aromatic C-H str), 2970 (aliphatic C-H str), 1637 (carbonyl group), 1596, 1503 (C=C str) cm^{-1}. Figure 4.4 shows ^1H NMR spectrum in DMSO-d6. ^1H NMR: δ 1.05 and 1.13 (3H each, t, $J = 6.8$ Hz, 2× CH$_2$C*H$_3$*), 3.37 (4H, m, 2× –C*H$_2$*CH$_3$), 6.04 (2H, s, –OC*H$_2$*O–), 6.55 (1H, d, $J = 14.50$ Hz, –CH=C*H*CO), 6.75–7.1 (5H, m, olefinic and Ar-*H*), 7.21 (1H, dd, $J = 14.8, 3.9$ Hz, –C*H*=CHCO). ^{13}C NMR: δ 165.69, 148.37, 148.17, 109.86, 121.48, 131.37, 106.06, 101.58, 137.99, 126.28, 142.10, 123.15, 165.69, 42.24, 15.66, 13.32 (Figure 4.5). The ^{13}C spectrum

confirms the presence of 16 carbons, of which 4 of them were corresponding to the diethylamino analog as shown in the Figure 4.5 (88).

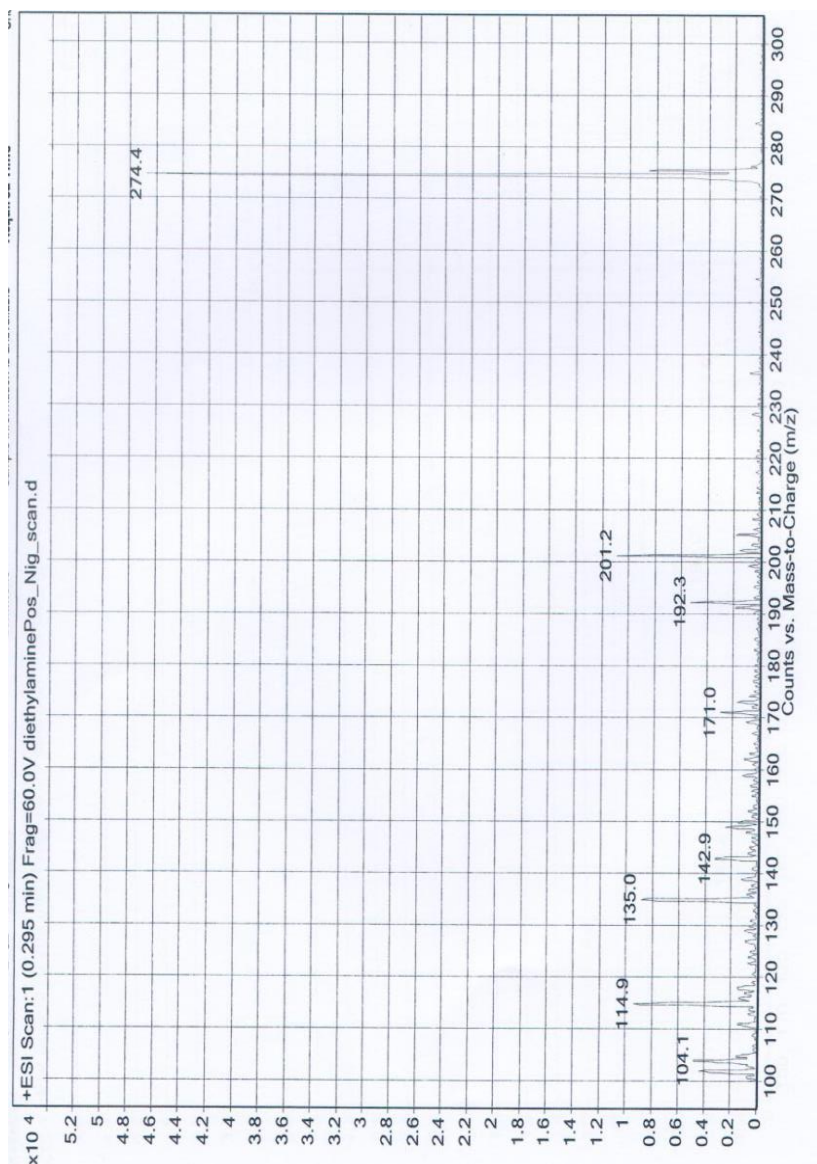**Figure 4.2:** The mass spectrum of **4** was recorded on an Agilent 6460 Triple Quadrupole LC/MS system using electrospray ionization (ESI) by direct injection technique and reported as $[M+1]^+$.
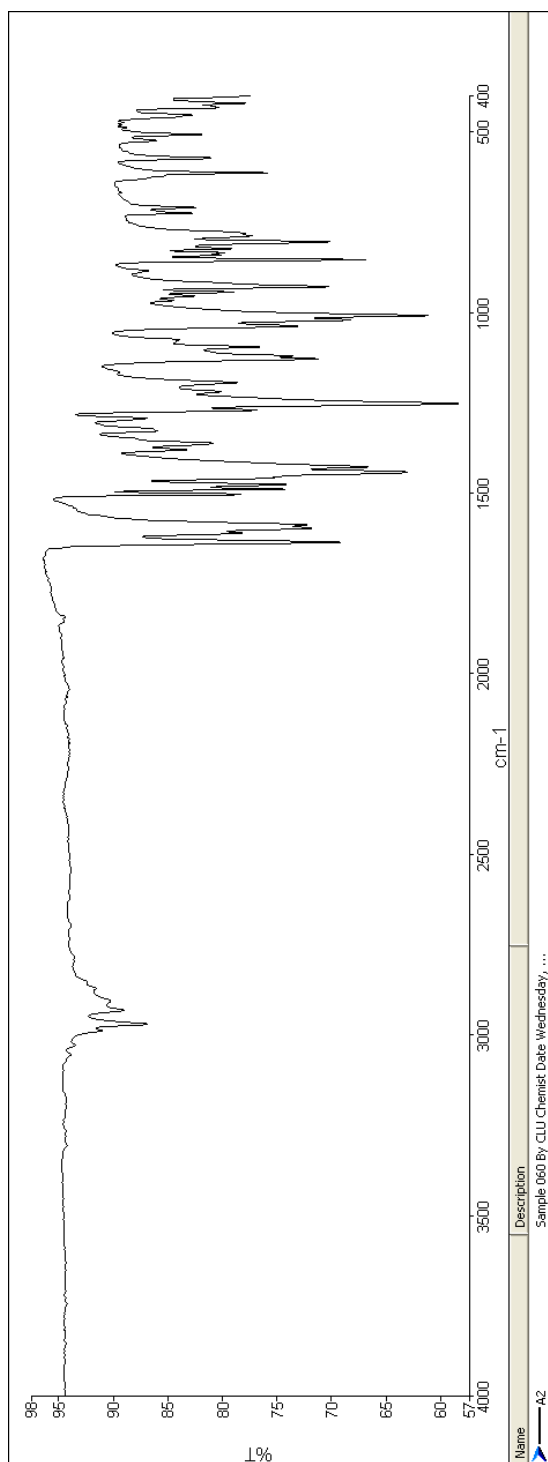
Figure 4.3: FTIR spectrum of **4** conducted on the solid sample using UATR.
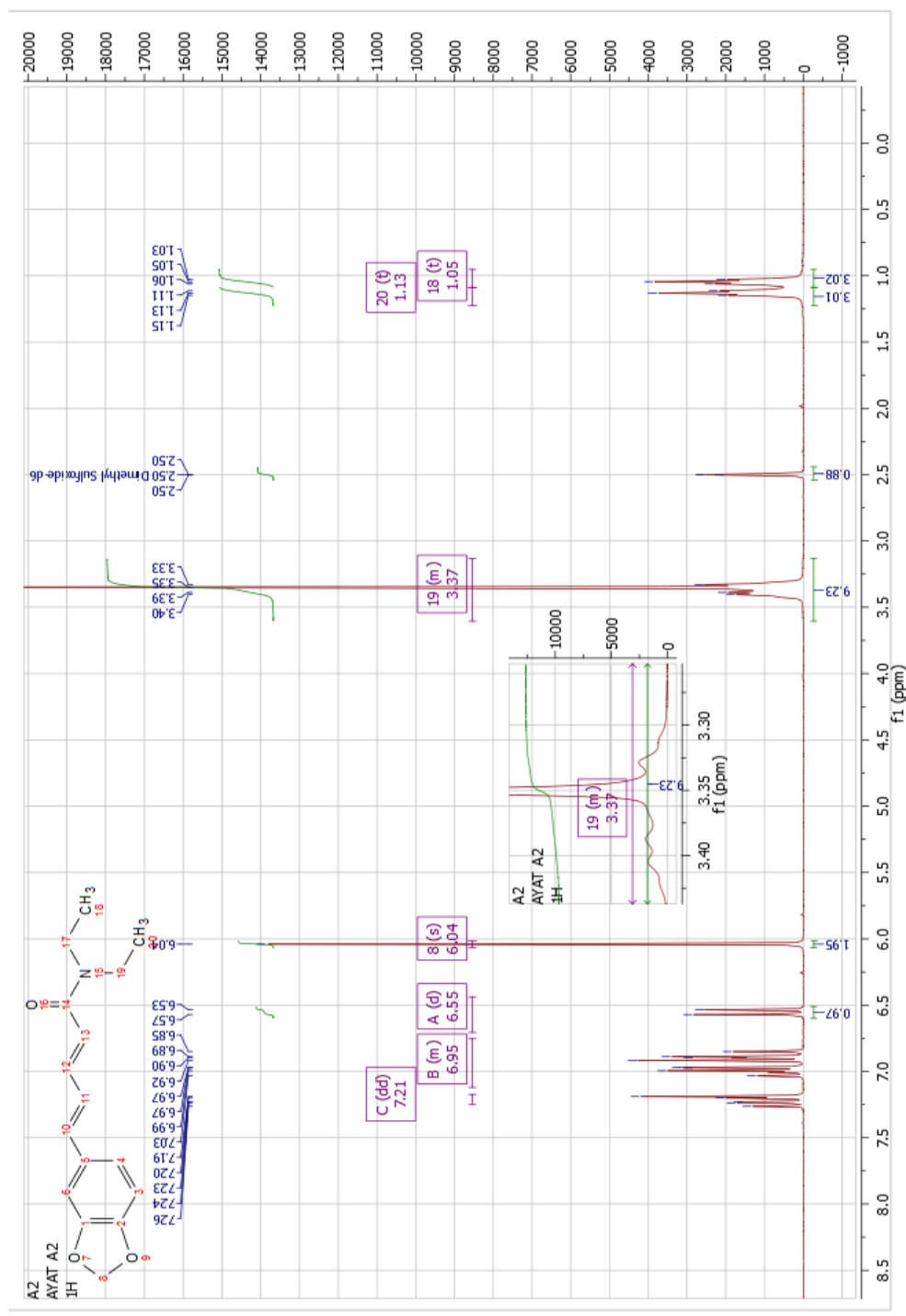
Figure 4.4: ^{1}H NMR spectrum of **4** in DMSO-d6.
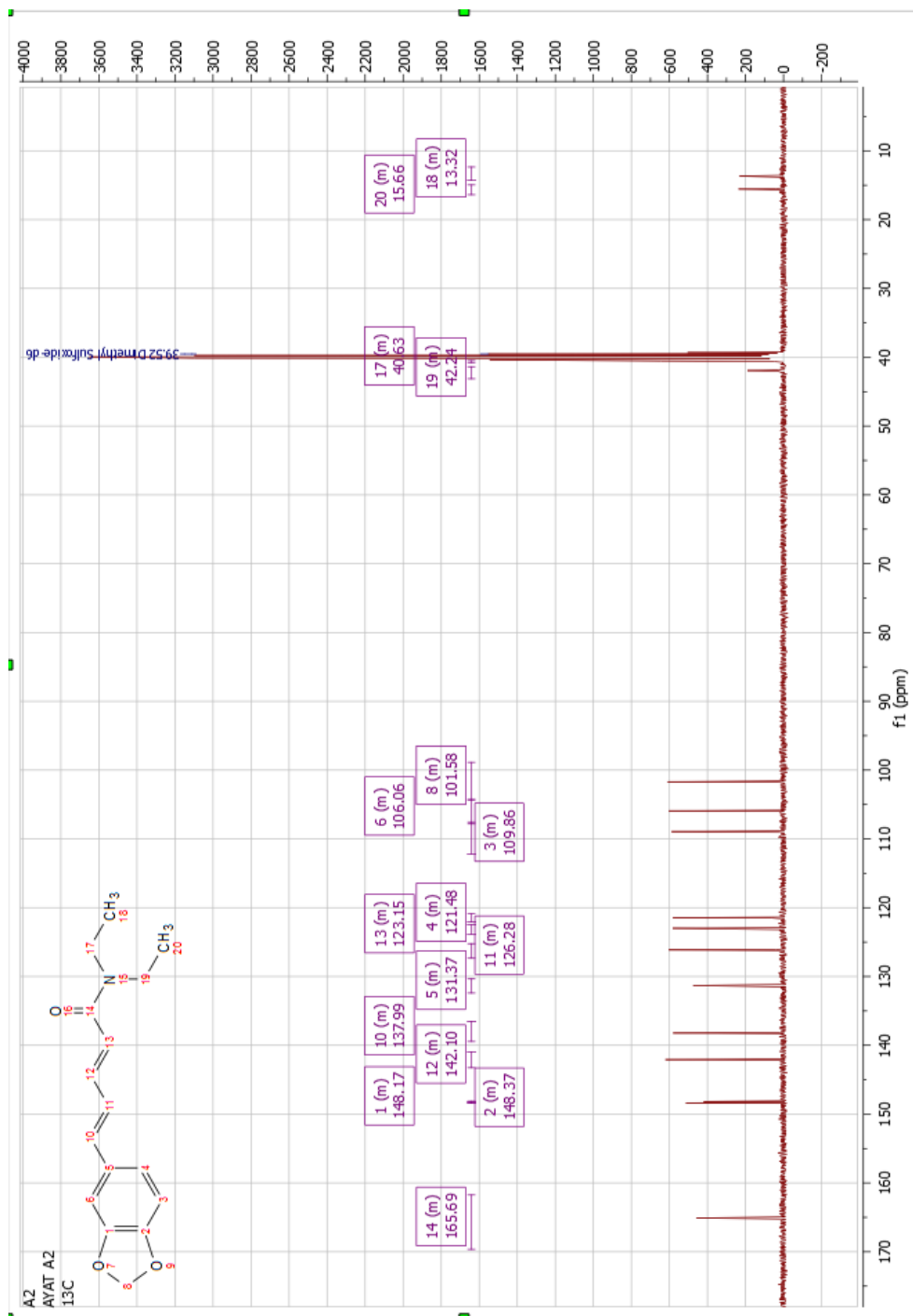
Figure 4.5: ¹³C NMR spectrum of **4** in DMSO-d6

4.2   Pharmacological Screening

4.2.1 *In vitro* model of Tunicamycin-induced ER stress and cell injury

4.2.1.1   *Cell Viability (MTT Assay)*

Several agents such as tunicamycin, thapsigargin, dithiothreitol (DTT) and palmitate are commonly used to induce ER stress in cells (51). The choice of tunicamycin as an ER stress inducer for our study using normal rat kidney (NRK-52E) cells was based on a previous study, which indicated that tunicamycin acts as a strong inducer of ER stress in comparison to other chemical inducers such as thapsigargin and DTT in NRK-52E cells (35).

Different concentrations at various time points were tested to identify an optimal model of ER stress using tunicamycin in normal rat kidney (NRK-52E) cells. Although several studies have utilized 24-hour exposure to tunicamycin (TM) to induce ER stress, in our pilot studies, we found that treatment with tunicamycin results in a dose-dependent and time-dependent loss of cell viability (measured by MTT assay) in NRK-52E cells, and it is evident even with 15 minutes exposure time.

As seen in the Figure 4.6, incubation of subconfluent cultures of NRK-52E cells with 0.5 μg/mL and 1 μg/mL of tunicamycin for 15 minutes and 2 hours resulted in significant loss of cell viability. Nevertheless, the induction of ER stress markers GRP78 and CHOP were prominent only at 2 hours of tunicamycin treatment (Figure 4.7). Thus,

we chose 0.5 µg/mL tunicamycin and 2 hours exposure time for our study and examined the effect of piperine and its analogs against tunicamycin-induced ER stress and cell death.
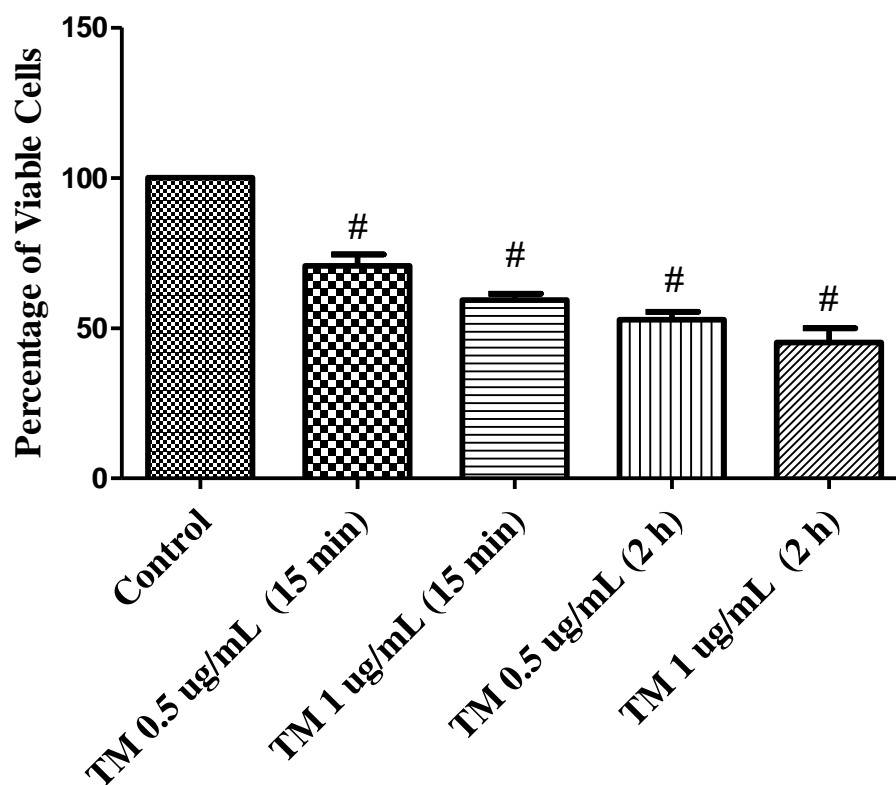

Figure 4.5: Dose-response studies with Tunicamycin (TM) in NRK-52E cells. Cell viability was determined by MTT assay, and values were expressed as percentage of control (Mean ± SEM; n=3). #$P < 0.05$ compared to control group.

4.2.1.2 Expression of ER Stress markers (Western Blotting)

4.2.1.2.1 GRP78

Induction of the ER chaperone GRP78 is considered as a hallmark of ER stress. In our study, TM treatment (0.5 µg/mL for 2 h) resulted in a robust increase in the expression of GRP78 compared to the control as shown in Figure 4.7.

Previous studies have shown the ability of TM to induce the expression of GRP78, which serves to improve the folding capacity of protein (63, 91). In the current study, we confirmed the ability of TM to induce GRP78 expression even with acute exposure and at concentrations as low as 0.5 µg/mL. To our knowledge, this is the first study to adopt an acute low-dose TM treatment in NRK-52E cells. We believe our findings would open the floor for further research on the signaling pathways that mediate acute TM-mediated ER stress in renal cells.

4.2.1.2.2 CHOP

CHOP is a ubiquitously expressed protein at low level in normal conditions, and several studies have documented its induction under conditions of ER stress (92, 93). TM is also known to be a strong inducer of CHOP (63, 93). Thus, to further investigate the involvement of other proteins involved in TM-induced ER stress, we examined the expression of this pro-apoptotic transcriptional regulator of ER stress.

As presented in the Figure 4.7, the expression of CHOP was significantly elevated in cells exposed to 0.5 µg/mL TM for 2 hours. Further, the elevated levels of CHOP level

suggest the involvement of PERK arm of the unfolded protein response in our model. Hence, future studies to investigate the upstream markers of PERK pathway such as eIF2α, ATF4 and PERK, would offer insights on the primary mediator involved in the induction of CHOP in this model.

In summary, exposure of NRK-52E cells to 0.5 μg/mL TM for 2 hours resulted in a significant decrease in cell viability (~50%) as shown in Figure 4.6, and a robust induction of GRP78 and CHOP proteins as shown in Figure 4.7.
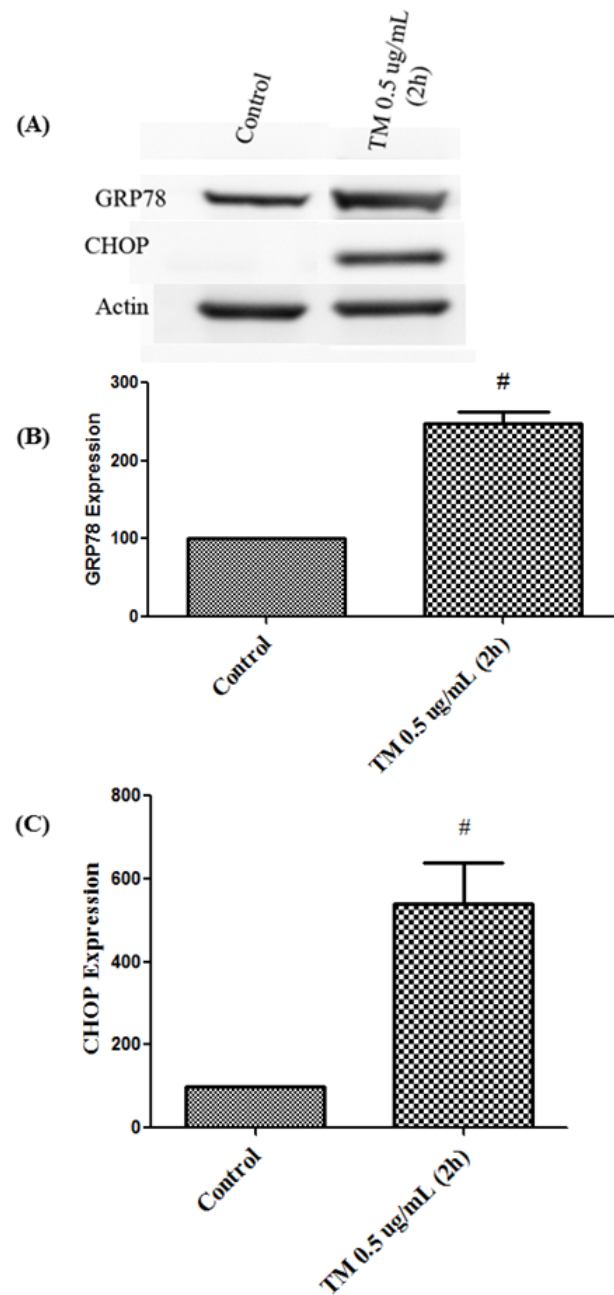
Figure 4.6: Effect of tunicamycin (TM) on GRP78 and CHOP expression in NRK-52E cells as determined by western blotting (A) and quantified using densitometry (B and C). Values were normalized using β-actin and expressed as percentage of control (Mean ± SEM; n=10). #$P < 0.05$ compared to control group.

4.3 Pharmacological Evaluation of Amide Piperine Analogs

4.3.1 Piperine (1)

4.3.1.1 Dose-Response Studies (Tolerability)

NRK-52E cells were treated with piperine at two different concentrations - 250 and 500 nM - for 24 hours and the control group received the highest vehicle concentration (0.1% DMSO) used in the study. Our results demonstrate that single doses of piperine of up to 500 nM were well tolerated by NRK-52E cells (Figure 4.8).
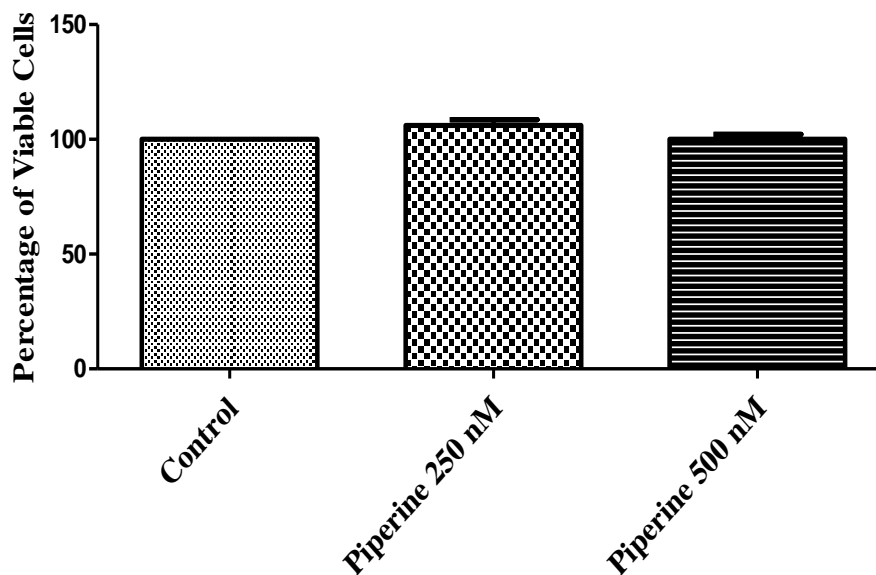
Figure 4.7: Tolerability of NRK-52E cells to Piperine **(1)** as measured by MTT assay. Values were expressed as percentage of control (Mean ± SEM; n=9).

4.3.1.2   *Effect on Cell Viability (MTT assay)*

NRK-52E cells were pre-treated with piperine for 24 hours and then exposed to tunicamycin (0.5 µg/ml for 2 h) as described in the experimental design (Figure 3.1). The effect of piperine on TM-induced loss of cell viability in NRK-52E cells was measured using MTT assay.

Results from MTT assay have demonstrated the ability of piperine to protect against TM-induced loss of viability in NRK-52E cells. As seen in Figure 4.9, piperine significantly improved the cell viability by about 13% at 250 nM concentration, and by about 8% at 500 nM concentration. Further studies are required to explain the decrease in cytoprotective efficacy observed with highest concentration (500 nM) of piperine used in the current study (Figure 4.9).
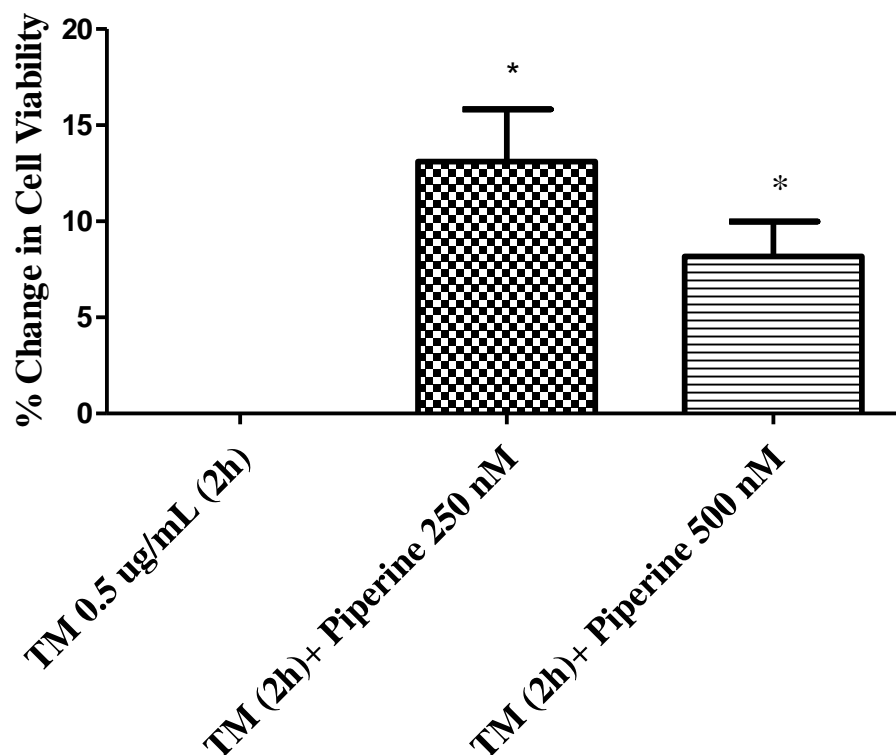
Figure 4.8: Effect of Piperine **(1)** on tunicamycin (TM)-induced loss of cell viability (measured by MTT assay) in NRK-52E cells. Values were normalized to TM-treated control and expressed as percentage change in cell viability (Mean $\pm$ SEM; n=3). *P < 0.05 compared to TM-treated group.

4.3.1.3 Expression of ER Stress Markers

To investigate the protective effect of piperine against TM-induced ER stress, NRK-52E cells were seeded on six-well plates and grown to sub-confluency were treated with piperine for 24 hours. After 24 hours treatment with piperine, cells were exposed to 0.5

μg/mL TM for 2 hours, and evaluated for the expression of GRP78 and CHOP at 24 hours post-tunicamycin exposure.

Consistent with the results from the *in vitro* model development (Figure 4.7), TM treatment for 2 hours induced a profound increase in the expression of GRP78 and CHOP in NRK-52E cells (Figure 4.10). Densitometry analysis showed decreased protein levels of GRP78 upon exposure to piperine at 250 nM and 500 nM for 24 hours (Figure 4.10B). Furthermore, pre-treatment of cells with piperine at 500 nM caused a statistically significant decrease in CHOP expression in cells exposed to TM (Figure 4.10C).

As expected, the protective effects of piperine against TM-induced upregulation of GRP78 and CHOP was dose-dependent, with the highest reduction in the levels of both protein markers observed at 500 nM concentration of piperine. Specifically, pre-treatment with 500 nM piperine has diminished the ability of TM to induce the expression of GRP78 by about 33%, and decreased the expression of CHOP by about 25% in comparison to TM-treated group (Figure 4.10).
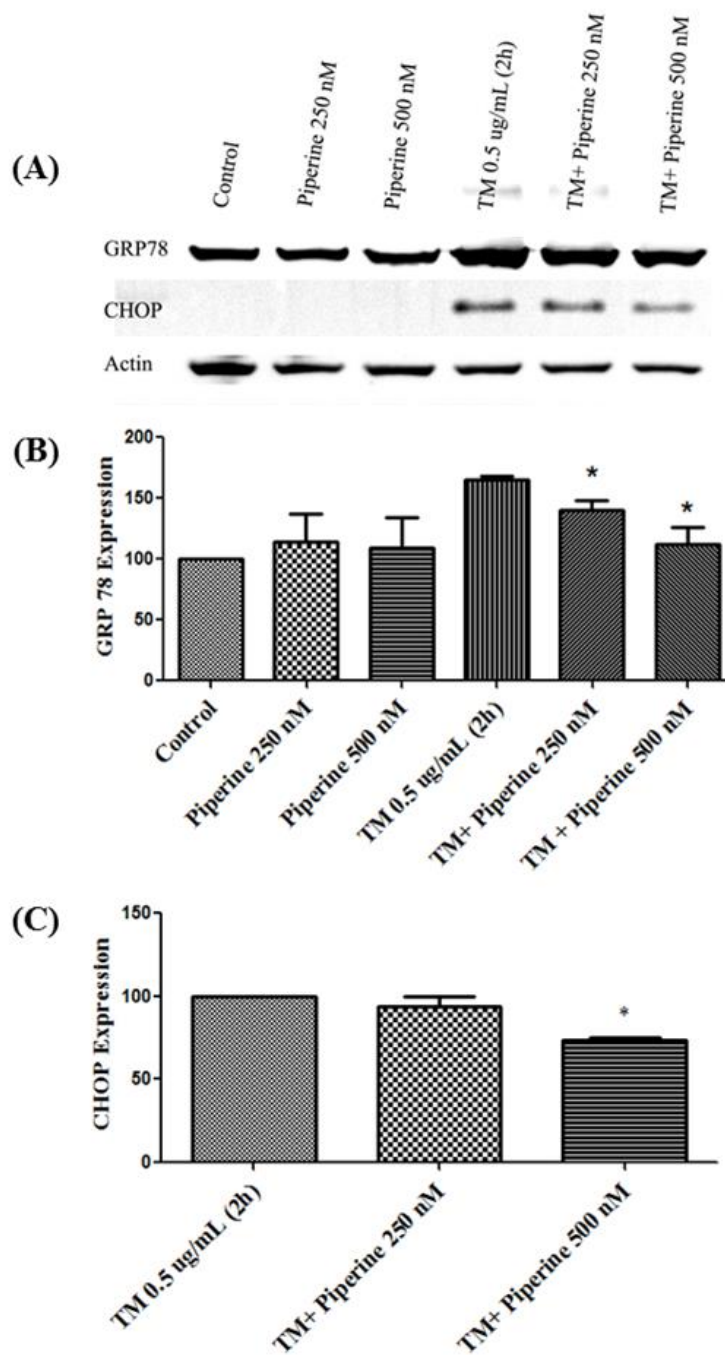
Figure 4.9: Effect of Piperine (**1**) on GRP78 and CHOP expression in NRK-52E cells as determined by western blotting (A) and quantified using densitometry (B and C). Values

were normalized to β-actin and expressed as percentage of control for GRP78 and percentage of tunicamycin (TM)-treated group for CHOP (Mean ± SEM; n=3). *P < 0.05 compared to TM-treated group.

4.3.2   4-PBA
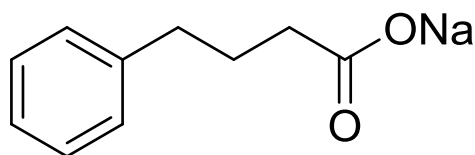
Figure 4.10: Chemical structure of Sodium 4-phenylbutyrate (4-PBA)

4.3.2.1   Dose-Response Studies (Tolerability)

4-phenylbutyrate (4-PBA) is a well-known chemical chaperone with clinical utility in urea cycle disorders (62). However, it is effective only when used at millimolar (mM) concentrations ranging from 1 to 10 mM. In this study, 4-PBA is used as a reference standard - at 1 mM and 2 mM concentrations (based on the literature) - to compare the efficacy of piperine and its analogs against TM-induced ER stress. As seen in Figure 4.12, 4-PBA was well tolerated by NRK-52E cells at concentration of 1 mM for 24 hours. However, at the highest concentration used (2 mM), it caused about 10% decrease (not statistically significant) in cell viability compared to control (Figure 4.12).
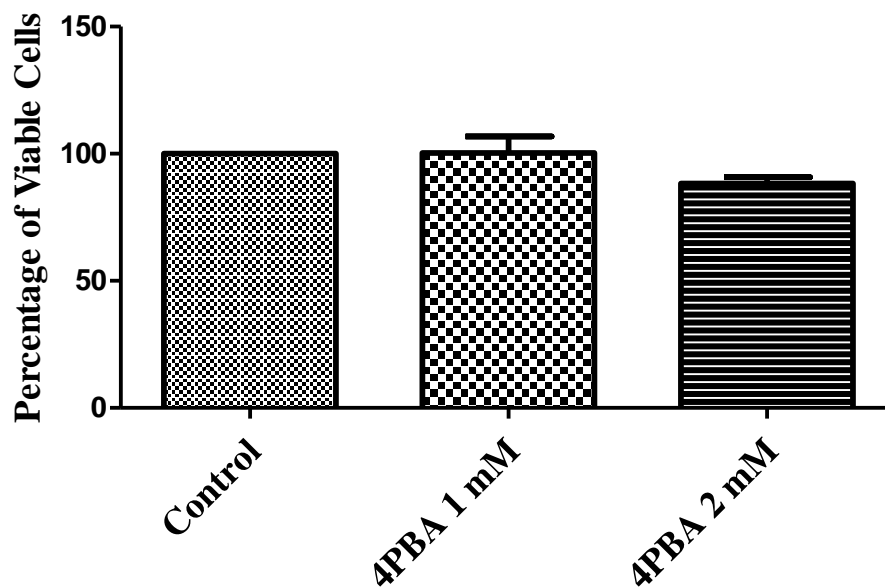
Figure 4.11: Tolerability of NRK-52E cells to 4-PBA as measured by MTT assay.

Values were expressed as percentage of control (Mean ± SEM; n=3).

4.3.2.2 Effect on Cell Viability (MTT assay)

As shown in the Figure 4.13, treatment with 4-PBA didn't have any impact on TM-induced loss of cell viability in NRK-52E cells.

Figure 4.12: Effect of 4-PBA on tunicamycin (TM)-induced loss of cell viability (measured by MTT assay) in NRK-52E cells. Values were expressed as percentage of control (Mean ± SEM; n=3).

4.3.2.3 Expression of ER Stress Markers

Given the fact that 4-PBA would protect against ER stress, we decided to investigate its effect on the protein expression of GRP78 and CHOP in NRK-52E cells exposed to TM. As demonstrated in Figure 4.14, 4-PBA decreased the expression of GRP78 (~15%), and CHOP (~70%) compared to TM-treated group. These results are in consistence with a previous *in vivo* study, which revealed that the principal mechanism behind the chaperone effects of 4-PBA is through repression of CHOP expression (63).

Figure 4.13: Effect of 4-PBA on GRP78 and CHOP in NRK-52E cells as determined by western blotting (A) and quantified using densitometry (B and C). Values were

normalized to β-actin and expressed as percentage of control for GRP78 and percentage of tunicamycin (TM)-treated group for CHOP (Mean ± SEM; n=3). *P < 0.05 compared to TM-treated group.

4.3.3 Piperic Acid (2)
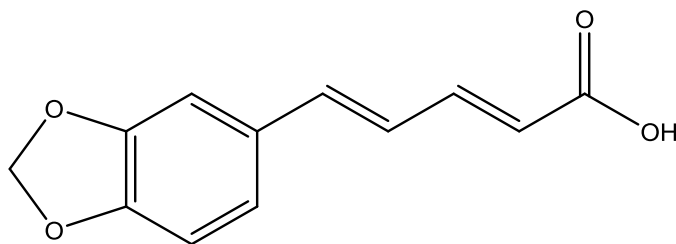
Figure 4.14: Chemical structure of piperic acid [(2*E*,4*E*)-5-(benzo[*d*][1,3]dioxol-5-yl)penta-2,4-dienoic acid] **(2)**

4.3.3.1 Dose-Response Studies (Tolerability)

Piperic acid was well tolerated by the NRK-52E cells at both concentrations (250 and 500 nM) used in the study (Figure 4.16).
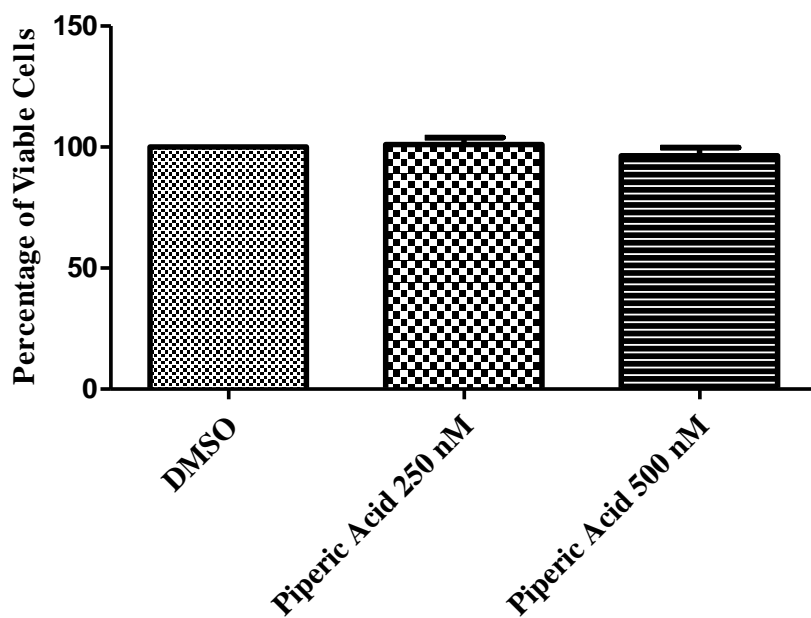
Figure 4.15: Tolerability of NRK-52E cells to Piperic acid (**2**) as measured by MTT assay. Values were expressed as percentage of control (Mean $\pm$ SEM; n=4).

4.3.3.2 Effect on Cell Viability (MTT assay)

Based on the results obtained from the MTT assay, it is clear that piperic acid lacks the ability to protect against TM-induced cell death (Figure 4.17). In fact, a decline in viability was observed in cells treated with 500 nM piperic acid.
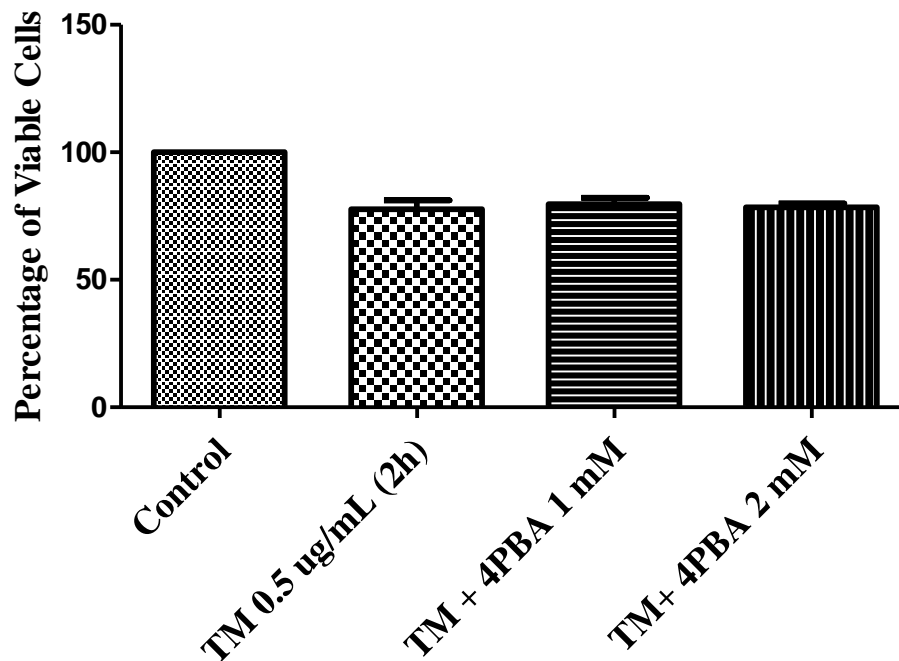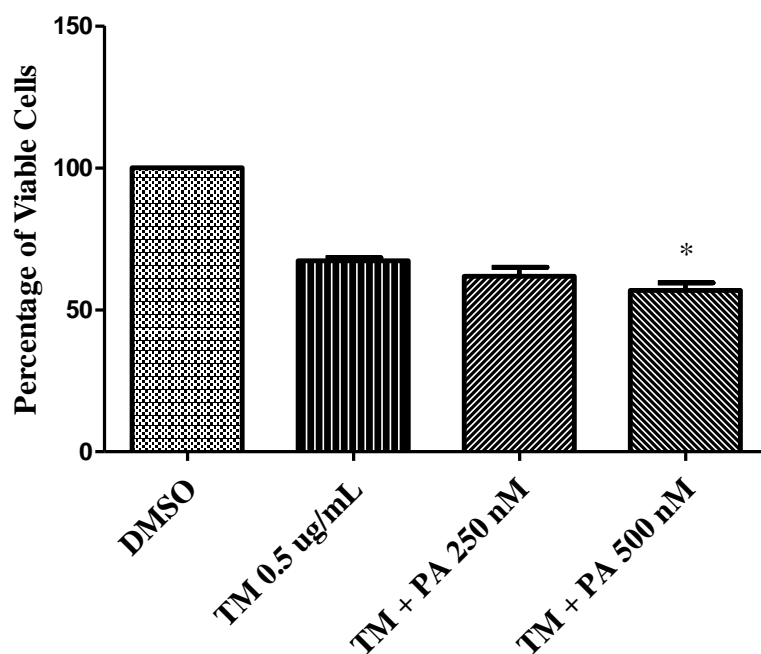

Figure 4.16: Effect of Piperic acid (**2**) on tunicamycin (TM)-induced loss of cell viability (measured by MTT assay) in NRK-52E cells. Values were expressed as percentage of control (Mean ± SEM; n=4). *P < 0.05 compared to TM-treated group.

4.3.3.3 Expression of ER Stress Markers

Further investigation on the levels of ER stress markers revealed that piperic acid does not affect the expression of GRP78 or CHOP (Figure 4.18).

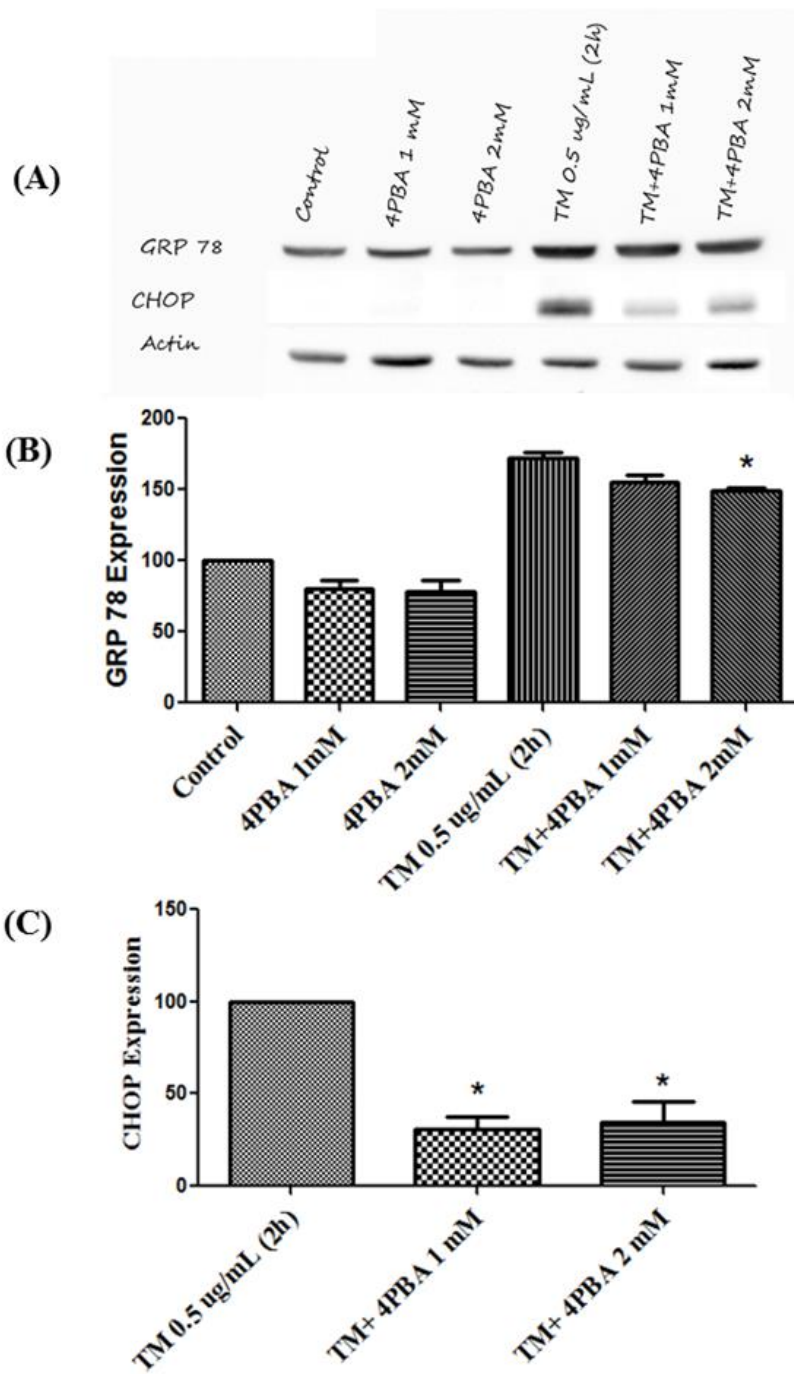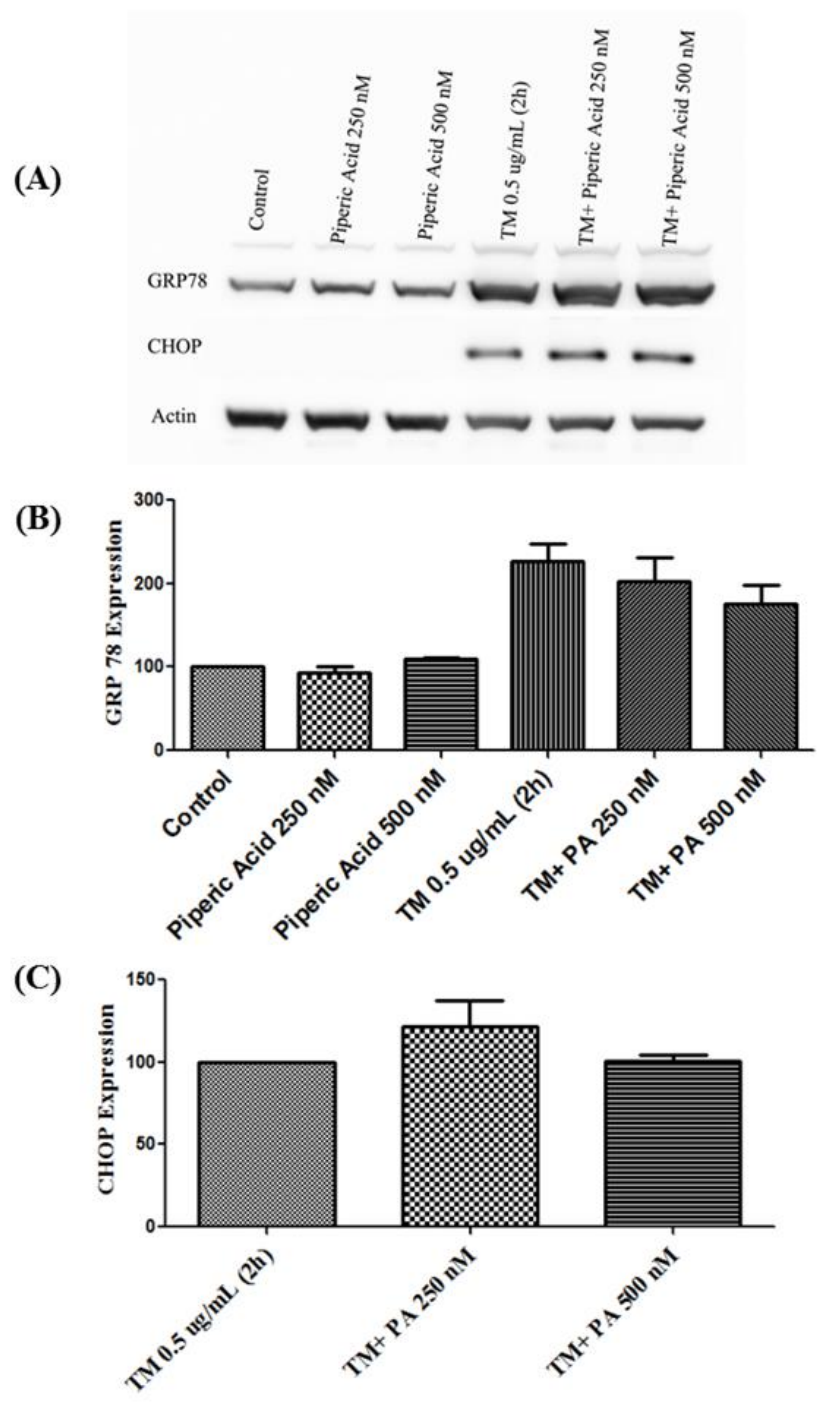**Figure 4.17:** Effect of Piperic acid **(2)** on tunicamycin (TM)-induced expression of GRP78 and CHOP in NRK-52E cells as determined by western blotting (A) and quantified using densitometry (B and C). Values were expressed as percentage of

control for GRP78 and percentage of tunicamycin (TM)-treated group for CHOP (Mean ±SEM; n=3).

4.3.4 Cyclohexylamino Analog (3)
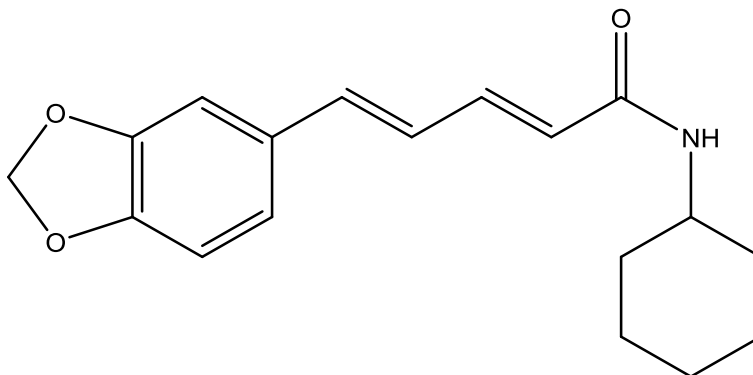
Figure 4.18: Chemical structure of cyclohexylamino analog [(2*E*,4*E*)-5-(benzo[*d*][1,3]dioxol-5-yl)-*N*-cyclohexylpenta-2,4-dienamide] **(3)**

4.3.4.1 Dose-Response Studies (Tolerability)

Cyclohexylamino analog **(3)** was well tolerated by cells at 250 and 500 nM concentrations (Figure 4.20).

Figure 4.19: Tolerability of NRK-52E cells to Cyclohexylamino analog **(3)** as measured by MTT assay. Values were expressed as percentage of control (Mean ± SEM; n=5).

4.3.4.2   Effect on Cell Viability (MTT assay)

Pre-treatment with **3** at 250 nM, but not 500 nM concentration, improved the viability of NRK-52E cells (by about 11%) following exposure to TM compared to untreated TM group (Figure 4.21).

Figure 4.20: Effect of Cyclohexylamino analog **(3)** on tunicamycin (TM)-induced loss of cell viability (measured by MTT assay) in NRK-52E cells. Values were normalized to TM-treated control and expressed as percentage change in cell viability (Mean ± SEM; n=4). *P < 0.05 compared to TM-treated group.

4.3.4.3   Expression of ER Stress Markers

Cells treated with compound **3** showed decreased expression of GRP78 (by about 25%) and CHOP (by about 30%) in comparison to TM-treated group. Similar to piperine, although both doses reduced GRP78 expression, significant reduction in CHOP expression was observed only at 500 nM concentration (Figure 4.22).
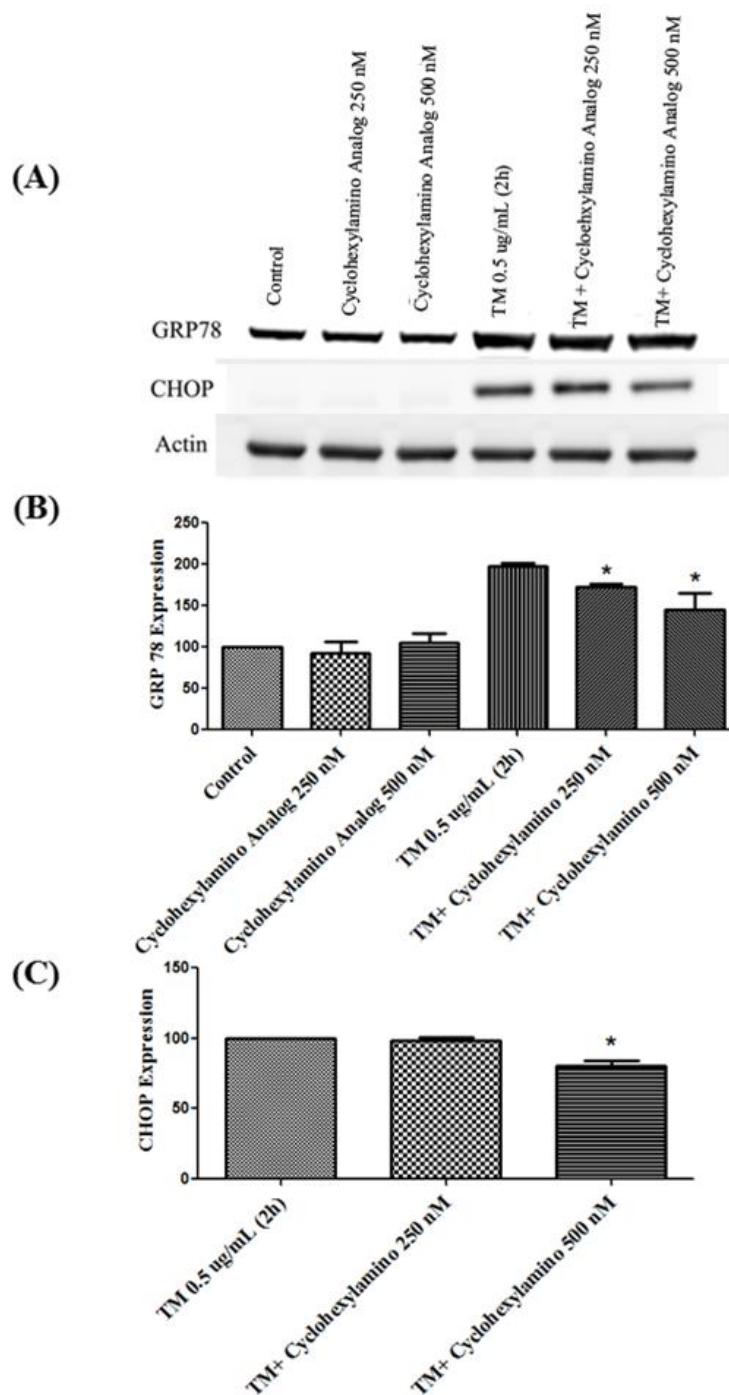
Figure 4.21: Effect of cyclohexylamino analog **(3)** on tunicamycin (TM)-induced expression of GRP78 and CHOP as determined by western blotting (A) and quantified using densitometry (B and C). Values were normalized using β-actin and expressed as

percentage of control for GRP78 or percentage of tunicamycin-treated group for CHOP

(Mean ± SEM; n=3). *P < 0.05 compared to TM-treated group.

4.3.5 Diethylamino Analog (4)
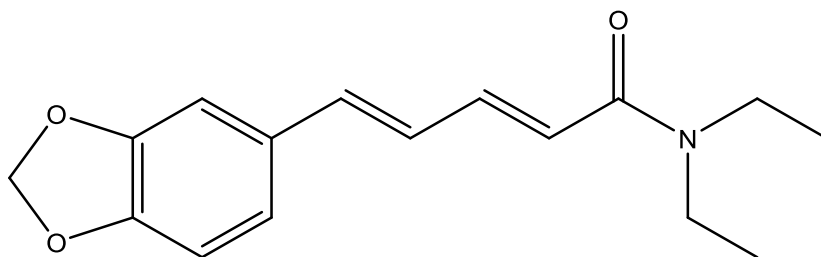
Figure 4.22: Chemical structure of diethylamino analog [(2*E*,4*E*)-5-(benzo[*d*][1,3]dioxol-5-yl)-*N*,*N*-diethylpenta-2,4-dienamide] **(4)**

4.3.5.1 Dose-Response Studies (Tolerability)

Diethylamino analog was well tolerated by NRK-52E cells at the concentrations of 250 nM and 500 nM tested in the current study (Figure 4.24).
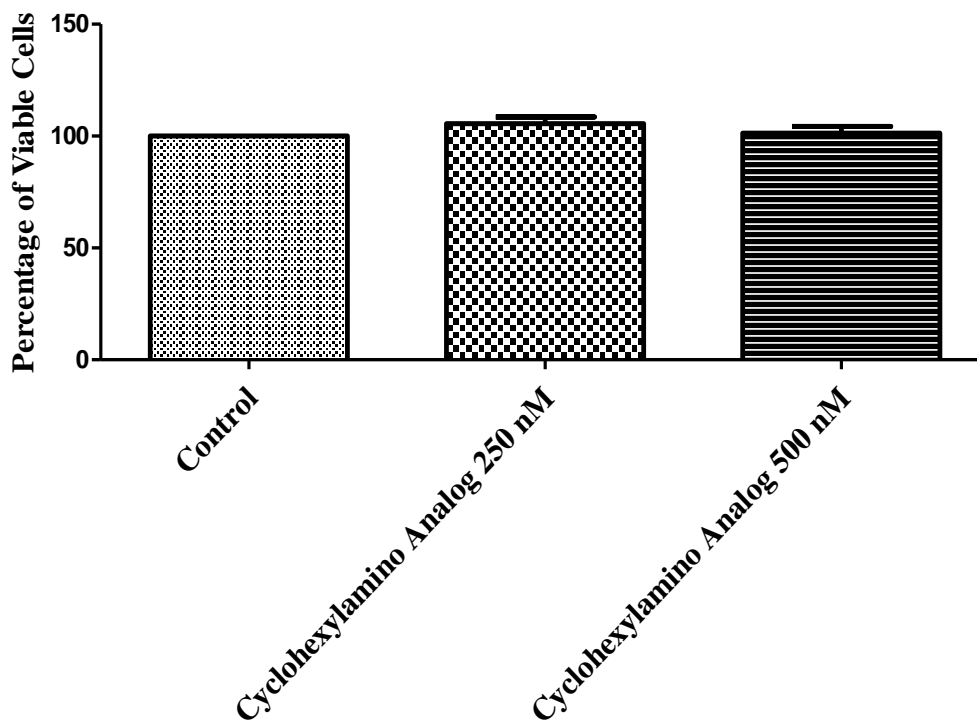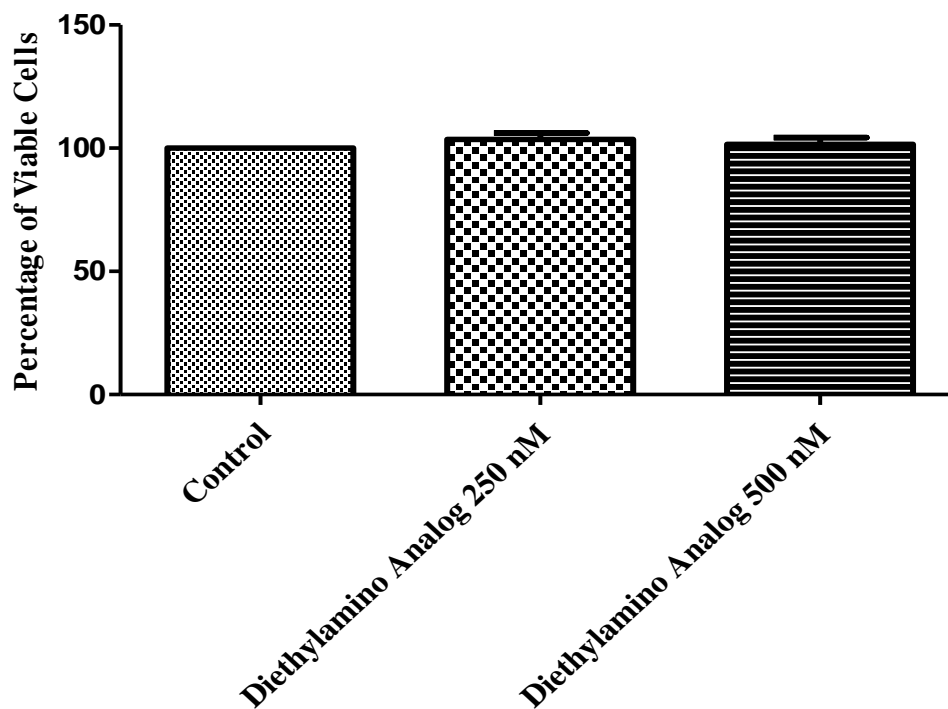
Figure 4.23: Tolerability of NRK-52E cells to Diethylamino analog **(4)** as measured by MTT assay. Values were expressed as percentage of control (Mean ± SEM; n=3).

4.3.5.2   Effect on Cell Viability (MTT assay)

The MTT results illustrate the inability of the diethylamino analog to improve the cell viability even at the highest concentration used (500 nM) (Figure 4.25). These results indicate that replacement of the piperidine ring in piperine with diethylamine led to loss of pharmacological activity.
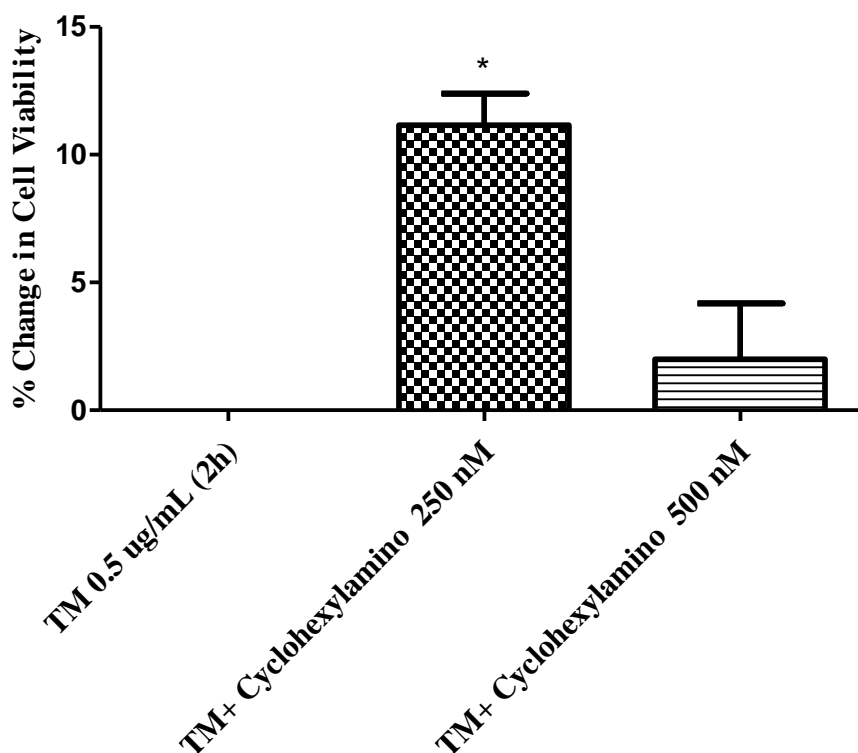
Figure 4.24: Effect of Diethylamino analog **(4)** on tunicamycin (TM)-induced loss of cell viability (measured by MTT assay) in NRK-52E cells. Values were expressed as percentage of control (Mean ± SEM; n=3).

4.3.5.3 Expression of ER Stress Markers

Consistent to the results from MTT assay, no reduction in the induction of GRP78 was observed in cells pre-treated with diethylamino analog. Moreover, a paradoxical increase (~69%) in the expression of CHOP was observed in cells treated with diethylamine and exposed to tunicamycin (Figure 4.26).

Figure 4.25: Effect of Diethylamino analog **(4)** on tunicamycin (TM)-induced expression of GRP78 and CHOP in NRK-52E cells as determined by western blotting (A) and quantified using densitometry (B and C). Values were normalized using β-actin

and expressed as percentage of control for GRP78 or percentage of tunicamycin-treated

group for CHOP (Mean ± SEM; n=3). *P < 0.05 compared to TM-treated group.

4.3.6 Pyrrolidinyl Analog (5)
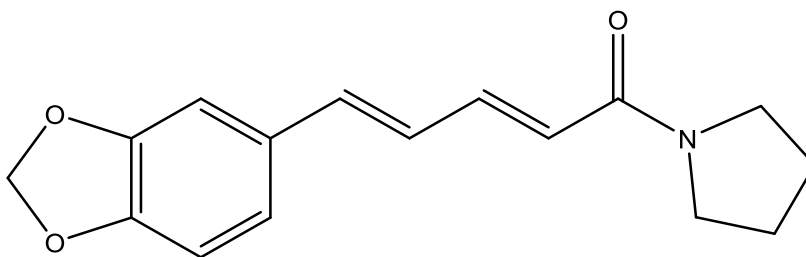
Figure 4.26: Chemical structure of Pyrrolidinyl analog (2*E*,4*E*)-5-(benzo[*d*][1,3]dioxol-

5-yl)-1-(pyrrolidin-1-yl)penta-2,4-dien-1-one) **(5)**

4.3.6.1   Dose-Response Studies (Tolerability)

Pyrrolidinyl analog was well tolerated by NRK-52E cells at the concentrations of 250

nM and 500 nM tested in the current study (Figure 4.28).
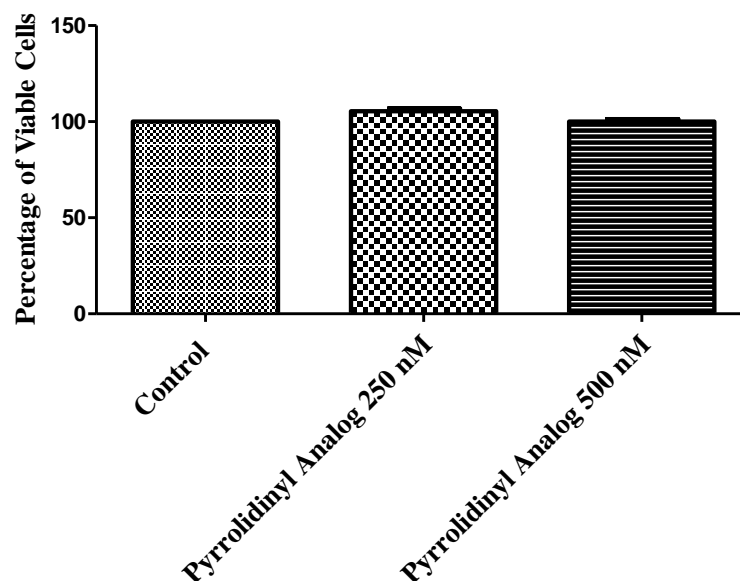
Figure 4.27: Tolerability of NRK-52E cells to Pyrrolidinyl analog **(5)** as measured by MTT assay. Values were expressed as percentage of control (Mean ± SEM; n=3).

4.3.6.2 *Effect on Cell Viability (MTT assay)*

Pre-treatment with Pyrrolidinyl analog has improved the cell viability (~11% increase compared to TM-treated control) at 250 nM concentration in NRK-52E cells exposed to TM (Figure 4.29). Similar to the Cyclohexylamino analog, a paradoxical decrease in cytoprotective efficacy was observed with Pyrrolidinyl analog at 500 nM concentration.
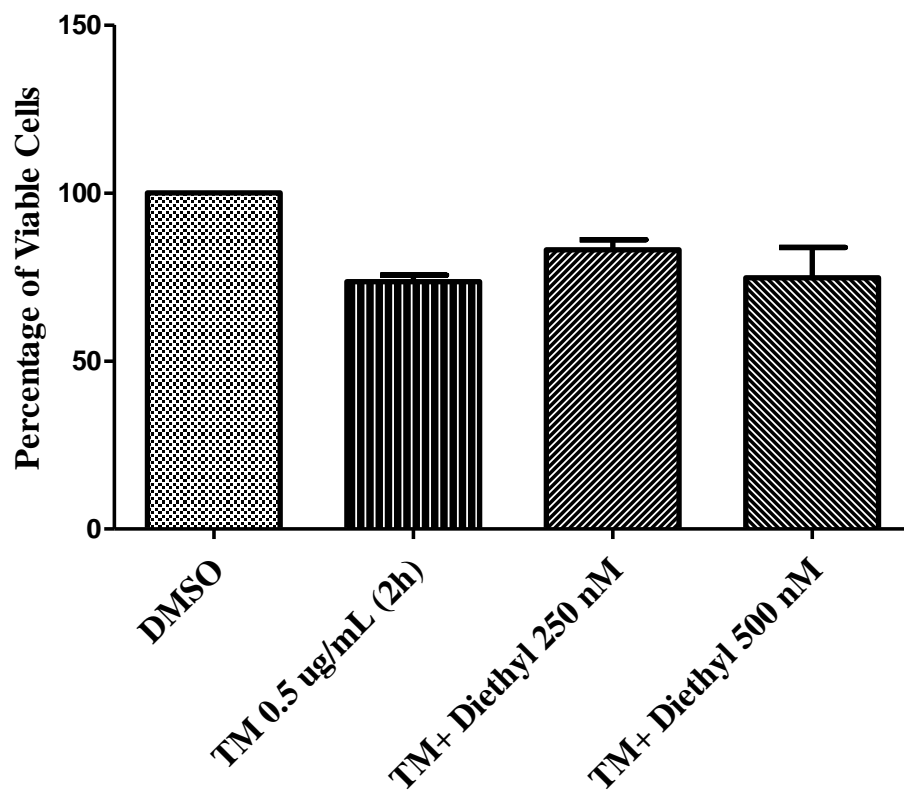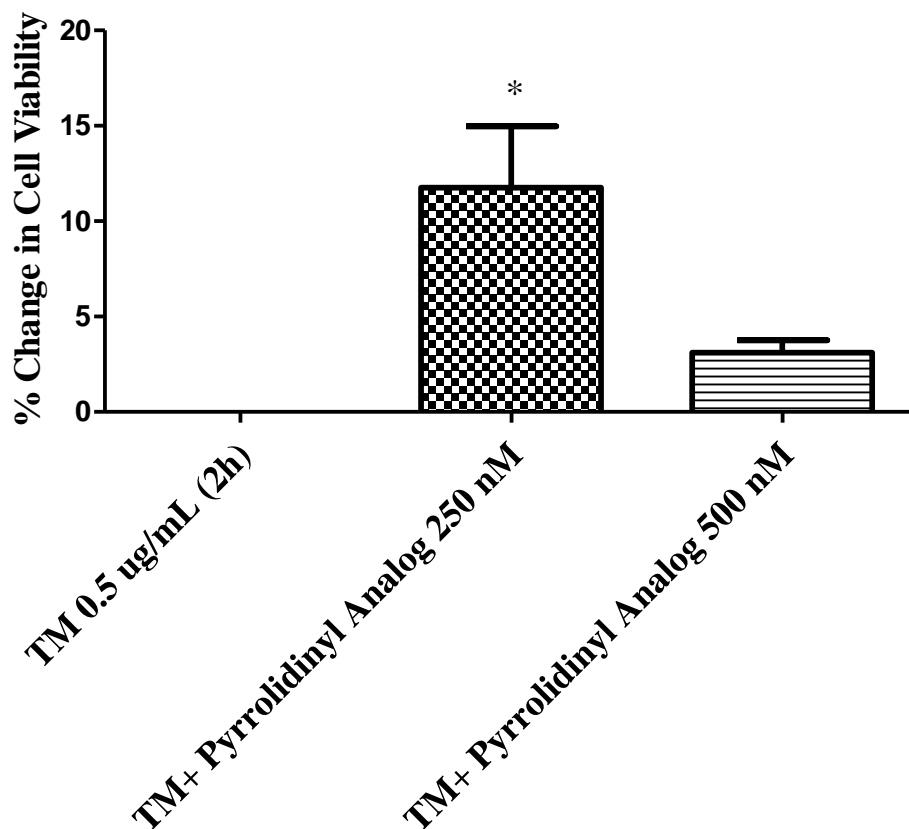
Figure 4.28: Effect of Pyrrolidinyl analog **(5)** on tunicamycin (TM)-induced loss of cell viability (measured by MTT assay) in NRK-52E cells. Values were normalized to TM-treated control and expressed as percentage change in cell viability (Mean ± SEM; n=3). *P < 0.05 compared to TM-treated group.

4.3.6.3 Expression of ER Stress Markers

Contrary to the results from MTT assay, data obtained from the western blots indicates that pre-treatment with pyrrolidine analog doesn't alter the expression of GRP78 or CHOP in NRK-52E cells (Figure 4.30).
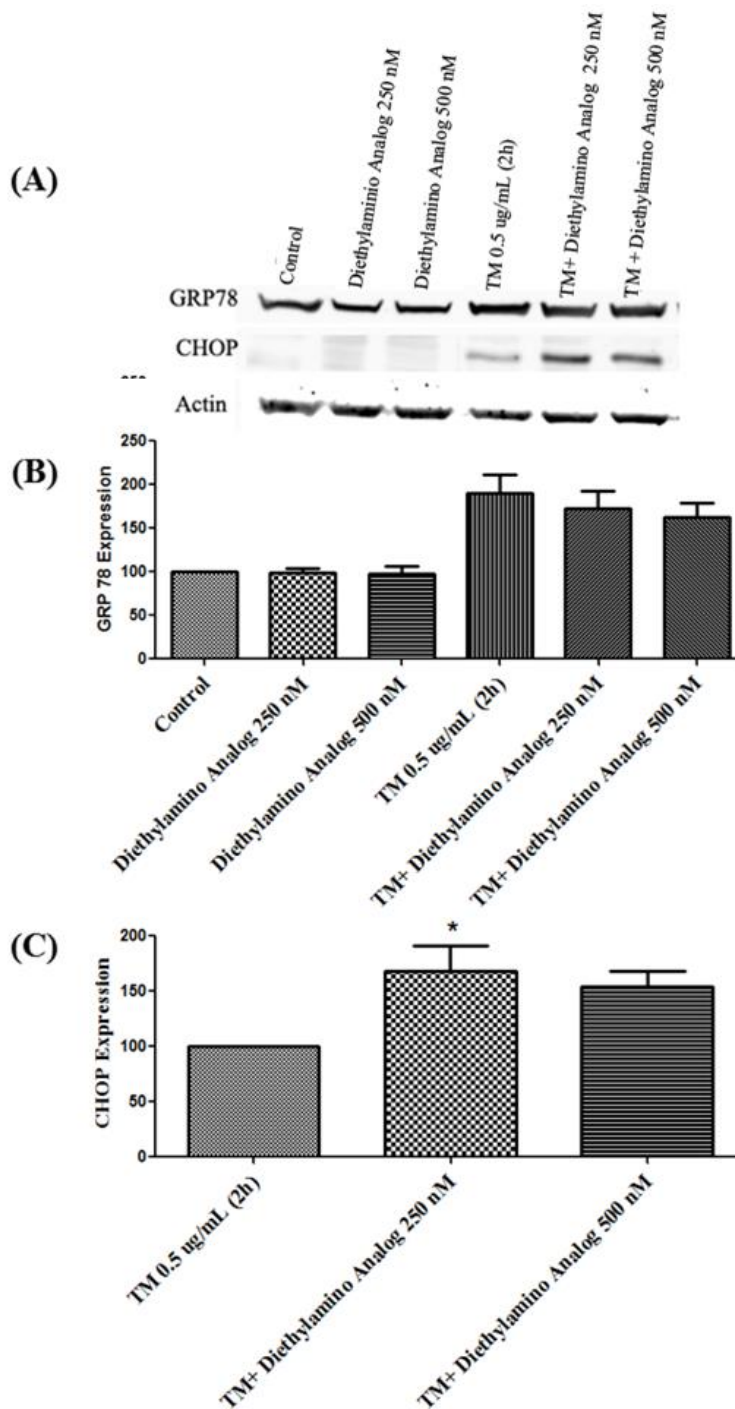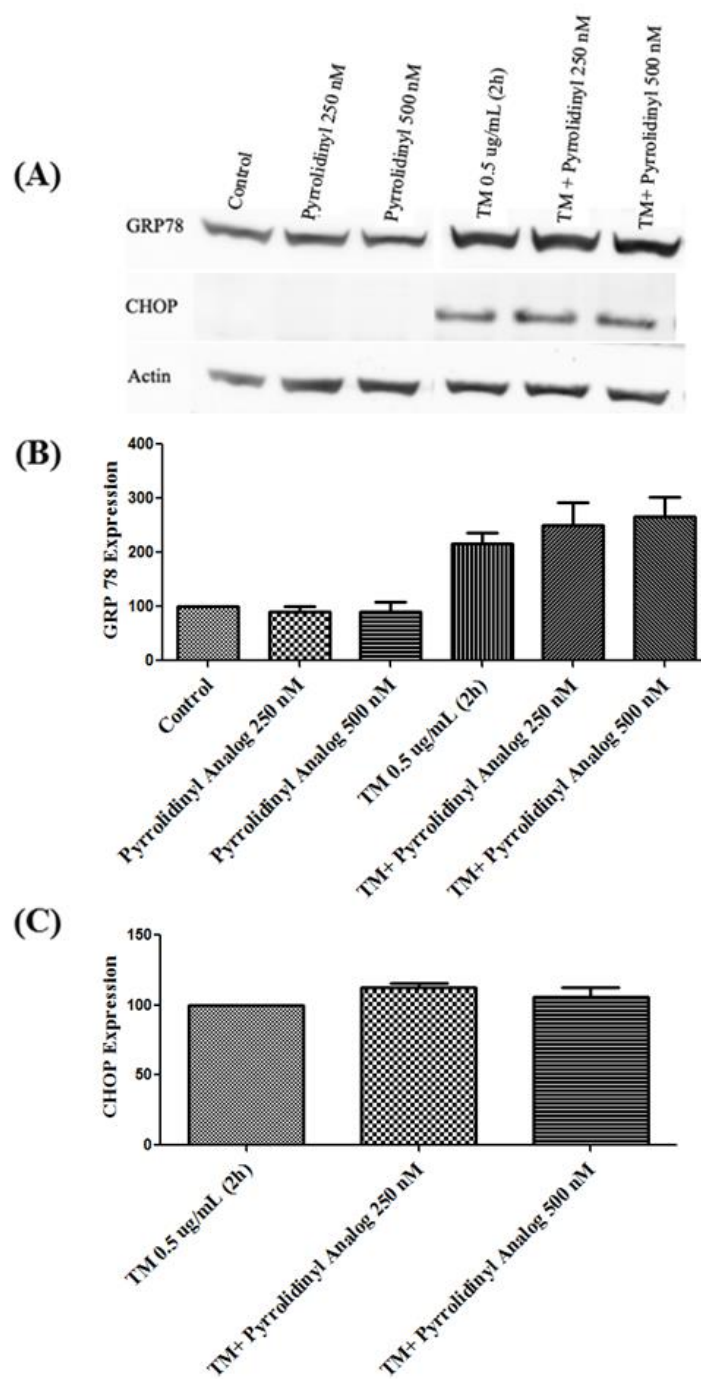
Figure 4.29: Effect of Pyrrolidinyl analog **(5)** on tunicamycin (TM)-induced expression of GRP78 and CHOP in NRK-52E cells as determined by western blotting (A) and quantified using densitometry (B and C). Values were normalized using β-actin and

expressed as percentage of control for GRP78 or percentage of tunicamycin-treated group for CHOP (Mean ± SEM; n=3).

5. Discussion

Piperine, the major ingredient of pepper species, is reported to possess multiple activities including antioxidant, neuroprotectant, and anti-inflammatory effects (94). Chemically, piperine is composed of a basic piperidine moiety that is connected to side chain through carbonylamide, a side chain with conjugated double bonds, and a methylenedioxyphenyl (MDP) ring (82). Based on its structure, any of its three components can be modified to evaluate their impact on the efficacy and potency of the parent compound piperine. A previous study conducted by Koul et al. has revealed that the piperidine moiety possess differential sensitivity for inhibition of CYP450 (82). On the other hand, the MDP ring in piperine, which could contribute to its activity, is a common component in many natural compounds (82). Therefore, in the current study, we focused on the modification of the piperidine moiety and evaluated its effect on the pharmacological activity against ER stress.

In this study, piperic acid (**2**) was prepared by the alkaline hydrolysis of piperine (**1**). Three amide piperine analogs (**3 to 5**) were synthesized from **2** and characterized as described in the experimental section. The analogs were designed and prepared based on their similarity to the parent compound piperine and screened for pharmacological activity against TM-induced ER stress and cell death in renal cells.

To establish an *in vitro* model of ER stress in renal cells, we chose tunicamycin (TM), an N-glycosylation inhibitor and a chemical inducer of ER stress (57). Our choice to utilize TM was based on a previous study conducted by Peyrou et al., which compared

the efficacy of TM with other chemical inducers of ER stress such as thapsigargin and oxidized dithiothreitol (ox-DTT) in four different renal cell lines - the porcine LLC-PK1, rat NRK-52E, canine MDCK and human HEK-293 cells (35). Results from the study have indicated that tunicamycin is the most potent inducer of ER stress among other chemical inducers tested in the model (35). Their findings also highlighted that the TM-induced ER stress response varies across different renal cell lines. For example, TM caused significant cell death in NRK-52E and HEK-293 cells; while its effect was significantly lowered in LLC-PK1 and MDCK cell lines (35). Thus, in our current study, we decided to use TM to induce ER stress in NRK-52E cells.

We assessed the major hallmarks proteins induced during ER stress response such as the ER chaperone glucose-regulated protein 78 (GRP78) and the pro-apoptotic growth arrest and DNA damage-inducible protein 153 (CHOP/GADD153). GRP78 is an important resident chaperone that maintains cellular homeostasis by ensuring the proper folding of protein in the ER (95), whereas, CHOP is a pro-apoptotic protein, which is induced by all the three arms of UPR - ATF6, IRE1 and PERK-eIF-2α pathways (53). Our results confirmed the ability of TM (at 0.5 µg/mL for 2 hours) to induce ER stress (marked by the induction of GRP78 and CHOP), and cell death (evidenced by ~ 60% reduction in cell viability) in NRK-52E cells.

To compare the efficacy of piperine and its analogs, we chose to use 4-PBA, a well-known chemical chaperone, as our reference standard. 4-PBA is a nontoxic butyrate analog, which has the ability to enhance the protein folding capacity of ER, and improve

the trafficking of mutant proteins (96). In our study, we found that 4-PBA protects against TM-induced expression of both GRP78 and CHOP. However, a higher magnitude of reduction was observed on CHOP expression (63). Our findings are in line with a previous study in HK-2 cells by Dickhout et al., where 4-PBA has been shown to prevent TM-induced CHOP expression without affecting the expression of GRP78 (57).

The pharmacological screening of the prepared analogs started with its parent compound piperine. Piperine is the major lipophilic component of black pepper with several recognized pharmacological activities (97). It is used as food additive for ages, and several studies *in vitro* and *in vivo* have demonstrated its safety and tolerability (82). In this study, we attempted to evaluate the chaperone activity of piperine against TM-induced ER stress, and assess the impact of modifications to its structure on its chaperone potential.

Five piperine analogs (Piperic acid, 3 amide piperine analogs and 1 ester piperine analog) were synthesized and their structures were elucidated by pertinent spectroscopic techniques. Each analog (except the ester analog) was tested - at two different concentrations (250 and 500 nM) - for its pharmacological activity to relieve ER stress induced by TM in renal cells, and compared against its parent compound piperine and reference standard 4-PBA. The Table 5.1 summarizes the effect of prepared analogs in comparison to piperine and 4-PBA.

Table 5.1: Summary of the effect of Piperine and its analogs against tunicamycin (TM)-induced ER Stress and cell death in NRK-52E cells

Compound	Concentration Tested	Cell Viability	Western blotting	
			GRP78	**CHOP**
4-PBA (Reference standard)	1 and 2 mM	N.C	▼ (~15%)	▼ (~70%)
Piperine (**1**)	250 and 500 nM	▲ (~13%)	▼ (~33%)	▼ (~25%)
Piperic acid (**2**)	250 and 500 nM	N.C	N.C	N.C
Cyclohexylamino analog (**3**)	250 and 500 nM	▲ (~11%)	▼ (~25%)	▼ (~30%)
Diethylamino analog (**4**)	250 and 500 nM	N.C	N.C	▲ (~69%)
Pyrrolidinyl analog (**5**)	250 and 500 nM	▲ (~11%)	N.C	N.C

Note: ▲ represents increase, ▼ represents decrease, and N.C represents no change compared to TM-treated control.

Based on the literature, all the prepared analogs were used in nanomolar (250 and 500 nM) concentrations, whereas the reference standard 4-PBA was used in millimolar (1

and 2 mM) concentration. Although the effects of piperine were similar to that of 4-PBA, its effects were mainly mediated through reduction in the expression of GRP78. In contrast, 4-PBA appears to mediate its effects mainly through reduction in CHOP expression. Thus, future studies could examine the synergistic effects expected out of combination of 4-PBA and piperine as a strategy to prevent ER stress in renal cells. Moreover, a previous study revealed the ability of piperine to down-regulate the mRNA expression of GRP78 and the protein expression on XBP1 and ATF6 in the livers of HFD-fed mice ([87]). Thus, future studies could also examine the effect of piperine and its analogs on the expression of the XBP and ATF6 in NRK-52E cells exposed to TM.

The second most potent compound in our study was the cyclohexylamino analog. Similar to piperine, it decreased the expression of GRP78 and CHOP in NRK-52E cells. Thus, its effects could be potentially mediated through either IRE1 and/or ATF6 arms of the UPR. Further studies to investigate the effect of this analog on the expression of XBP1 and JNK would help to unravel the mechanism(s) behind its protective effects against ER stress.

Intriguingly, the diethylamino analog (**4**) caused a paradoxical increase in the expression of CHOP. Thus, further studies are required to understand their impact on the CHOP expression, and to determine whether its effects on CHOP are transient or permanent. On the other hand, piperic acid (**2**) did not affect the expression of CHOP and GRP78. Similarly, pyrrolidinyl analog (**5**) did not alter the induction of ER stress markers GRP78 and CHOP; however, it was the only compound, which showed improvements in

cell viability. Further studies with different side chains and amine substituents in the aromatic moiety are required to elucidate the structure–activity relationship of these compounds. Nevertheless, based on our research findings, we were able to identify and propose the following.

1) Piperine and its analogs are pharmacologically active at nanomolar (nM) concentrations.

2) Similar to 4-PBA, piperine **(1)** and its cyclohexylamino analog **(3)** can decrease the expression of GRP78 and CHOP in renal cells, and attenuate ER stress.

3) Opening of piperidine ring structure in piperine (diethylamino analog **(4)**) causes a paradoxical increase in CHOP expression, which might aggravate ER stress.

4) Removal of the piperidine ring by hydrolysis of piperine **(1)** or replacement of six-membered ring with a five-membered ring (pyrrolidinyl analog **(5)**) appears to result in loss of pharmacological activity against ER stress.

5) Compounds **1**, **3**, and **5** also possess cytoprotective properties against ER stress-induced cell death.

6) In terms of potency, piperine and its analogs (used in nanomolar concentrations) are about 4,000 times more potent when compared to the reference standard 4-PBA (used in millimolar concentration).

In conclusion, considering their high potency (used in nM), efficacy and a wide margin of safety, piperine **(1)** and its cyclohexylamino analog **(3)** appear to be

promising drug candidates for further investigation *in vivo* for prevention of ER

stress, and potential application to treat ER stress-related renal disorders in patients.

6. References

1.   Brandizzi F, Frigerio L, Howell SH, Schafer P. Endoplasmic reticulum-shape and function in stress translation. Frontiers in plant science. 2014;5:425.
2.   Staehelin LA. The plant ER: a dynamic organelle composed of a large number of discrete functional domains. The Plant journal : for cell and molecular biology. 1997;11(6):1151-65.
3.   Zhuang A, Forbes JM. Stress in the kidney is the road to pERdition: is endoplasmic reticulum stress a pathogenic mediator of diabetic nephropathy? The Journal of endocrinology. 2014;222(3):R97-111.
4.   Voeltz GK, Rolls MM, Rapoport TA. Structural organization of the endoplasmic reticulum. EMBO reports. 2002;3(10):944-50.
5.   Walter P, Ron D. The unfolded protein response: from stress pathway to homeostatic regulation. Science. 2011;334(6059):1081-6.
6.   Lynes EM, Simmen T. Urban planning of the endoplasmic reticulum (ER): how diverse mechanisms segregate the many functions of the ER. Biochimica et biophysica acta. 2011;1813(10):1893-905.
7.   Spear ED, Ng DTW. Stress Tolerance of Misfolded Carboxypeptidase Y Requires Maintenance of Protein Trafficking and Degradative Pathways. Molecular biology of the cell. 2003;14(7):2756-67.
8.   Hoyer-Hansen M, Jaattela M. Connecting endoplasmic reticulum stress to autophagy by unfolded protein response and calcium. Cell death and differentiation. 2007;14(9):1576-82.
9.   Travers KJ, Patil CK, Wodicka L, Lockhart DJ, Weissman JS, Walter P. Functional and genomic analyses reveal an essential coordination between the unfolded protein response and ER-associated degradation. Cell. 2000;101(3):249-58.
10.   Nagelkerke A, Bussink J, Sweep FC, Span PN. The unfolded protein response as a target for cancer therapy. Biochimica et biophysica acta. 2014;1846(2):277-84.
11.   Hotamisligil GS. Endoplasmic reticulum stress and the inflammatory basis of metabolic disease. Cell. 2010;140(6):900-17.
12.   Sen D, Balakrishnan B, Jayandharan GR. Cellular unfolded protein response against viruses used in gene therapy. Frontiers in microbiology. 2014;5:250.
13.   Jager R, Bertrand MJ, Gorman AM, Vandenabeele P, Samali A. The unfolded protein response at the crossroads of cellular life and death during endoplasmic reticulum stress. Biology of the cell / under the auspices of the European Cell Biology Organization. 2012;104(5):259-70.
14.   Sano R, Reed JC. ER stress-induced cell death mechanisms. Biochimica et biophysica acta. 2013;1833(12):3460-70.
15.   Saito A, Ochiai K, Kondo S, Tsumagari K, Murakami T, Cavener DR, et al. Endoplasmic reticulum stress response mediated by the PERK-eIF2(alpha)-ATF4 pathway is involved in osteoblast differentiation induced by BMP2. The Journal of biological chemistry. 2011;286(6):4809-18.

16.   Marciniak SJ, Garcia-Bonilla L, Hu J, Harding HP, Ron D. Activation-dependent substrate recruitment by the eukaryotic translation initiation factor 2 kinase PERK. The Journal of cell biology. 2006;172(2):201-9.

17.   Brush MH, Weiser DC, Shenolikar S. Growth arrest and DNA damage-inducible protein GADD34 targets protein phosphatase 1 alpha to the endoplasmic reticulum and promotes dephosphorylation of the alpha subunit of eukaryotic translation initiation factor 2. Molecular and cellular biology. 2003;23(4):1292-303.

18.   Sovolyova N, Healy S, Samali A, Logue SE. Stressed to death - mechanisms of ER stress-induced cell death. Biological chemistry. 2014;395(1):1-13.

19.   Shiraishi H, Okamoto H, Yoshimura A, Yoshida H. ER stress-induced apoptosis and caspase-12 activation occurs downstream of mitochondrial apoptosis involving Apaf-1. Journal of cell science. 2006;119(Pt 19):3958-66.

20.   Gupta S, Cuffe L, Szegezdi E, Logue SE, Neary C, Healy S, et al. Mechanisms of ER Stress-Mediated Mitochondrial Membrane Permeabilization. International journal of cell biology. 2010;2010:170215.

21.   Rao RV, Castro-Obregon S, Frankowski H, Schuler M, Stoka V, del Rio G, et al. Coupling endoplasmic reticulum stress to the cell death program. An Apaf-1-independent intrinsic pathway. The Journal of biological chemistry. 2002;277(24):21836-42.

22.   Hacker G. ER-stress and apoptosis: molecular mechanisms and potential relevance in infection. Microbes and infection / Institut Pasteur. 2014;16(10):805-10.

23.   Gallerne C, Prola A, Lemaire C. Hsp90 inhibition by PU-H71 induces apoptosis through endoplasmic reticulum stress and mitochondrial pathway in cancer cells and overcomes the resistance conferred by Bcl-2. Biochimica et biophysica acta. 2013;1833(6):1356-66.

24.   Wang X, Olberding KE, White C, Li C. Bcl-2 proteins regulate ER membrane permeability to luminal proteins during ER stress-induced apoptosis. Cell death and differentiation. 2011;18(1):38-47.

25.   Chipuk JE, Moldoveanu T, Llambi F, Parsons MJ, Green DR. The BCL-2 Family Reunion. Molecular cell. 2010;37(3):299-310.

26.   Morishima N, Nakanishi K, Takenouchi H, Shibata T, Yasuhiko Y. An endoplasmic reticulum stress-specific caspase cascade in apoptosis. Cytochrome c-independent activation of caspase-9 by caspase-12. The Journal of biological chemistry. 2002;277(37):34287-94.

27.   Zou H, Henzel WJ, Liu X, Lutschg A, Wang X. Apaf-1, a Human Protein Homologous to C. elegans CED-4, Participates in Cytochrome c–Dependent Activation of Caspase-3. Cell.90(3):405-13.

28.   Szegezdi E, Logue SE, Gorman AM, Samali A. Mediators of endoplasmic reticulum stress-induced apoptosis. EMBO reports. 2006;7(9):880-5.

29.   Davis RJ. Signal transduction by the JNK group of MAP kinases. Cell. 2000;103(2):239-52.

30.   Rao RV, Ellerby HM, Bredesen DE. Coupling endoplasmic reticulum stress to the cell death program. Cell death and differentiation. 2004;11(4):372-80.

31.   Hetz C, Bernasconi P, Fisher J, Lee AH, Bassik MC, Antonsson B, et al. Proapoptotic BAX and BAK modulate the unfolded protein response by a direct interaction with IRE1alpha. Science. 2006;312(5773):572-6.

32.   Henriquez FL, Nickdel MB, McLeod R, Lyons RE, Lyons K, Dubremetz JF, et al. Toxoplasma gondii dense granule protein 3 (GRA3) is a type I transmembrane protein that possesses a cytoplasmic dilysine (KKXX) endoplasmic reticulum (ER) retrieval motif. Parasitology. 2005;131(Pt 2):169-79.

33.   Inagi R. Endoplasmic reticulum stress as a progression factor for kidney injury. Current opinion in pharmacology. 2010;10(2):156-65.

34.   Markan S, Kohli H, Joshi K, Minz R, Sud K, Ahuja M, et al. Up regulation of the GRP-78 and GADD-153 and down regulation of Bcl-2 proteins in primary glomerular diseases: a possible involvement of the ER stress pathway in glomerulonephritis. Molecular and cellular biochemistry. 2009;324(1-2):131-8.

35.   Peyrou M, Cribb AE. Effect of endoplasmic reticulum stress preconditioning on cytotoxicity of clinically relevant nephrotoxins in renal cell lines. Toxicology in vitro : an international journal published in association with BIBRA. 2007;21(5):878-86.

36.   Muntner P, Levin A. Chapter 6 - Epidemiology of Chronic Kidney Disease: Scope of the Problem. In: Kimmel PL, Rosenberg ME, editors. Chronic Renal Disease. San Diego: Academic Press; 2015. p. 57-68.

37.   Shigidi MM, Ramachandiran G, Rashed AH, Fituri OM. Demographic data and hemodialysis population dynamics in Qatar: A five year survey. Saudi journal of kidney diseases and transplantation : an official publication of the Saudi Center for Organ Transplantation, Saudi Arabia. 2009;20(3):493-500.

38.   Drawz P, Hostetter TH, Rosenberg ME. Chapter 49 - Slowing Progression of Chronic Kidney Disease. In: Kimmel PL, Rosenberg ME, editors. Chronic Renal Disease. San Diego: Academic Press; 2015. p. 598-612.

39.   Rogers M, Goettsch C, Aikawa E. Medial and intimal calcification in chronic kidney disease: stressing the contributions. Journal of the American Heart Association. 2013;2(5):e000481.

40.   Dronavalli S, Duka I, Bakris GL. The pathogenesis of diabetic nephropathy. Nature clinical practice Endocrinology & metabolism. 2008;4(8):444-52.

41.   Schena FP, Gesualdo L. Pathogenetic mechanisms of diabetic nephropathy. Journal of the American Society of Nephrology : JASN. 2005;16 Suppl 1:S30-3.

42.   Molitch ME, DeFronzo RA, Franz MJ, Keane WF, Mogensen CE, Parving HH, et al. Nephropathy in diabetes. Diabetes care. 2004;27 Suppl 1:S79-83.

43.   Araki E, Oyadomari S, Mori M. Endoplasmic reticulum stress and diabetes mellitus. Internal medicine. 2003;42(1):7-14.

44.   Back SH, Kaufman RJ. Endoplasmic reticulum stress and type 2 diabetes. Annual review of biochemistry. 2012;81:767-93.

45.   Laybutt DR, Preston AM, Akerfeldt MC, Kench JG, Busch AK, Biankin AV, et al. Endoplasmic reticulum stress contributes to beta cell apoptosis in type 2 diabetes. Diabetologia. 2007;50(4):752-63.

46.   Åkerfeldt MC, Howes J, Chan JY, Stevens VA, Boubenna N, McGuire HM, et al. Cytokine-Induced β-Cell Death Is Independent of Endoplasmic Reticulum Stress Signaling. Diabetes. 2008;57(11):3034-44.

47.   Kooptiwut S, Mahawong P, Hanchang W, Semprasert N, Kaewin S, Limjindaporn T, et al. Estrogen reduces endoplasmic reticulum stress to protect against glucotoxicity induced-pancreatic β-cell death. The Journal of steroid biochemistry and molecular biology. 2014;139(0):25-32.

48.   Fonseca SG, Burcin M, Gromada J, Urano F. Endoplasmic reticulum stress in beta-cells and development of diabetes. Current opinion in pharmacology. 2009;9(6):763-70.

49.   Nakatani Y, Kaneto H, Kawamori D, Yoshiuchi K, Hatazaki M, Matsuoka TA, et al. Involvement of endoplasmic reticulum stress in insulin resistance and diabetes. The Journal of biological chemistry. 2005;280(1):847-51.

50.   Liu G, Sun Y, Li Z, Song T, Wang H, Zhang Y, et al. Apoptosis induced by endoplasmic reticulum stress involved in diabetic kidney disease. Biochemical and biophysical research communications. 2008;370(4):651-6.

51.   Cunard R, Sharma K. The endoplasmic reticulum stress response and diabetic kidney disease. American journal of physiology Renal physiology. 2011;300(5):F1054-61.

52.   Kimura K, Jin H, Ogawa M, Aoe T. Dysfunction of the ER chaperone BiP accelerates the renal tubular injury. Biochemical and biophysical research communications. 2008;366(4):1048-53.

53.   Katsoulieris E, Mabley JG, Samai M, Sharpe MA, Green IC, Chatterjee PK. Lipotoxicity in renal proximal tubular cells: relationship between endoplasmic reticulum stress and oxidative stress pathways. Free radical biology & medicine. 2010;48(12):1654-62.

54.   Fujii Y, Khoshnoodi J, Takenaka H, Hosoyamada M, Nakajo A, Bessho F, et al. The effect of dexamethasone on defective nephrin transport caused by ER stress: a potential mechanism for the therapeutic action of glucocorticoids in the acquired glomerular diseases. Kidney international. 2006;69(8):1350-9.

55.   Cybulsky AV, Takano T, Papillon J, Bijian K. Role of the endoplasmic reticulum unfolded protein response in glomerular epithelial cell injury. The Journal of biological chemistry. 2005;280(26):24396-403.

56.   Inagi R, Nangaku M, Onogi H, Ueyama H, Kitao Y, Nakazato K, et al. Involvement of endoplasmic reticulum (ER) stress in podocyte injury induced by excessive protein accumulation. Kidney international. 2005;68(6):2639-50.

57.   Schonthal AH. Endoplasmic reticulum stress: its role in disease and novel prospects for therapy. Scientifica. 2012;2012:857516.

58.   Cybulsky AV, Takano T, Papillon J, Bijian K, Guillemette J, Kennedy CR. Glomerular epithelial cell injury associated with mutant alpha-actinin-4. American journal of physiology Renal physiology. 2009;297(4):F987-95.

59.   Xie Q, Khaoustov VI, Chung CC, Sohn J, Krishnan B, Lewis DE, et al. Effect of tauroursodeoxycholic acid on endoplasmic reticulum stress-induced caspase-12 activation. Hepatology. 2002;36(3):592-601.

60.   Ozcan U, Yilmaz E, Ozcan L, Furuhashi M, Vaillancourt E, Smith RO, et al. Chemical chaperones reduce ER stress and restore glucose homeostasis in a mouse model of type 2 diabetes. Science. 2006;313(5790):1137-40.
61.   Gao X, Fu L, Xiao M, Xu C, Sun L, Zhang T, et al. The nephroprotective effect of tauroursodeoxycholic acid on ischaemia/reperfusion-induced acute kidney injury by inhibiting endoplasmic reticulum stress. Basic & clinical pharmacology & toxicology. 2012;111(1):14-23.
62.   Basseri S, Lhotak S, Sharma AM, Austin RC. The chemical chaperone 4-phenylbutyrate inhibits adipogenesis by modulating the unfolded protein response. Journal of lipid research. 2009;50(12):2486-501.
63.   Carlisle RE, Brimble E, Werner KE, Cruz GL, Ask K, Ingram AJ, et al. 4-Phenylbutyrate Inhibits Tunicamycin-Induced Acute Kidney Injury via CHOP/GADD153 Repression. PloS one. 2014;9(1):e84663.
64.   Choi S-E, Lee Y-J, Jang H-J, Lee K-W, Kim Y-S, Jun H-S, et al. A chemical chaperone 4-PBA ameliorates palmitate-induced inhibition of glucose-stimulated insulin secretion (GSIS). Archives of biochemistry and biophysics. 2008;475(2):109-14.
65.   Hiroi T, Wei H, Hough C, Leeds P, Chuang DM. Protracted lithium treatment protects against the ER stress elicited by thapsigargin in rat PC12 cells: roles of intracellular calcium, GRP78 and Bcl-2. Pharmacogenomics J. 2005;5(2):102-11.
66.   Huang S, Zhu M, Wu W, Rashid A, Liang Y, Hou L, et al. Valproate pretreatment protects pancreatic beta-cells from palmitate-induced ER stress and apoptosis by inhibiting glycogen synthase kinase-3beta. Journal of biomedical science. 2014;21:38.
67.   Kudo T, Kanemoto S, Hara H, Morimoto N, Morihara T, Kimura R, et al. A molecular chaperone inducer protects neurons from ER stress. Cell death and differentiation. 2007;15(2):364-75.
68.   Nakanishi T, Shimazawa M, Sugitani S, Kudo T, Imai S, Inokuchi Y, et al. Role of endoplasmic reticulum stress in light-induced photoreceptor degeneration in mice. Journal of neurochemistry. 2013;125(1):111-24.
69.   Kim I, Shu CW, Xu W, Shiau CW, Grant D, Vasile S, et al. Chemical biology investigation of cell death pathways activated by endoplasmic reticulum stress reveals cytoprotective modulators of ASK1. The Journal of biological chemistry. 2009;284(3):1593-603.
70.   Gao B, Zhang XY, Han R, Zhang TT, Chen C, Qin ZH, et al. The endoplasmic reticulum stress inhibitor salubrinal inhibits the activation of autophagy and neuroprotection induced by brain ischemic preconditioning. Acta pharmacologica Sinica. 2013;34(5):657-66.
71.   Neuber C, Uebeler J, Schulze T, Sotoud H, El-Armouche A, Eschenhagen T. Guanabenz interferes with ER stress and exerts protective effects in cardiac myocytes. PloS one. 2014;9(6):e98893.
72.   Doucette CD, Greenshields AL, Liwski RS, Hoskin DW. Piperine blocks interleukin-2-driven cell cycle progression in CTLL-2 T lymphocytes by inhibiting multiple signal transduction pathways. Toxicology letters. (0).

73.   Yoon YC, Kim S-H, Kim MJ, Yang HJ, Rhyu M-R, Park J-H. Piperine, a component of black pepper, decreases eugenol-induced cAMP and calcium levels in non-chemosensory 3T3-L1 cells. FEBS open bio. 2015;5(0):20-5.

74.   Greenshields AL, Doucette CD, Sutton KM, Madera L, Annan H, Yaffe PB, et al. Piperine inhibits the growth and motility of triple-negative breast cancer cells. Cancer letters. 2015;357(1):129-40.

75.   Meghwal M, Goswami TK. Piper nigrum and piperine: an update. Phytotherapy research : PTR. 2013;27(8):1121-30.

76.   Srinivasan K. Black pepper and its pungent principle-piperine: a review of diverse physiological effects. Critical reviews in food science and nutrition. 2007;47(8):735-48.

77.   Kumar A, Sasmal D, Sharma N. Immunomodulatory role of piperine in Deltamethrin induced thymic apoptosis and altered immune functions. Environmental Toxicology and Pharmacology. (0).

78.   Koul S, Koul JL, Taneja SC, Dhar KL, Jamwal DS, Singh K, et al. Structure-activity relationship of piperine and its synthetic analogues for their inhibitory potentials of rat hepatic microsomal constitutive and inducible cytochrome P450 activities. Bioorganic & medicinal chemistry. 2000;8(1):251-68.

79.   Ferreira C, Soares DC, Barreto-Junior CB, Nascimento MT, Freire-de-Lima L, Delorenzi JC, et al. Leishmanicidal effects of piperine, its derivatives, and analogues on Leishmania amazonensis. Phytochemistry. 2011;72(17):2155-64.

80.   Faas L, Venkatasamy R, Hider RC, Young AR, Soumyanath A. In vivo evaluation of piperine and synthetic analogues as potential treatments for vitiligo using a sparsely pigmented mouse model. The British journal of dermatology. 2008;158(5):941-50.

81.   Wattanathorn J, Chonpathompikunlert P, Muchimapura S, Priprem A, Tankamnerdthai O. Piperine, the potential functional food for mood and cognitive disorders. Food and chemical toxicology : an international journal published for the British Industrial Biological Research Association. 2008;46(9):3106-10.

82.   Koul S, Koul JL, Taneja SC, Dhar KL, Jamwal DS, Singh K, et al. Structure–activity relationship of piperine and its synthetic analogues for their inhibitory potentials of rat hepatic microsomal constitutive and inducible cytochrome P450 activities. Bioorganic & medicinal chemistry. 2000;8(1):251-68.

83.   Yaffe PB, Power Coombs MR, Doucette CD, Walsh M, Hoskin DW. Piperine, an alkaloid from black pepper, inhibits growth of human colon cancer cells via G1 arrest and apoptosis triggered by endoplasmic reticulum stress. Molecular carcinogenesis. 2014.

84.   Ouyang D-y, Zeng L-h, Pan H, Xu L-h, Wang Y, Liu K-p, et al. Piperine inhibits the proliferation of human prostate cancer cells via induction of cell cycle arrest and autophagy. Food and Chemical Toxicology. 2013;60(0):424-30.

85.   Pradeep CR, Kuttan G. Effect of piperine on the inhibition of lung metastasis induced B16F-10 melanoma cells in mice. Clin Exp Metastasis. 2002;19(8):703-8.

86.   Lai L-h, Fu Q-h, Liu Y, Jiang K, Guo Q-m, Chen Q-y, et al. Piperine suppresses tumor growth and metastasis in vitro and in vivo in a 4T1 murine breast cancer model. Acta pharmacologica Sinica. 2012;33(4):523-30.

87.   Jwa H, Choi Y, Park U-H, Um S-J, Yoon SK, Park T. Piperine, an LXRα antagonist, protects against hepatic steatosis and improves insulin signaling in mice fed a high-fat diet. Biochemical pharmacology. 2012;84(11):1501-10.

88.   Sangwan PL, Koul JL, Koul S, Reddy MV, Thota N, Khan IA, et al. Piperine analogs as potent Staphylococcus aureus NorA efflux pump inhibitors. Bioorganic & medicinal chemistry. 2008;16(22):9847-57.

89.   Atal S, Agrawal RP, Vyas S, Phadnis P, Rai N. Evaluation of the effect of piperine per se on blood glucose level in alloxan-induced diabetic mice. Acta poloniae pharmaceutica. 2012;69(5):965-9.

90.   Venkatasamy R, Faas L, Young AR, Raman A, Hider RC. Effects of piperine analogues on stimulation of melanocyte proliferation and melanocyte differentiation. Bioorganic & medicinal chemistry. 2004;12(8):1905-20.

91.   Raiter A, Yerushalmi R, Hardy B. Pharmacological induction of cell surface GRP78 contributes to apoptosis in triple negative breast cancer cells. Oncotarget. 2014;5(22):11452-63.

92.   Oyadomari S, Mori M. Roles of CHOP/GADD153 in endoplasmic reticulum stress. Cell death and differentiation. 2004;11(4):381-9.

93.   Galehdar Z, Swan P, Fuerth B, Callaghan SM, Park DS, Cregan SP. Neuronal apoptosis induced by endoplasmic reticulum stress is regulated by ATF4-CHOP-mediated induction of the Bcl-2 homology 3-only member PUMA. The Journal of neuroscience : the official journal of the Society for Neuroscience. 2010;30(50):16938-48.

94.   Zhang J, Zhu X, Li H, Li B, Sun L, Xie T, et al. Piperine inhibits proliferation of human osteosarcoma cells via G2/M phase arrest and metastasis by suppressing MMP-2/-9 expression. International immunopharmacology. 2015;24(1):50-8.

95.   Rovetta F, Stacchiotti A, Consiglio A, Cadei M, Grigolato PG, Lavazza A, et al. ER signaling regulation drives the switch between autophagy and apoptosis in NRK-52E cells exposed to cisplatin. Experimental cell research. 2012;318(3):238-50.

96.   Humeres C, Montenegro J, Varela M, Ayala P, Vivar R, Letelier A, et al. 4-Phenylbutyric acid prevent cytotoxicity induced by thapsigargin in rat cardiac fibroblast. Toxicology in Vitro. 2014;28(8):1443-8.

97.   Hu D, Wang Y, Chen Z, Ma Z, You Q, Zhang X, et al. The protective effect of piperine on dextran sulfate sodium induced inflammatory bowel disease and its relation with pregnane X receptor activation. Journal of ethnopharmacology. 2015;169(0):109-2

ملخص

المقدمة: تعتبر الشبكة الاندوبلازمية مكون اساسي من مكونات الخلايا وهي المسؤولة عن عملية طي البروتينات ونضجها. بالتالي فإن حدوث خلل في عملها يفعلينشط عدد من المسارات الحيوية لافراز مركبات لضمان صحة الخلايا. وقد أثبتت العديد من الدراسات دور الخلل في الشبكة الاندوبلازمية في امراض الكلى. لذلك فهنالك حاجة ملحة لاكتشاف علاج جديد لهذا الخلل. من ضمن المواد الشائعة (الببرين وهو أحد مكونات الفلفل الأسود) وقد اثبتت الدراسات المعملية تمتعه بالعديد من الخصائص الدوائية الا ان تاثيره على امراض الكلى الناتجة عن حدوث خلل في الشبكة الاندوبلازمية لم يدرس بعد. لذلك فان الهدف من هذا البحث هو تشييد بعض المركبات الشبيهة للببرين واختبار تاثيرها العلاجي على خلايا الانابيب الكلوية للجرذان.

الطريقة: تم تحضيربعض المركبات الشبيهة للببرين واثبات تركيبها الكيميائي باستخدام مختلف التقنيات التحليلية . وقد تم ايضا احداث المرض في خلايا الكلى المستخدمة باستخدام مركب تونيكاميسن. وتم دراسة تاثير المركبات على حماية الخلايا.

النتائج: تم تشييد خمسة مركبات مشابهة للببرين والتاكد من تركيبها الكيميائي. النتائج التي توصلنا اليها تشير الى ان استخدام تونيكاميسن لمدة ساعتين وبتركيز 0.5 ميكروغرام \ مل يؤدي الى انخفاض في صحة الخلايا بنسبة 60%. في حين ان استخدام الببرين او المركب المشتق باستخدام سيكلوهيكسيل امين يقلل من انتاج البروتينات الناتجة عن الخلل. واثبتت النتائج الاولية ان استخدام المركبات المصنعة بتركيز نانوغرام ينتج فاعالية مشابهة للمركب المعتمد عند استخدامه بتركيز ميلي غرام وبذلك فانها تتمتع فعالية اكبر بـ4000 ضعف.

الخلاصة: نتائجنا تثبت ان الببرين والمركبات المشابهة له تقلل الخلل في الشبكة الاندوبلازمية بطرق تفاضليه وتمثل مواد مثيرة لعلاج امراض الكلى الناتجة عن الخلل في الشبكة الاندوبلازمية

7. Appendix

7.1 Piperic Acid (2)
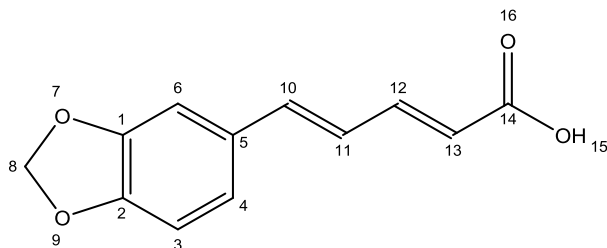
(2*E*,4*E*)-5-(benzo[*d*][1,3]dioxol-5-yl)penta-2,4-dienoic acid
Chemical Formula: $C_{12}H_{10}O_4$
Molecular Weight: 218.21
Elemental Analysis: C, 66.05; H, 4.62; O, 29.33

2 was obtained by alkaline hydrolysis of piperine. The positive mode ESI mass spectrum of **2** (Figure 7.1) showed $[M+1]^+$ peak at m/z 219 (calculated value 218). Elemental analysis for $C_{12}H_{10}O_4$; found C 65.00, H 4.57, O 29.25%; calculated C 66.05, H 4.62, O 29.33%. Figure 7.2 shows ^{1}H NMR spectrum in DMSO-d6. ^{1}H NMR: δ 6.05(H8), 7.23 (H12), 5.93 (H13), 12.02 (H15). Figure 7.3 represents ^{13}C NMR spectrum in DMSO-d6: δ 148.59 (C1), 148.44 (C2), 106.03 (C3), 123.69 (C4), 131.12 (C5), 108.94 (C6), 101.69 (C8), 139.45 (C10), 125.6 (C11), 144.88 (C12), 121.53 (C13), 167.65 (C14). IR (conducted on the solid sample using UATR) : 3200-2500 (-OH stretching), 1673 (carbonyl group), and C=C stretching of benzene ring at 1599 and 1500 cm^{-1} (Figure 7.4). Melting point: 220-224 ^{0}C (value reported in literature 217 ^{0}C) (1).
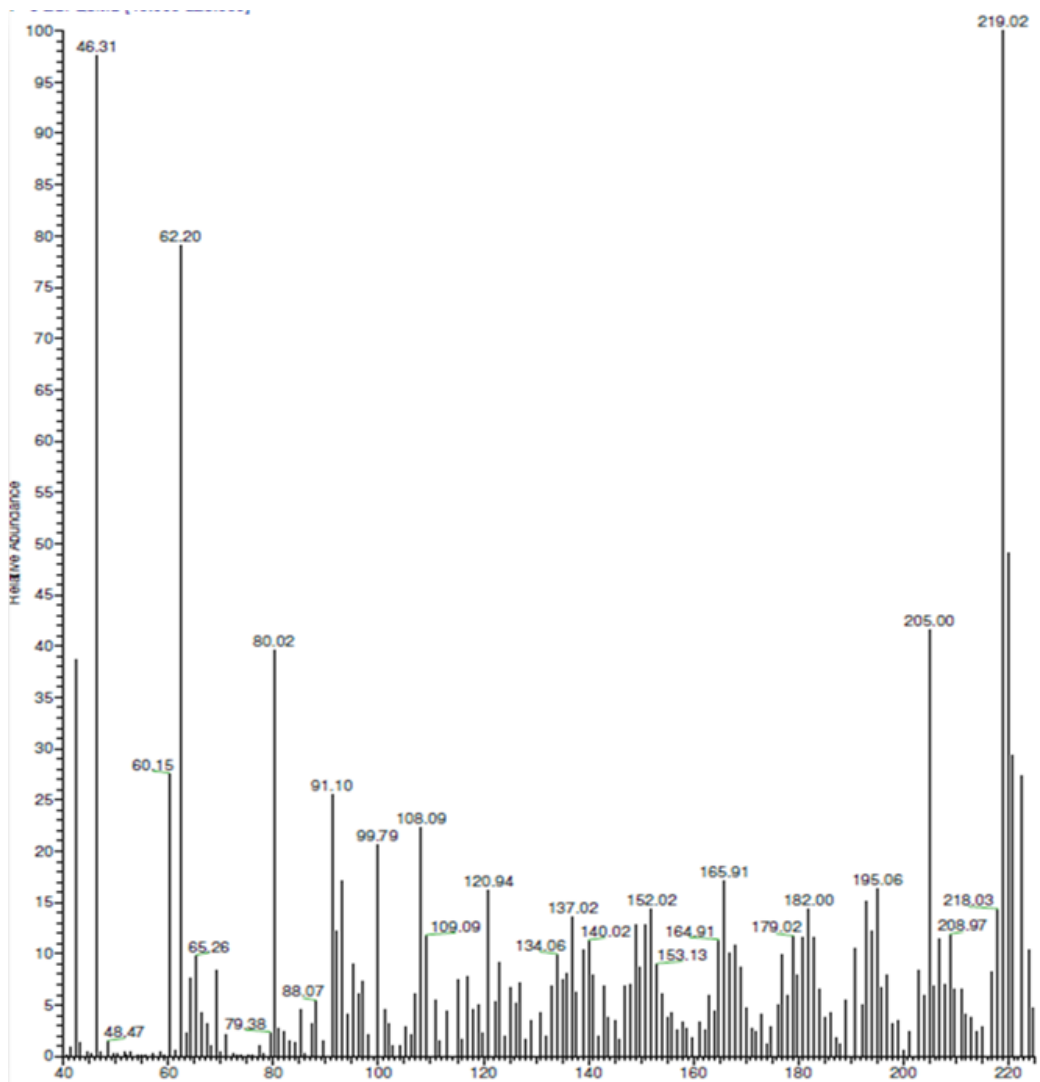
Figure 7.1: Mass spectrum of **2** using positive mode ESI.
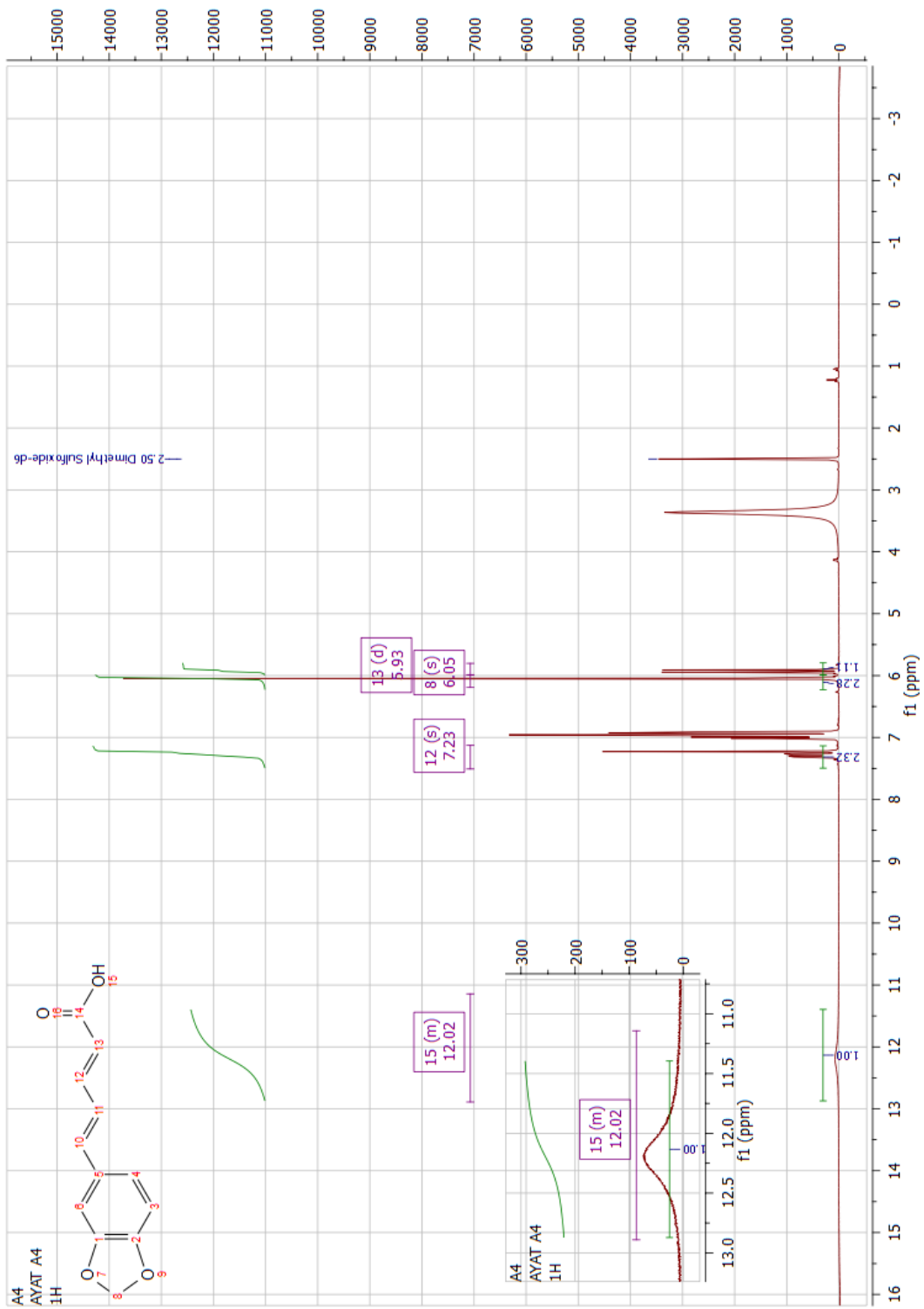
Figure 7.2: ^{1}H NMR spectrum of **2** in DMSO-d6.
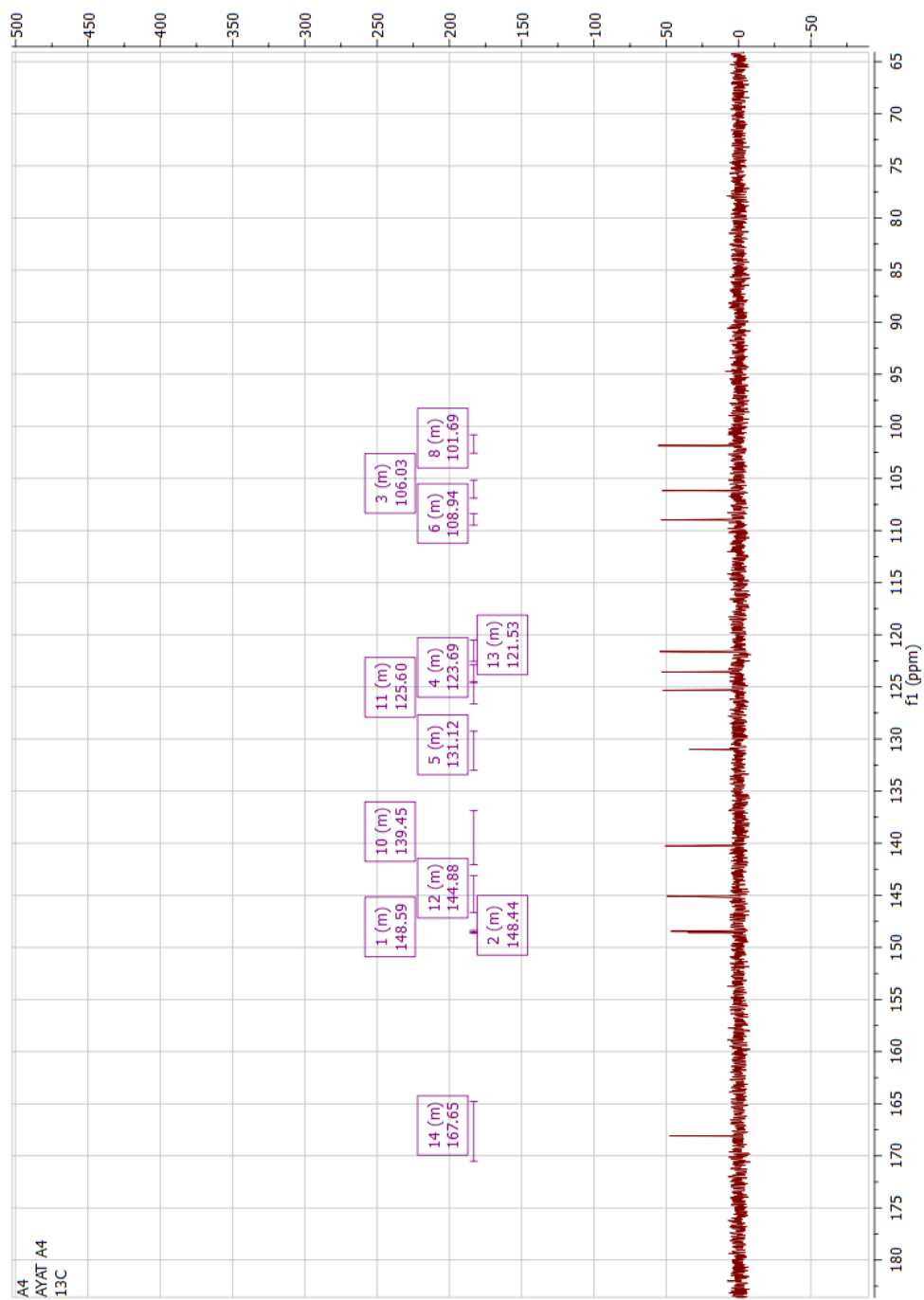
Figure 7.3: ^{13}C NMR spectrum of **2** in DMSO-d6
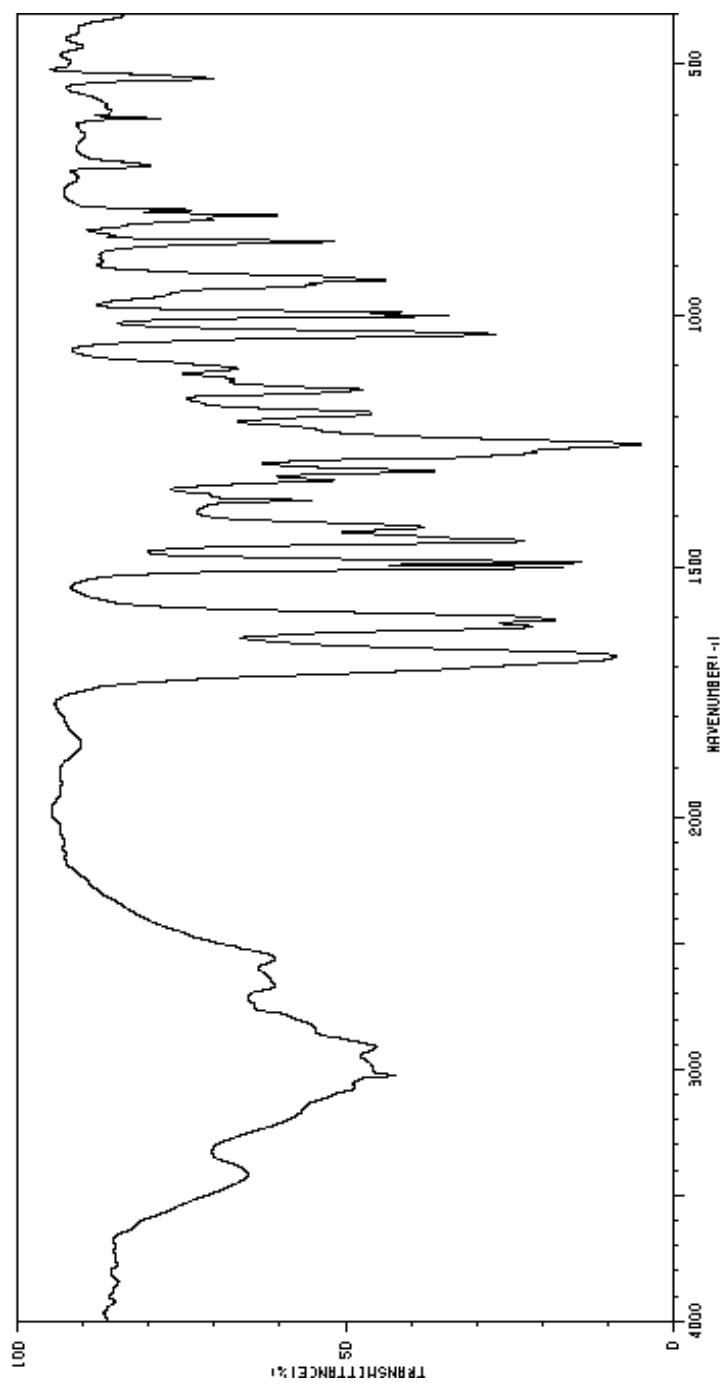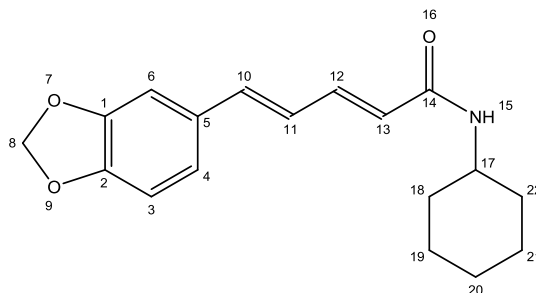
Figure 7.4: FTIR of **2** conducted on the solid sample using UATR.

7.2 Cyclohexylamino Analog (3)

(2*E*,4*E*)-5-(benzo[*d*][1,3]dioxol-5-yl)-*N*-cyclohexylpenta-2,4-dienamide
Chemical Formula: $C_{18}H_{21}NO_3$
Molecular Weight: 299.37
Elemental Analysis: C, 72.22; H, 7.07; N, 4.68; O, 16.03

All the obtained data were consistent with the previously reported in the literature. **3** was prepared from **2** and cyclohexylamine as described in the section 3.1.2.The positive mode ESI mass spectrum of **3** (Figure 7.5) showed [M+1]$^+$ at m/z 300 which is in accordance with the calculated molecular weight 299. Analysis for $C_{12}H_{10}O_4$; found C 71.99, H 7.15, N 4.55%; calculated C 72.22, H 7.07, N 4.68%. Figure 7.6 shows ^{1}H NMR spectrum in DMSO-d6. ^{1}H NMR: δ 6.10 (H3), 6.98 (H4), 7.1 (H6), 6.03 (H8), 6.87 (H10), 6.06 (H11), 7.25 (H12), 7.91 (H15), 3.36 (H17), 1.56 (H20), 1.19 (H21), 1.72 (H22). ^{13}C NMR spectrum in DMSO-d6: δ 148.4 (C1), 109.23 (C3), 125.41 (C4), 131.23 (C5), 106.05 (C6), 101.75 (C8), 137.95 (C10), 125.77 (C11), 123.07 (C13), 164.83 (C14), 48.4 (C17), 25.74 (C20), 25.03 (C21), 33.53 (C22) (Figure 7.7). The IR (conducted on the solid sample using UATR) spectrum, showed the absorption of C=O stretch of the amide group at 1642 cm^{-1}, N-H stretch of the amide group at 3305 cm^{-1} as a medium sharp peak (Figure 7.8): Melting point: 202-205 ^{0}C (reported value 199-200 ^{0}C)(2)**.**
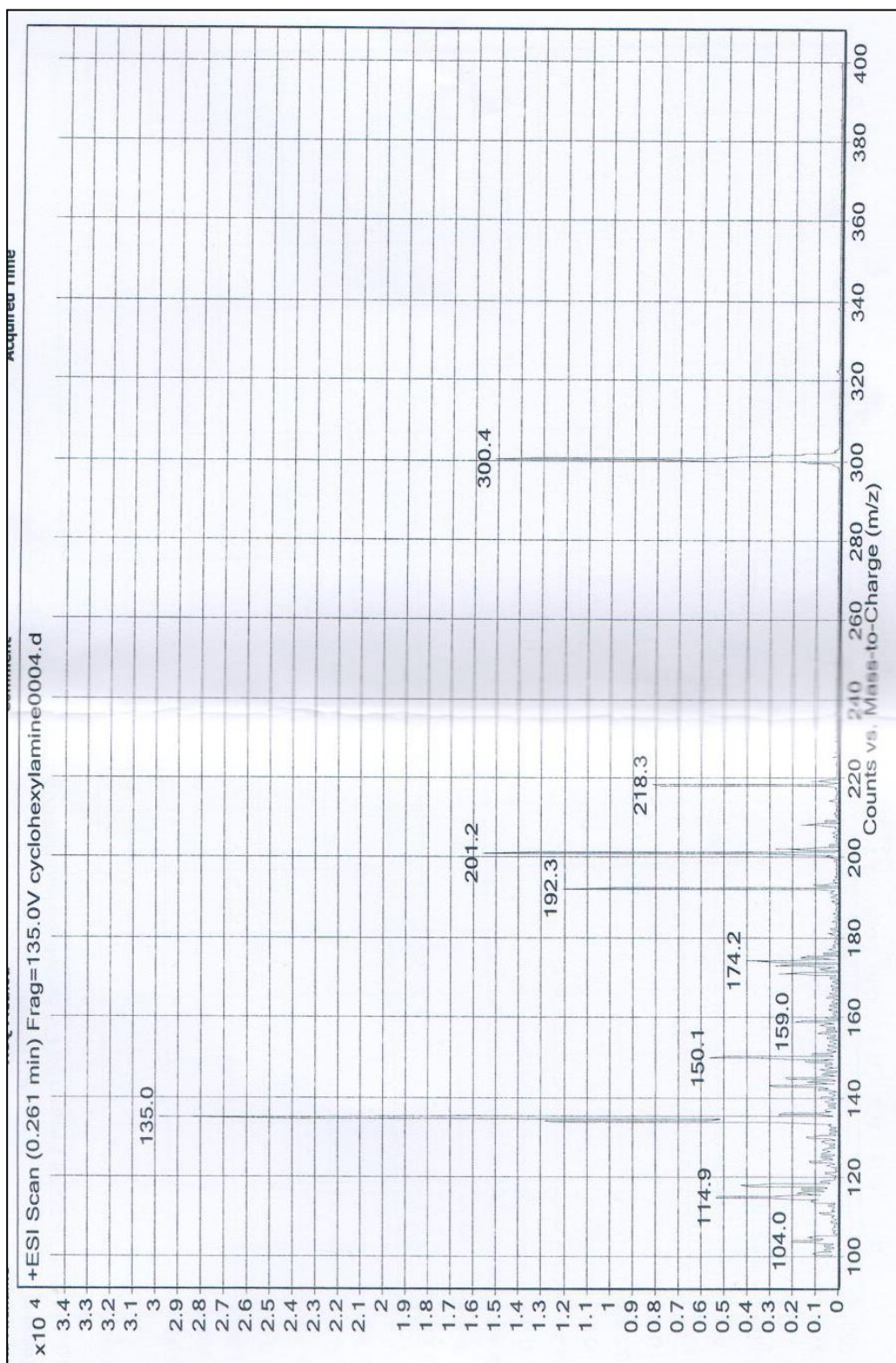
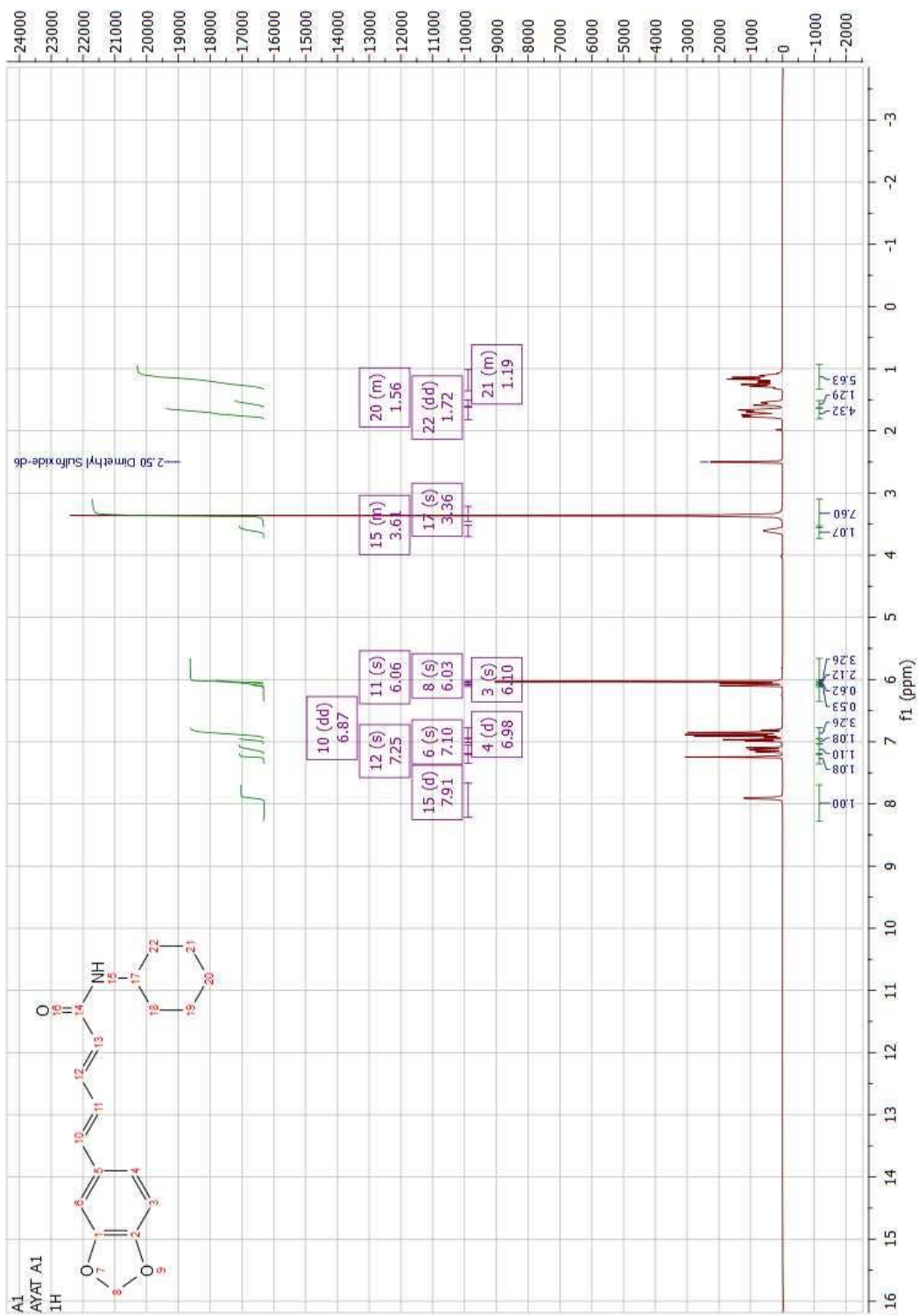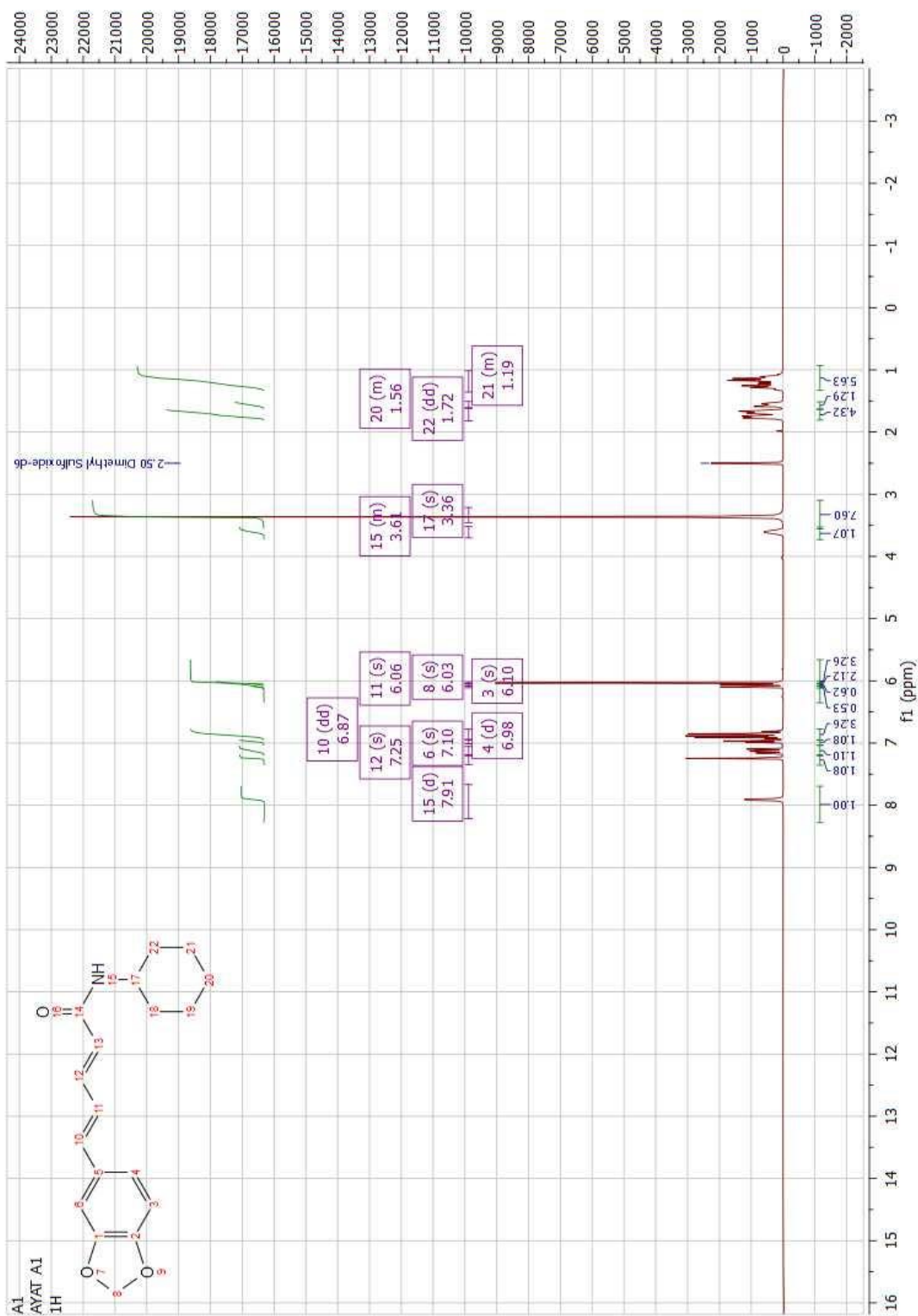**Figure 7.5:** Mass spectrum of 3 using positive mode ESI.

Figure 7.6: ^{1}H NMR spectrum of **3** in DMSO-d6.

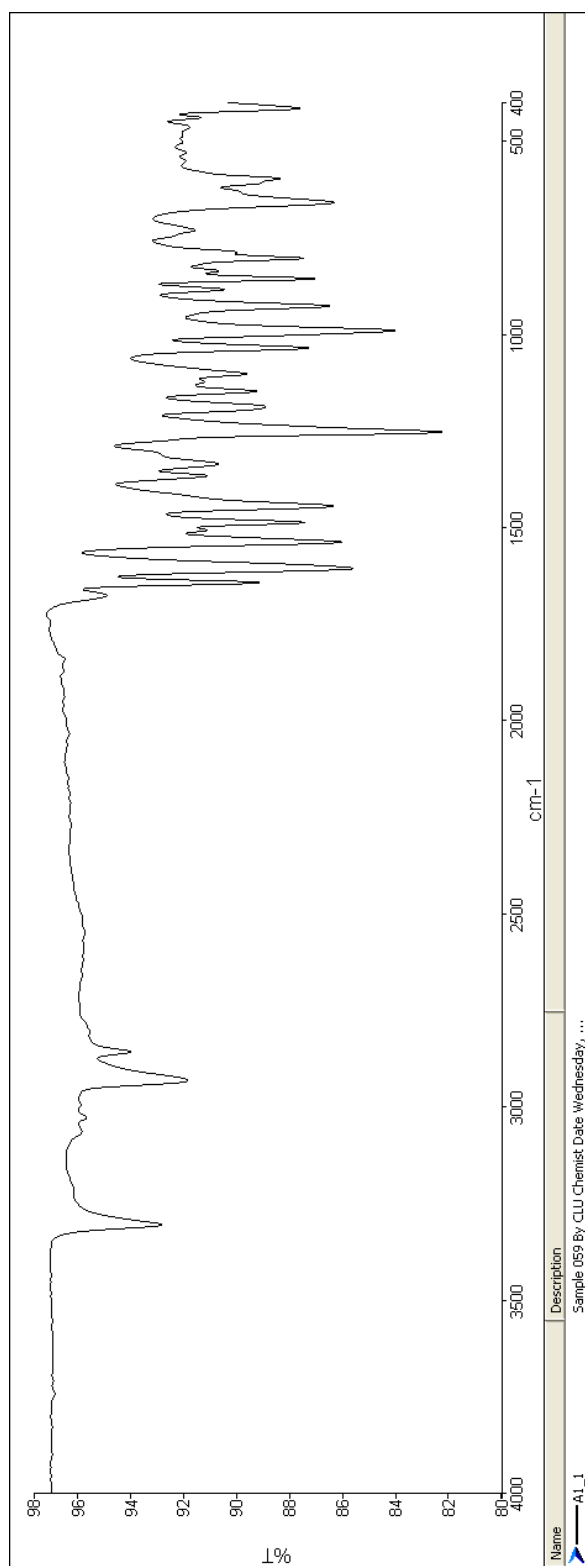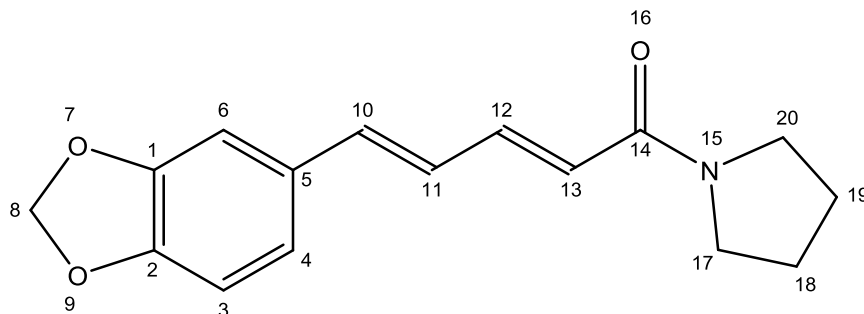**Figure 7.7:** ^{13}C NMR of 3 in DMSO-d6.

Figure 7.8: FTIR of **3** conducted on the solid sample using UATR.

7.3 Pyrrolidinyl Analog (5)

(2*E*,4*E*)-5-(benzo[*d*][1,3]dioxol-5-yl)-1-(pyrrolidin-1-yl)penta-2,4-dien-1-one
Chemical Formula: $C_{16}H_{17}NO_3$
Molecular Weight: 271.32
Elemental Analysis: C, 70.83; H, 6.32; N, 5.16; O, 17.69

All the obtained data were consistent with the previously reported in the literature. **5** was prepared from **2** and pyrrolidine as described in the section 3.1.2. The positive mode ESI mass spectrum of **5** (Figure 7.9) showed [M+1]$^{+}$ appearing at m/z 272, and confirmed the molecular weight of the prepared, which was calculated to be 271. Analysis for $C_{16}H_{17}O_3N$; found C 70. 50, H 6.34, N 5.00%; calculated C 70.83, H 6.32, N 5.16%. Figure 7.10 shows ^{1}H NMR spectrum in DMSO-d6. ^{1}H NMR: δ 6.04 (H8), 6.93 (H10), 6.41 (H11), 7.20 (H12), 3.39 (H13), 2.5 (20), 1.83 (H19). ^{13}C NMR spectrum in DMSO-d6: δ 148.41 (C1), 148.23 (C2), 108.93 (C3), 123.17 (C4), 131.29 (C5), 105.9 (C6), 100.98 (C8), 138.6 (C10), 125.83 (C11), 141.26 (C12), 122.71 (C13), 164.18 (C14), 23.35 (C19), 46.47 (C20) (Figure 7.11). FTIR (conducted on the solid sample using UATR) results showed the absorption of C=O stretch of the amide group at 1635 cm^{-1} (Figure 7.12). Melting point: 143-146 ^{0}C (value reported in literature 144-146 ^{0}C) (1, 2).
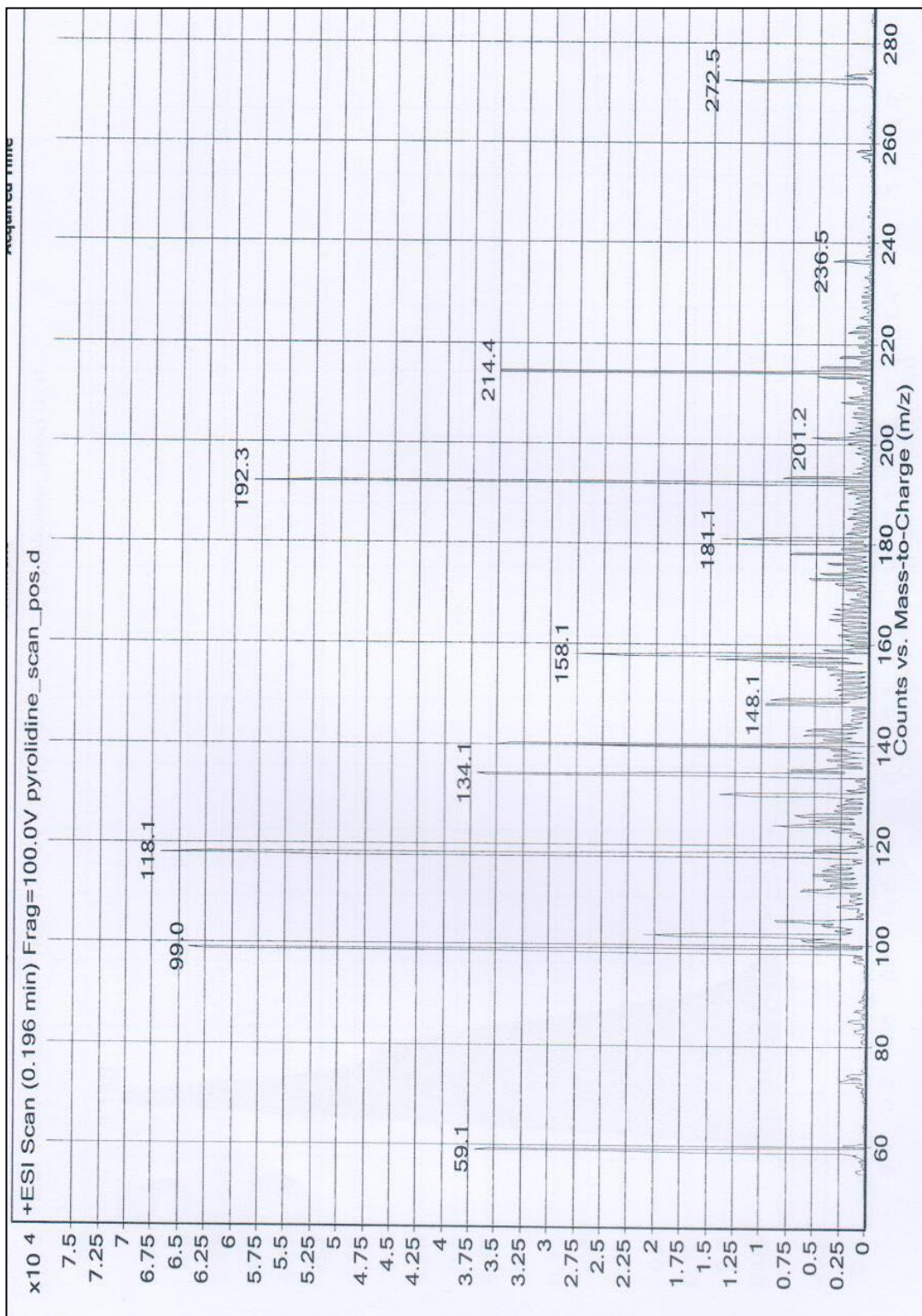
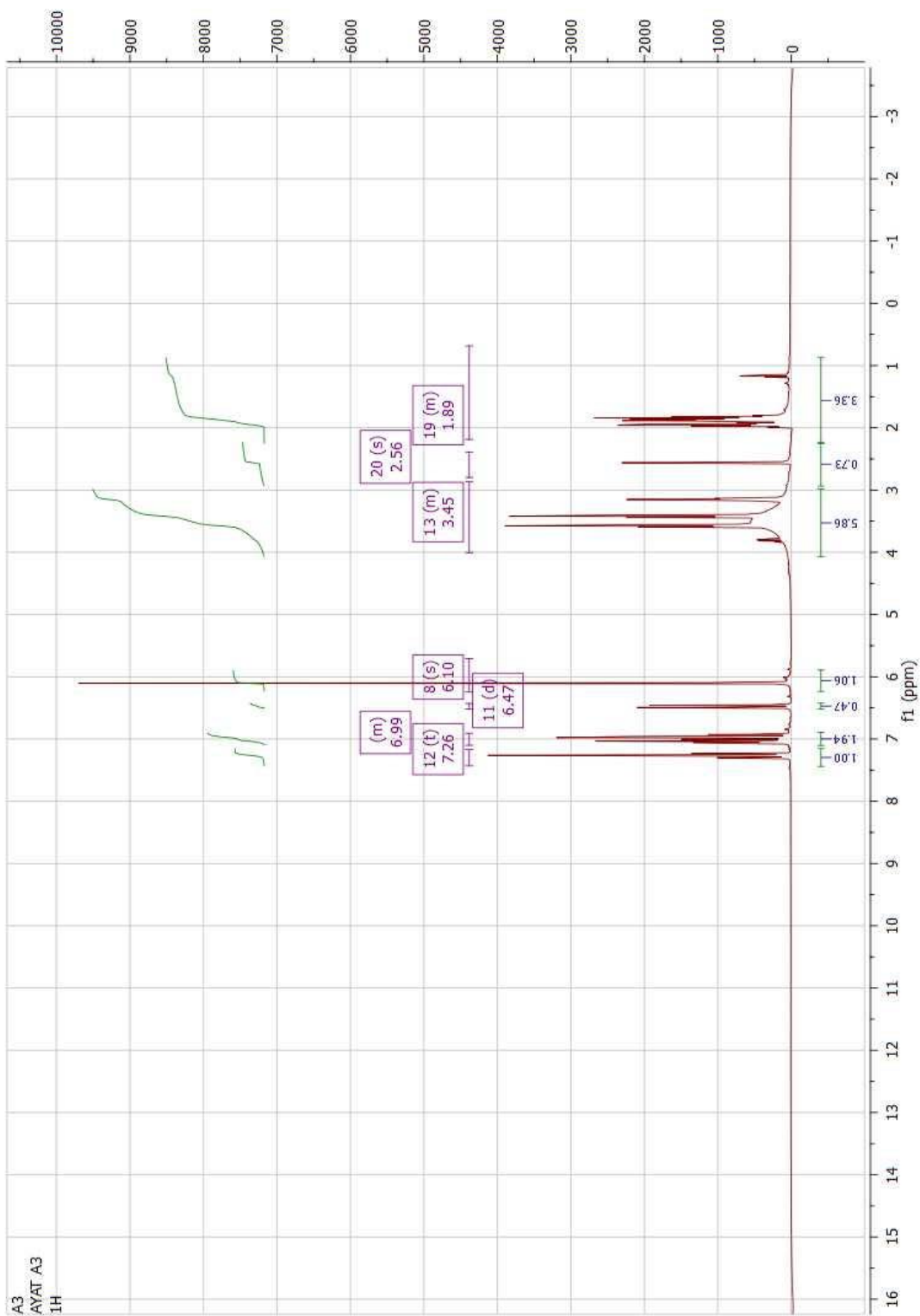**Figure 7.9:** Mass spectrum of **5** using positive mode ESI.

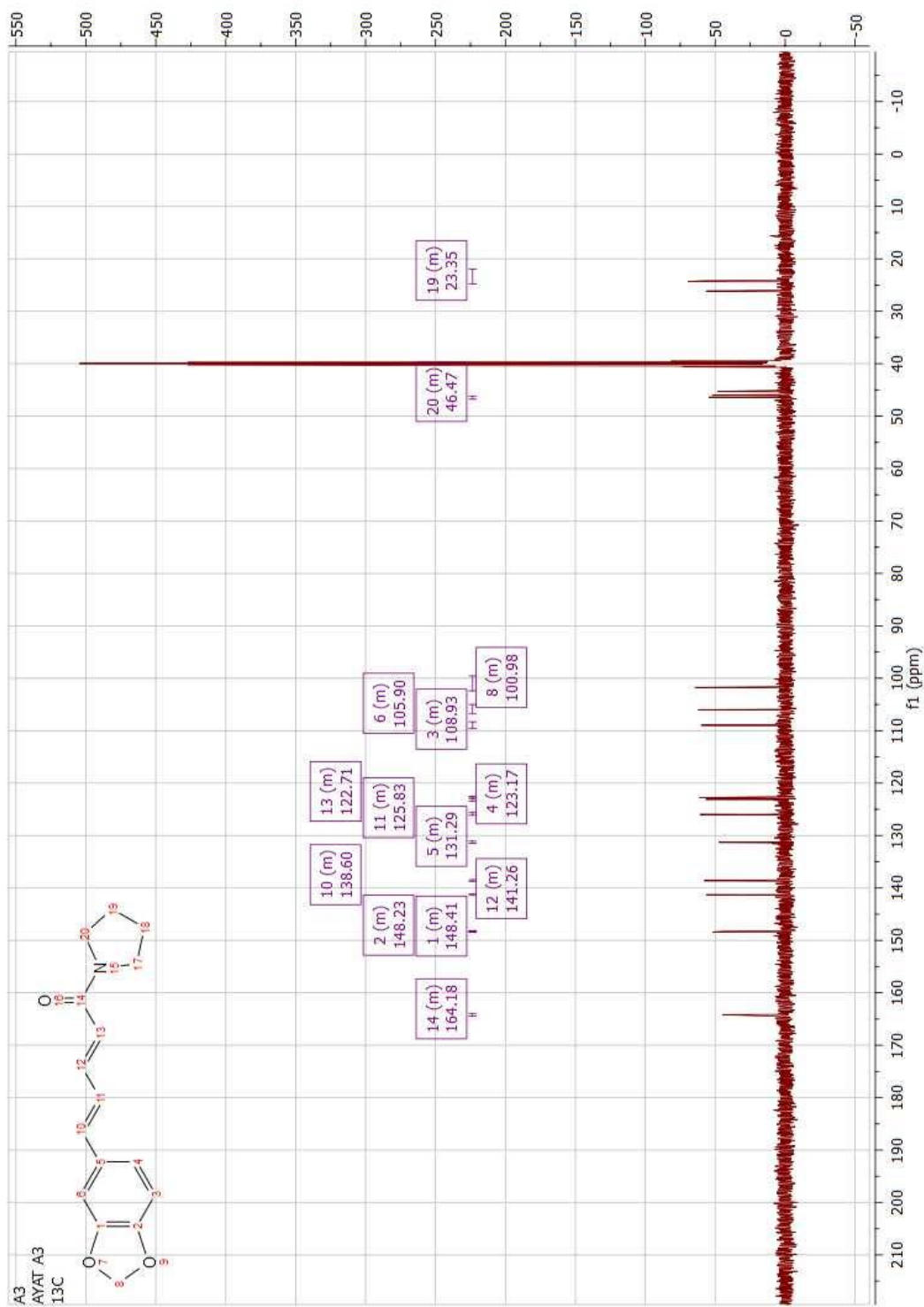**Figure 7.10:** ^{1}H NMR spectrum of **5** in DMSO-d6.

Figure 7.11: ^{13}C NMR spectrum of **5** in DMSO-d6.
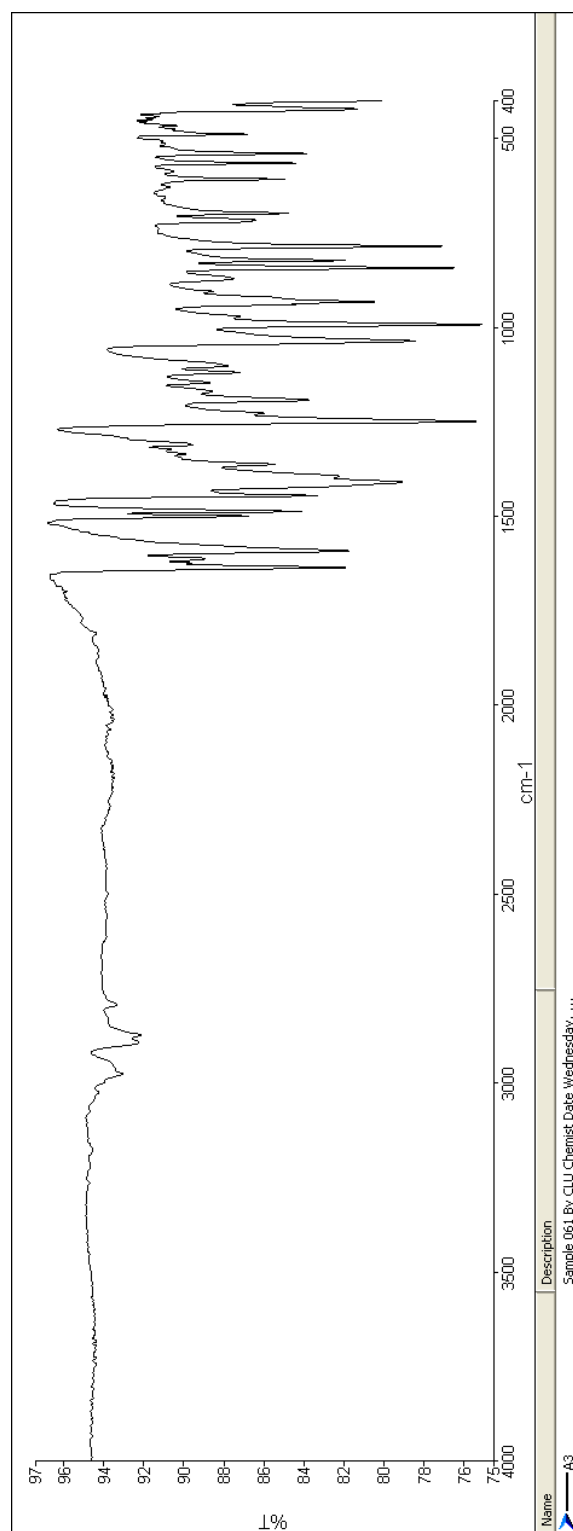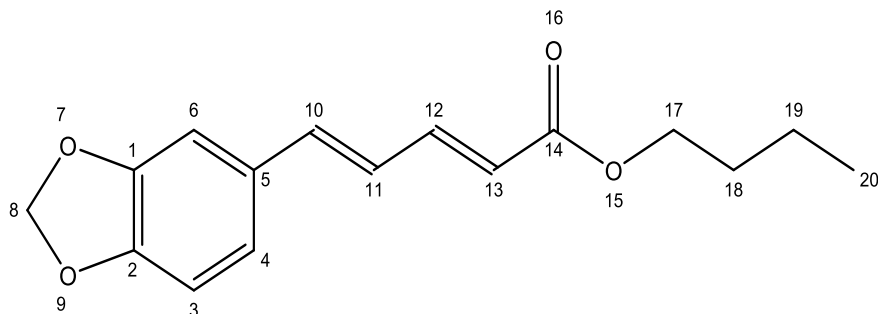
Figure 7.12: FTIR of **5** conducted on the solid sample using UATR.

7.4 Butyl Ester Analog (6)

butyl (2*E*,4*E*)-5-(benzo[*d*][1,3]dioxol-5-yl)penta-2,4-dienoate
Chemical Formula: $C_{16}H_{18}O_4$
Molecular Weight: 274.32
Elemental Analysis: C, 70.06; H, 6.61; O, 23.33

6 was prepared from piperic acid (**2**) and butanol as described in the section 3.1.2. The ^{1}H NMR spectrum in DMSO-d6 of butyl amide: δ 7.22 (H6), 6.05 (H8), 7.38 (H12), 5.99 (H13), 4.09 (H17), 1.59 (H18), 1.35 (H19), 0.9 (H20) (Figure 7.14). ^{13}C NMR spectrum in DMSO-d6: δ 148.7 (C1), 148.47 (C2), 108.92 (C3), 123.63 (C4), 131.08 (C5), 106.17 (C6), 101.63 (C8), 140.41 (C10), 125.32 (C11), 145.53 (C12), 120.44 (C13), 165.58 (C14), 64.35 (C17), 29.52 (C18), 19.01 (C19), 13.95 (C20) (Figure 7.15). FTIR results showed the absorption of C=O stretch of the ester group at 1701 cm^{-1} (Figure 7.16).
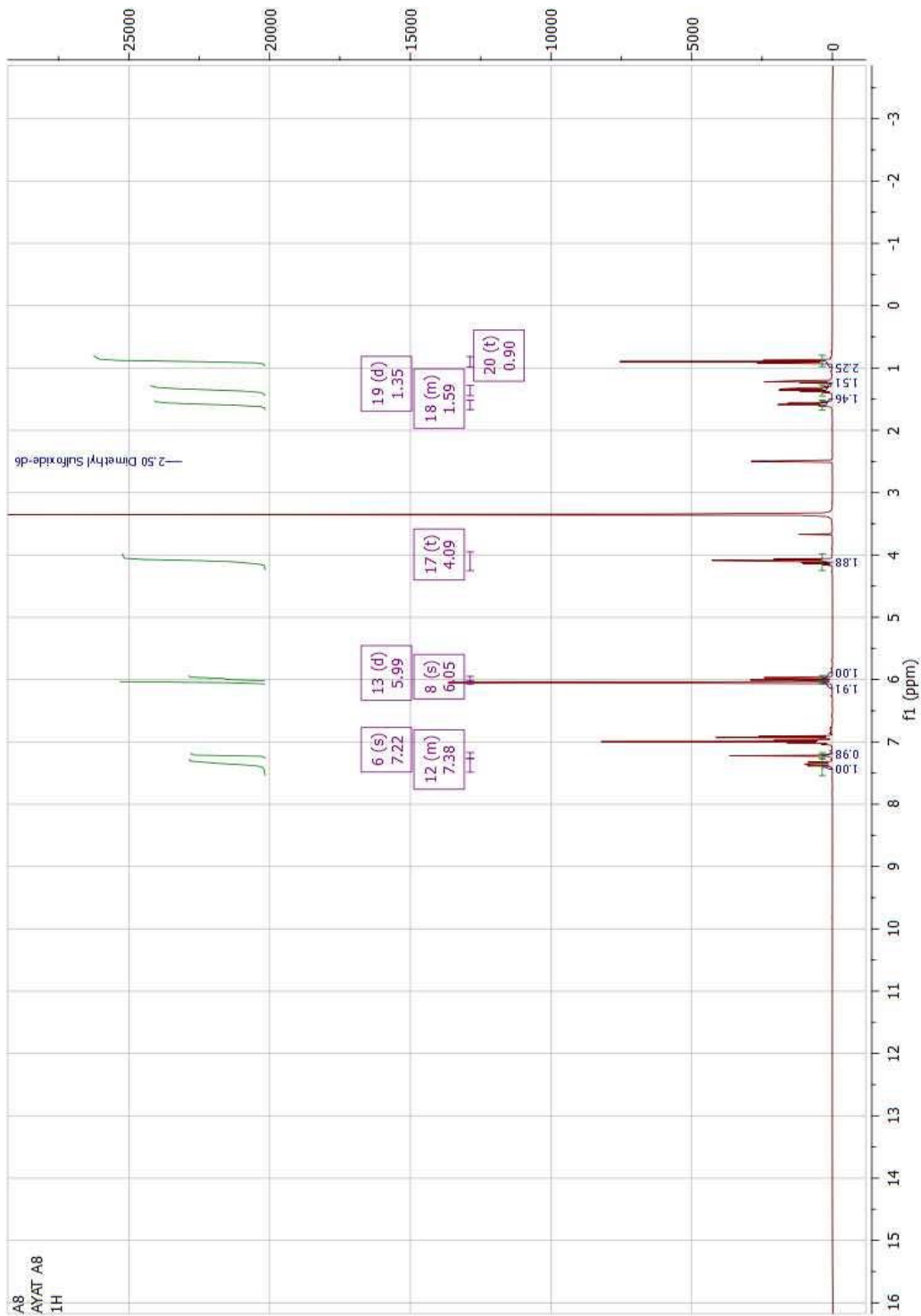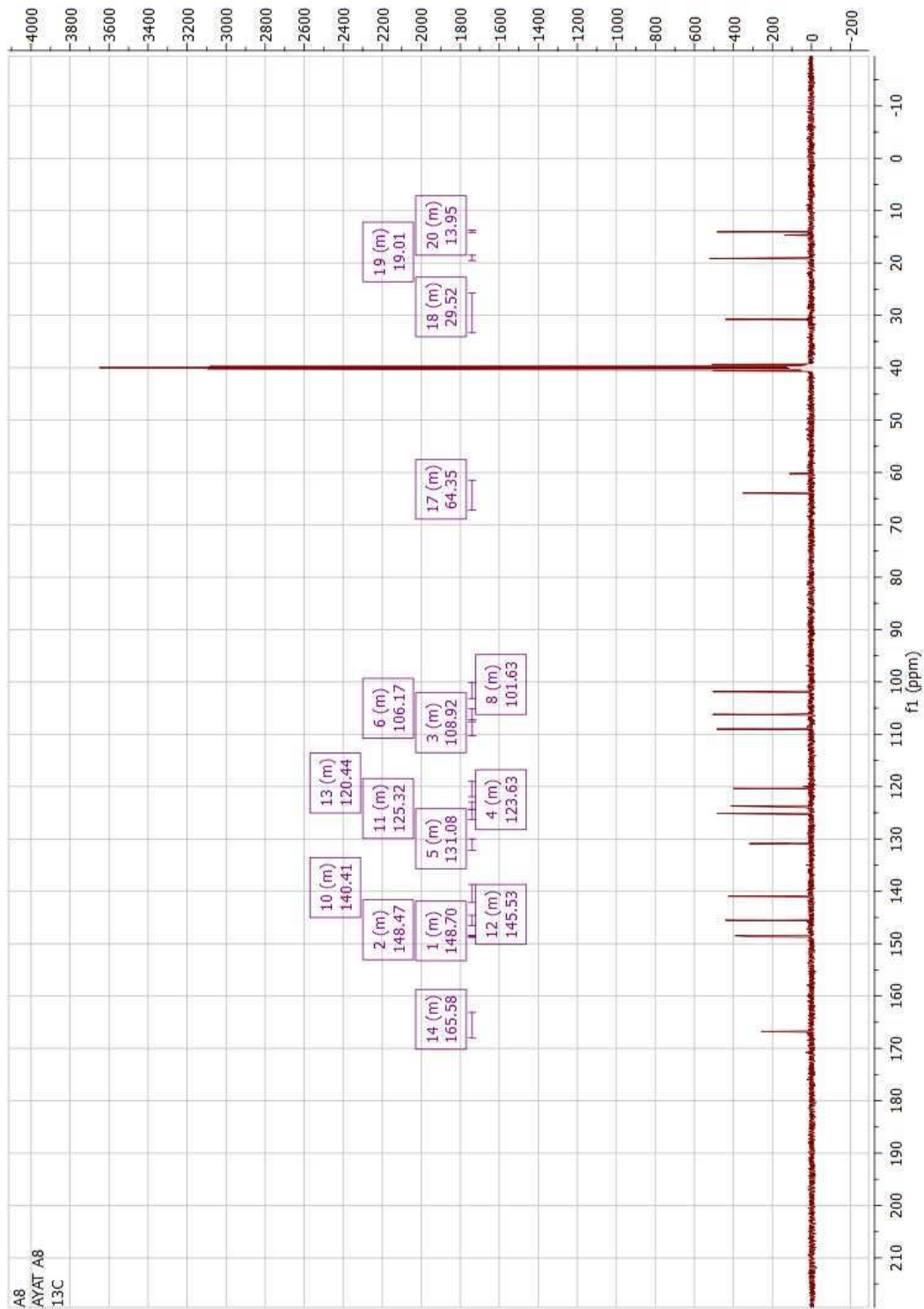
Figure 7.14: ^{1}H NMR spectrum of butyl ester analog **(6)**

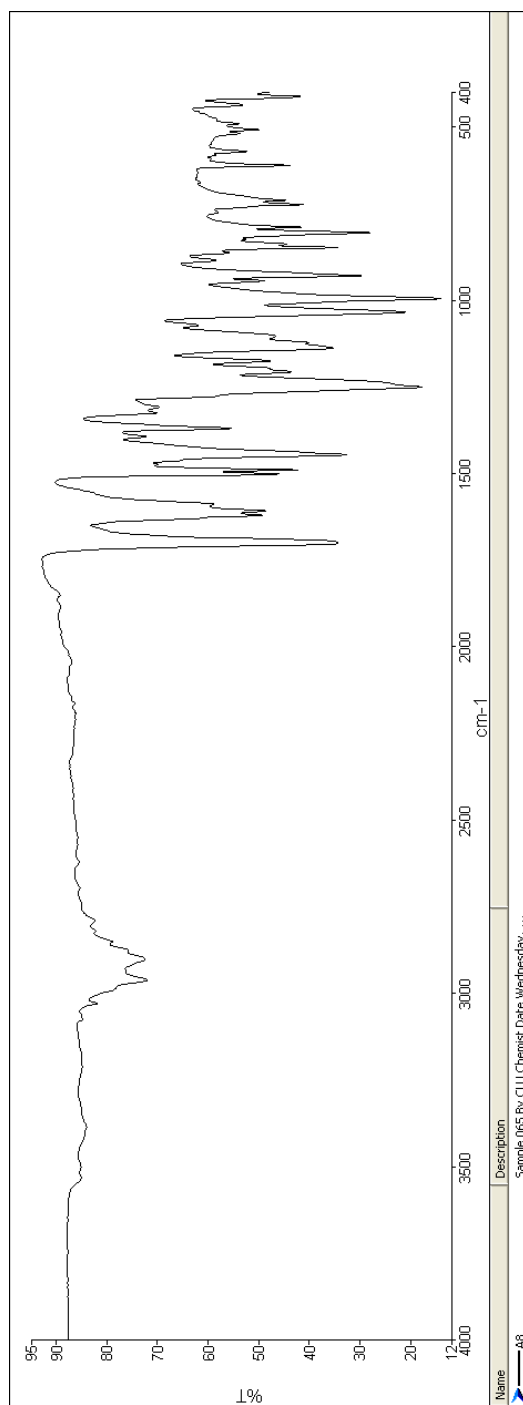**Figure 7.15:** ^{13}C NMR spectrum of butyl ester analog (**6**)

Figure 7.16: FTIR of butyl ester analog (**6**)

Note: Due to time constraints, the butyl ester analog was excluded from pharmacological screening.

7.5 References

1.   Koul S, Koul JL, Taneja SC, Dhar KL, Jamwal DS, Singh K, et al. Structure-activity relationship of piperine and its synthetic analogues for their inhibitory potentials of rat hepatic microsomal constitutive and inducible cytochrome P450 activities. Bioorganic & medicinal chemistry. 2000;8(1):251-68.

2.   Venkatasamy R, Faas L, Young AR, Raman A, Hider RC. Effects of piperine analogues on stimulation of melanocyte proliferation and melanocyte differentiation. Bioorganic & medicinal chemistry. 2004;12(8):1905-20.